ASSESSMENT OF MASONRY ARCH BRIDGES BY MECHANISM METHOD

by

Onur Özer

B.S., in C.E., Middle East Technical University, 2004

Submitted to the Institute for Graduate Studies in
Science and Engineering in partial fulfillment of
the requirements for the degree of
Master of Science

Graduate Program in Civil Engineering

Boğaziçi University

2006

Bana daima inanan ve güvenen babama

ACKNOWLEDGEMENTS

I would like to express my sincere gratitude to Dr. Cem Yalçın, my thesis advisor, for his guidance, support, encouragement and friendly attitude. The brainstorming hours we had with him has contributed enormously to this study.

I am grateful to Dr. Erhan Karaesmen for his tremendous support and assistance while pursuing both my academic and personal goals. His well-known love for historic structures has been an appreciable inspiration for me to select the subject as my research topic.

I would also like to thank Prof. Cengiz Karakoç for his involvement in my thesis committee.

My thanks also go to my roommates, Numan Aral and Serdar Yüksel for their unchanging friendship.

I owe my heartfelt gratitude to my family for their support, love and friendship all throughout my life. Finally, I would like to thank my dear friend, Bilge Alıcıoğlu; without her, my life in Istanbul would have never been the same.

ABSTRACT

ASSESSMENT OF MASONRY ARCH BRIDGES BY MECHANISM METHOD

There exists several arch assessment methods in the literature which predict the ultimate load carrying capacities of masonry arch bridges. The present study elaborates specifically on the Mechanism Method.

In the first part of this thesis, an algorithm and corresponding computer program has been developed to predict the collapse load of masonry arch bridges. The collapse mechanism is based on the formation of four plastic hinges throughout the structure. The algorithm examines all possible sets of such hinge formations and returns the critical one that leads to collapse.

The second part of this study concerns a non-dimensional analysis. The aim is to extract a quick estimate for the collapse load of an existing bridge without using any arch assessment technique. The proposed method uses the non-dimensional geometric properties of the bridge of interest along with those of tested one(s) for which the geometric properties and corresponding experimental collapse load are available. The method is validated by means of both hypothetical and experimental data.

.

ÖZET

TAŞ KEMERLİ KÖPRÜLERİN MEKANİZMA METODU İLE YÜK TAŞIMA KAPASİTESİ HESABI

Literatürde taş kemerli köprülerin taşıma kapasitelerini öngören bir çok değerlendirme metodu vardır. Bu çalışma, özelde Mekanizma Metoduna yoğunlaşmaktadır.

Bu tezin ilk kısmında, taş kemerli köprülerin taşıma kapasitesini hesaplayan bir algoritma ve neticesindeki bilgisayar programı geliştirilmiştir. Taş kemerli köprülerin yıkılma mekanizması 4 – plastik – mafsal oluşumundan kaynaklanmaktadır. Geliştirilen program tüm mafsal oluşum kümelerini inceleyip, yıkıma neden olabilecek en krıtik kümeyi seçmektedir.

Çalışmanın ikinci kısmı geliştirilen bilgisayar programıyla yapılan boyutsuz analizi içermektedir. Herhangi bir metot kullanmadan, mevcut köprülerin taşıma kapasitelerini pratik bir şekilde tahmin edebilen bir yöntem geliştirilmesi amaçlanmıştır. İleri sürülen yöntem, mevcut köprünün boyutsuz geometrik özellikleriyle birlikte önceden deneylerle incelenmiş olan köprülerin geometrik özelliklerini ve taşıma kapasitelerini kullanmaktadır. Bu yöntem, farazi ve deneysel veriler yardımıyla doğrulanmıştır.

TABLE OF CONTENTS

LIST OF FIGURES

LIST OF TABLES

LIST OF SYMBOLS/ABBREVIATIONS

3-D	3 Dimensional
A	Area
b	Width of a rectangular cross section
c	A constant
e	Eccentricity
f	Rise at the crown
f_e	Rise of the existing bridge
f_t	Rise of the tested bridge
F_i	Force fraction at node i
F_j	Force fraction at node j
H	Fill depth at the crown
H_e	Fill depth of the existing bridge
H_t	Fill depth of the tested bridge
HT	Horizontal abutment thrust
h	Height of a rectangular cross section
L	Span length
L_e	Span of the existing bridge
L_t	Span of the tested bridge
M	Bending moment
N	Normal force
N_0	Ultimate axial load capacity
n	Number of segments
P	Collapse load
P_e	Collapse load of existing bridge
P_t	Collapse load of tested bridge
r	Ring thickness

r_e	Ring thickness of the existing bridge
r_t	Ring thickness of the tested bridge
R	Correlation coefficient
VT	Vertical abutment thrust
w	The width of the live load
θ	Dispersion angle
σ_i	Stress fraction at node i
σ_j	Stress fraction at node j
σ_x	Horizontal soil pressure
σ_{xz}	Shear stress
σ_z	Vertical soil pressure
σ_o	Ultimate compressive strength
FEA	Finite element analysis
FEM	Finite element method
gfill	Specific weight of the fill
GMF	Geometric multiplication factor
gring	Specific weight of the ring
har	Hypothetical arch ratio
MEXE	Military Engineering Experimental Establishment
PAL	Provisional axle load
SF	Scaling factor
TRL	Transport Research Laboratory

1. INTRODUCTION

There are more than 250 masonry arch bridges still existing in Turkey with various spans, shapes and materials which were constructed in different eras. They were built for social and economical purposes as well as strategic purposes such as passageway for the army or showing the power of the empire. Due to the over conservative design methods used in the earlier times, most of these bridges are able to carry the ever-increasing live loads from modern day traffic without risk of collapse. Some have witnessed serious earthquakes, and these earthquakes have hardly caused the collapse of these bridges since many of them are still standing.

There are mainly two reasons why these bridges survived until today without any repair. First reason is that the materials used in the masonry construction are extremely durable. As the five-minute theorem for masonry may be stated; if the timber centering of the arch is removed on completion of the stonework, and the work stands for 5 minutes, then it will stand for 500 years. 500 years is the time period for decaying of the material [1].

Second reason is that these masonry arches are well-designed despite the fact that no engineering calculations and material testing were performed. A structural feeling through practical experience is attained. The ancient master builders, then, learned that in order to span large openings, the true shape of the structure should be in the form of an arch as it can be seen also in the nature.

- *Landscape Arch, National Park, USA: The world's second longest natural span with a span of 88 m. It is less than 1.6 m thick at its thinner part (see Figure 1.1)* [2].

The arch is, therefore, a complete example of form following function. Its aesthetic appeal lies in the variety of forms which can be used to express unity, balance, proportion, scale and character. Its structural advantage results from the fact that under uniform load, the induced stresses are principally compressive. Because brick or stone has greater

resistance to compression and are weak in tension, the masonry arch is frequently the most efficient structural element to span openings.

Figure 1.1. Landscape arch [2]

Out of so many bridges constructed in a long period of time, many of them survived until the present days. Nevertheless, this does not mean that the survival is eternal. Moreover, it should be controlled whether the arch is able to carry the current axle loads safely. Furthermore, as vehicle weight limits steadily amplify, the need for strengthening the old bridges is ever-increasing. In order to determine whether the old bridge really needs any repair or not, the engineer's first duty is to determine the critical load that causes collapse. Previous studies on this subject show that; collapse must be viewed as a geometrical problem rather than a problem in strength of materials; i.e., failure of an arch is not related to crushing of the material but only its shape [1, 3].

1.1. Masonry as Material and Construction Technique for Structural Systems

In our days, the materials used in the masonry construction vary a lot: stone, brick, adobe, processed concrete hollow or plain blocks, etc. In this group, stone still occupies a very special place. Throughout the developments in construction techniques and in structural forms, stone has preserved the dominant place among materials [4].

It should be remembered that, all construction materials including the most sophisticated ones are all obtained by processing raw materials existing in nature. Boulders and loose stone pieces as abundant raw materials on earth were further easily handled and transported by early man for sheltering and protection purposes. Men living in caves where spaces were covered by arched rock components became familiar with stones and curved linings. This early familiarity with curved forms perhaps has led to a structural conceptualization. It is clear that man imitated reliable forms with stone as observed in nature. Moreover, wide use of arched bridges with stones gave this material a prestigious place in construction field. Later, needs for proper binding and connecting stone pieces in vertical or curved structural elements were observed. Giving rise to use of auxiliary material as mortar and thus resulting in requirement of special workmanship in masonry construction techniques [5].

1.2. Objectives and Outline of the Thesis

This study focuses mainly on two major issues; the assessment of masonry arch bridges and the investigation of the effect of the geometry on the capacity of masonry arch bridges. An algorithm and its corresponding computer program is developed in order to predict the capacity of such arch bridges, and furthermore, the results were validated with previous experimental studies. As a result, a simple and useful method is offered for the prediction of the capacity of existing bridges.

This thesis comprises 3 parts and includes 8 Chapters. The first part; Chapters 2, 3 and 4, is a condensed summary of the subject. The second part, Chapter 5, is the development of an analysis algorithm and a computer program. The last part, Chapters 6 and 7, involves parametric study using the computer program.

Chapter 2 describes an overview of the main characteristics of the masonry arch bridges. Structural forms and construction techniques are presented. Development of the arch form is briefly introduced

Chapter 3 includes the review of the masonry arch behavior. Basic concepts such as Line of Thrust, Middle Third Rule and Theory of Limit Analysis are introduced. An introduction to failure modes of masonry arch bridges is also presented.

Chapter 4 is devoted to the assessment of masonry arch bridges. Four different arch assessment methods, namely MEXE, Pinned-Elastic, Finite Element and Mechanism Methods, are introduced. The background to each of these methods is presented. Each method is evaluated against the selected criteria and conclusions are drawn on their suitability for assessment.

Chapter 5 explains the implementation of the computer program that predicts the ultimate load carrying capacities of single span masonry arch bridges by the Mechanism Method. The details about the program algorithm together with a test run are given. The program's results are validated by comparing them with the available experimental results.

In Chapter 6, the influence of the change in arch geometry on the collapse load is studied. The relationship between the capacity of the arch and the non-dimensional parameters are investigated.

In Chapter 7, a very simple and useful arch assessment method is proposed and validated.

2. CHARACTERISTIC FEATURES AND DEVELOPMENT OF MASONRY ARCH BRIDGES

2.1. The Parts of a Masonry Arch Bridge

The arch ring consists of shaped blocks that compress together under vertical loads. The outward thrust at the base of the arch must be countered by the abutments. Figure 2.1 illustrates the technical terminology for arches. Voussoirs are the wedge-shaped bricks or blocks constituting the arch. The central one, which is sometimes emphasized by making it larger or projecting below and above, is the keystone. Extrados and Intrados are the external and internal curves of the arch, respectively. The highest point of the arch ring is the crown. The lower half of the arch between the crown and the skewbacks, which are the inclined surfaces of the abutments from which the arch springs, is the haunch. The intersection points of skewbacks and the intrados are the springing points. Abutments are the piers or the portion of wall supporting the arch [6, 7].

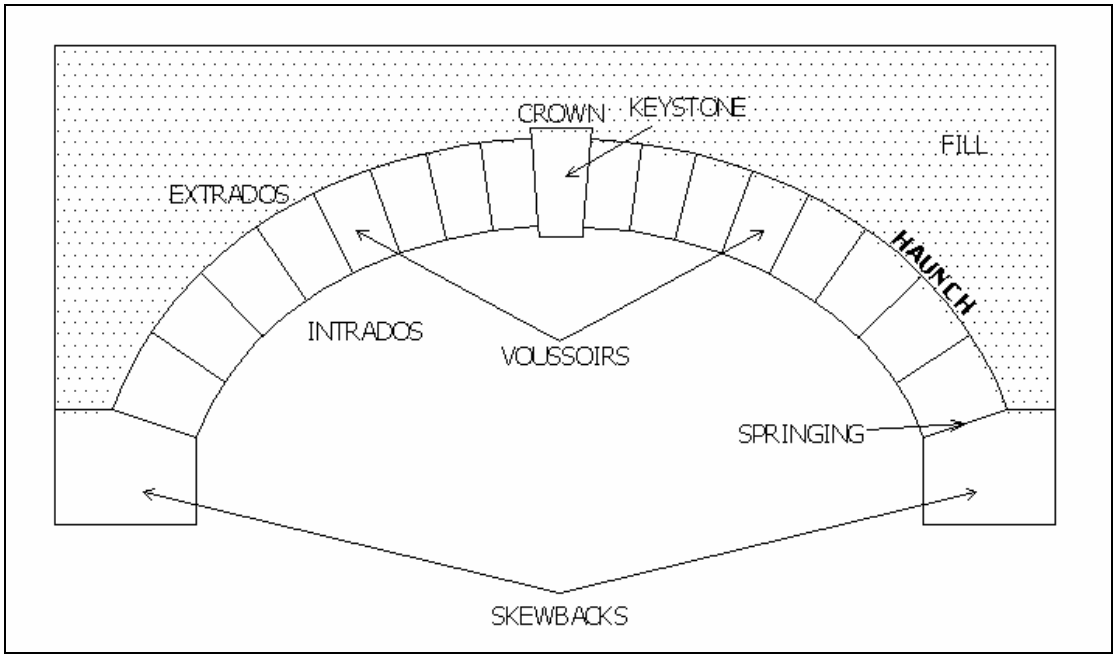

Figure 2.1. Masonry arch terms

2.2. Structural Forms of an Arch

It is possible to obtain different arch patterns by using various mortar thicknesses. The curve of intrados or extrados determines the name of the arch. The most common arch forms can be classified as semicircular, segmental, pointed, elliptical, flat, shallow and horse shoe shaped arches [8, 9, 10].

- Semicircular Arches: These arches were generally used for load bearing distances rather than small wall openings or on facades and preferred mostly by the Romans.
- Segmental Arches: These arches are less circular than semi circumference. They are stronger than semicircular arches, but since they apply more thrust to supports, strong abutments or tie rods may be required. They were generally used above doors and windows instead of semicircular or full-centered arches.
- Pointed Arches: These arches are formed by two curves meeting at the crown with a sharp angle. This type is known as Gothic arch as well, and has a wide spread use in the Middle Age and Gothic period. It is the most common arch form used by Seljuks [11, 12].

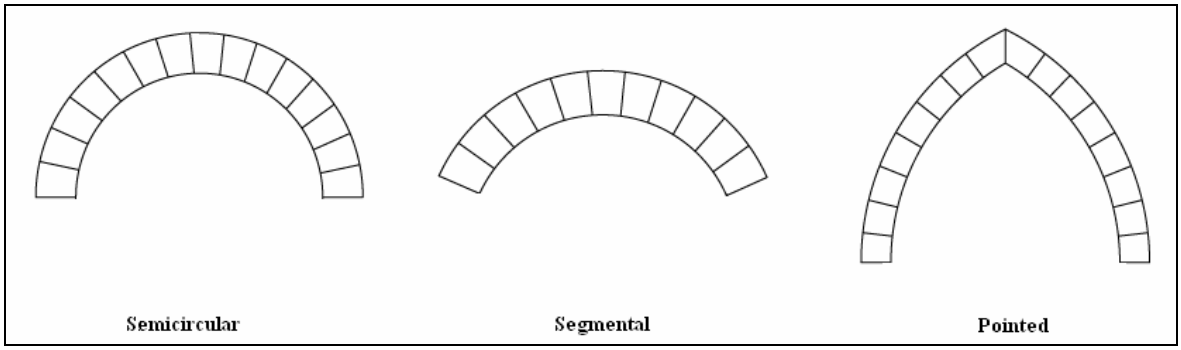

Figure 2.2. Examples of arch forms (Semicircular, Segmental, Pointed) [2]

- Elliptic Arches: In a true ellipse form, each joint is perpendicular to a tangent of the curve. Sometimes it takes the form of three consecutive curves; this is not the true ellipse form and called a*s* three-centered ellipse. In this case, each joint radiates from its own curve.
- Flat Arches: They were generally used to cover the remaining wall beyond the door or wall openings such as windows or doors with less than 2-meter spans. The intrados is curved slightly in order to avoid the appearance of sagging. They are not

expected to bear the loads without sagging or cracking unlike segmental or semicircular curves.

- Horse Shoe Shaped Arches: Every arch with its curve turning till the underneath of stirrup can be included into this group. It has four types as semicircular, pointed with two centers, single centered tangential and three centered with the upper part reverse curved.

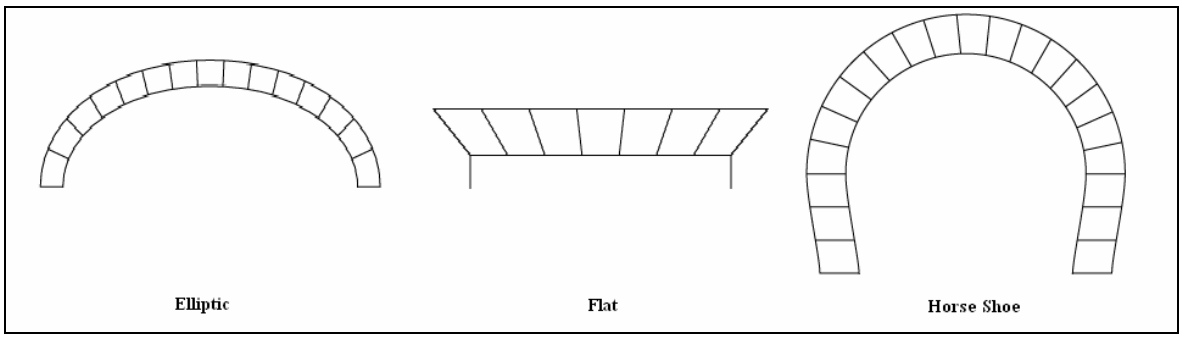

Figure 2.3. Examples of arch forms (Elliptic, Flat, Horse Shoe) [2]

2.3. A Brief Discussion on the Construction of Masonry Arch Bridges

An arch requires all of its elements to hold it together. Therefore, the entire weight during assembly is taken by the falsework, or centering until the arch itself has gained sufficient strength. An example of centering for an arch is shown in Figure 2.4.

After the construction of the centering, the arch is built by flat or wedge-shaped fieldstone since shaping the ring stones results in perfect arch. Subsequently, the spandrels are constructed. The sides or spandrels of the bridge are less crucial; their function is simply to retain the fill material for the roadway. Spandrels are often made up of rubble; i.e. randomly shaped stone. Finally, when the arch and spandrels are completed, large-size stones are placed between the spandrel walls to form the roadway.

Figure 2.4. A typical view of centering [13]

Immediately after removal of the centering, very slight downward displacement of the centering, termed easing, can be performed to cause the arch voussoirs to press against one another and compress the mortar joints between them. Easing helps to avoid separation cracks in the arch. In no case the centering is removed until it is absolutely certain that the masonry is capable of carrying all the imposed loads. Premature removal of the centering may result in collapse of the arch.

How much of the structural behavior was known to masons is one of the most tantalizing questions since it cannot be definitely answered. In some cases, authors of books or book chapters on the history of bridges use terms such as “primitive”, probably as opposed to the modern state-of-the-art engineering achievements. It is spoken of a lack of proper understanding, and of empirical methods. From today’s point of view it is easy to come up such a judgment, but one should be careful not to diminish the outstanding achievements of the early builders. In our technical age, equipped with well-developed computation techniques and tools, and heavy construction equipments that are readily available, it is relatively easy to forget about the real circumstances under which these structures were built. Since mathematics and the natural sciences had yet even begun being developed, it is not surprising that no engineering calculations and material testing as adhering to our modern understanding were performed. Accordingly, these ancient master builders had no means of calculating the amount of buttressing required by any particular design, and seem to have discovered the margins of safety through observation and

experience; they were additionally fortunate in then sense that the proportions to which they built happened to lie in the necessary limits of stability. More clearly; up until the 19th century, the “rule of thumb” was the only design method existed. A feeling for structures and materials was present in the minds of these ancient master builders. With this and much trial and error, they built extraordinary arch structures that are so solid and well engineered that many have survived over the centuries until today. Heyman [1995] describes in detail how these learned stone masons used their skills to build ever lasting masonry structures.

2.4. Development of the Arch Form

Along with timber, masonry is the oldest building material known to mankind. The placing of stone or brick blocks on top of each other, laid dry or bonded with mortar, has revealed itself to be a very successful technique, which is mainly justified by its simplicity and the durability of the constructions. Most likely, the first masonry was a simple mass of selected natural stones and mortar was packed between the stones. As tools became available and skills developed, stone elements were shaped in regular forms. The first bricks were made out of mud and clay, shaped to form bricks and dried under the sun. The bricks were then laid with mud mortar into walls. This simple process; namely adobe, has been widely used for millennia to construct dwellings, particularly in the valleys of the Nile and Mesopotamia [14].

Archaeological excavations have revealed masonry houses near Lake Hullen in Israel dated back 9000-8000 B.C., that are in the form of dry-stone huts, circular and semi-subterranean shapes were found, as one of the oldest building types. Another earliest example of building construction is the Walls of Jericho (8000 B.C.). These structures were built as military defense and were made from roughly worked limestone, where the joints were simply filled with earth. In the same area, archaeological surveys have found more recent walls (3000 B.C.) made from sun-dried bricks and mortar [14, 15].

2.4.1. First Examples of Arches in Structures

The first masonry structure in the form of true arch, dating to the third millennium B.C., is seen in Ur-Mesopotamia in underground tombs. Bricks, actually, were in plano-convex form; i.e. flat or planer on one side, and rounded on the other, rather than voussoir, with a span of few feet. The subterranean water canal, which was discovered in another Sumerian city, Nuffar, dating to 2900-2700 B.C., has an oval-shaped arch form with less than one meter span. The plano-convex shaped brick makes a contradiction for the recognition of this form as a true arch; and the same is relevant for the similar remains found in Khafaje and Fara [16].

The true arch found in Egypt, indicates that builders were indeed possessed keen knowledge about the structural possibilities of the arch at least simultaneously with the Sumerians. In the period of the Fifth Dynasty, 2560-2420 B.C., bricks in voussoir fashion, and in the period of the following dynasty, 2372-2266 B.C., cut stones in rough voussoir fashion were used. A combination of corbel and true arch was found belonging to the period of Rameses II, thirteenth century B.C. Since the fine quality of stones in Egypt, were enough to span long distances, voussoir arches were ignored despite the ease of using relatively small pieces. Therefore, this form was not developed effectively [16, 17].

Due to their familiarity with the corbel arch, people of Pre-Hellenic Crete and Greece used this form widely in their buildings. But, the voussoir arch was not that common in classical Greek and even in their further periods, despite their knowledge about its structural capacity [16].

Even though the true arch form was invented in Egypt or Mesopotamia, limited structural possibilities remained until the Roman period. The earliest examples for the Roman use of arch are seen as the vaulted passages covering the altar drains, which were made to carry the blood of victims. These passages may also be thought to have been the branches of Cloaca Maxima. The subterranean passage Cloaca Maxima, as seen Figure 2.5, probably dates to the period of Augustus (27 B.C.-A.D. 17) with three rows of voussoirs [16, 18].

Figure 2.5. Cloaca Maxima [19]

2.4.2. Use of Arch in Aqueducts and Bridges

Probably the oldest stone arch bridge, more complex structural type, can be found crossing the Melez creek with a single span in Smyrna (İzmir), Turkey. It is dated back to the 9th century B.C. [20]. Earliest cultures using such bridges, according to our current knowledge, were the Sumarians in Mesopotamia and the Egyptians, who used corbelled stone arches for the vaults of tombs [21]. However, the greatest bridge builders of antiquity were the Romans. They applied a vast civil engineering repertoire on an extraordinary grand scale and achieved impressive results. Roman engineering introduced four significant developments to the art of bridge building never being prominent before; the discovery and extensive use of natural cement (pozzolana), development of the coffer dam, development to near perfection and widespread application of semi-circular masonry arch, and the concept of public works.

Structural evolution achieved by Roman engineers is well noticeable in aqueducts, dam constructions, and highway bridges that relied on the development of concrete, and a growing awareness of its strength. The Romans mixed cement, pozzolana, found near the Italian town of Pozzuoli (ancient Puteoli), with lime, sand, and water to form a mortar that did not disintegrate when exposed to water. It was used as a binder in piers and arch spandrels, and mass-formed in foundations.

In the last centuries B.C., arch form became traditional due to its widely spread use on facades, above the entrance to porticoes and in city gates as signs for triumphal arches of the Roman Empire. Stones of the gateway, The Porta di Giove, at Falerii Novi, dating to the 3rd century B.C., are locked in each other without mortar as it is seen in Figure 2.6.

Figure 2.6. The Porta di Giove at Falerii Novi [22]

The Roman aqueducts, which were used to bring water from wide and steep valleys to the cities, were important revolutions that the arch form brought in utilitarian architecture. Aqua Marcia, which was built in 144-140 B.C., was an important revolution. Being divided into several pipes in order to reduce the pressure at inclinations, it brought water to both Rome and Lyons from different valleys. It was carried by arches, which were built of traditional Roman tufa ashlar as its piers. These structures dating from the ancient times are in the form of single arches as Metz and Tunis, or double arched as the one built in Segiova, or three-tiered as Pont du Gard (Figure 2.7), which is one of the wonders of all times with its perfect proportions. Pont du Gard, one of the best preserved examples of aqueducts, was built on River Garden, at the southern part of France, near Nimes in 14 A.D. It rises to a height of 55 meters above the stream, and built with monumental stones [23, 24].

Figure 2.7. Pont du Gard, France [2]

The appearance of this body is as perfect as its functional achievement. The two rows of larger arches are on top of each other, and the smaller arches at the third part were arranged in a manner that the width of three of them would be equal to the width of one arch at the lower parts. Since the central arch is wider than the others, four small arches take place above this arch.

Masonry arch bridges are also seen in China. There are some differences in the arch form with the Roman's as these bridges consist of mainly almost flat segmental arches. The An-Chi Bridge, in northern China, which was built between 590 and 616, has a span of 37.5 meters with a height of only 7 meters. In this bridge, all the voussoirs were connected to each other by iron clamps and openings were made at the upper parts of the spandrels so as to reduce the effect of water flow and lighten the weight of the structure. Its shallow segmental arch and open spandrels were strikingly different to the full semi-circular arches and filled spandrels typical of Roman arches [17, 23, 25].

The developments in bridges remained within the limits of only refinement for long centuries. The revolutionary techniques of Gothic period were not applied on the bridges. Structural principle could not reach to the "independent arch" until Perronet, who was one

of the greatest engineers of the 18th century. In order to transmit the thrust beyond, the vertical supports was used in the construction of flying buttresses, but he was the first to apply it to the bridges. The piers would take only the vertical loads and the thrust would be transmitted from one to another ending at the abutments. This enabled reducing the thickness of the piers about half of the usual dimensions. He made a sequence of bridges starting with Neuilly Bridge over the Seine in 1768-1774, which was demolished in 1938. The second bridge of Perronet is Ponte – Sainte - Maxence over the Oise and the third is Pont de la Concorde in Paris with a total length of 153 meters. The arches are symmetric about the main arch with span lengths as; 25 m. – 28 m. – 31 m. - 28 m. – 25 m. [17, 23, 24].

2.4.3. Examples of Bridges in Anatolia and Thrace

- Roman and Byzantine Period: Bölam (Cendere) Suyu Bridge, dating to the 2nd century, in southeastern Anatolia, around Kahta region, is a single arch bridge with 34.2 meters of span and 17 meters of height. It has a total length of 117.5 meters. As it is shown in Figure 2.8, the abutments were constructed on very stiff rock in order to transmit the lateral thrust coming from the arch effect to the foundation.

Figure 2.8. Cendere Bridge, Turkey [26]

The Karamagara Bridge in the region of Keban Dam around Ağin is also a single arch bridge. Its construction date is known to be the fifth or sixth century. The arch is

of pointed form, with 14.5 meters span and 9.5 meters height. The Justinianus Bridge around Adapazarı dates to 561, has 8 openings with a maximum span of 33 meters [27]. Güvercin Bridge, Seyhan Bridge, Misis Bridge and Asi Nehri Bridge are other important bridges constructed at Roman and Byzantine period.

- Seljuks Period: In Anatolia and Thracia, there are 32 bridges proved to be built by the Seljuks. Nine of them are on Kizilirmak, as Tekgöz Bridge with 27.0 meters of span length, which is the first bridge built by the Seljuks. The most important peculiarity of this bridge is the precise and perfect craftsmanship of interlocking cut stones [27].

  The Sividin Bridge with one pointed arch, Yıldızırmak Bridge with 13 openings, Yeşilırmak Bridge, Akköprü Bridge, Kesik Bridge, Kızılırmak Bridge are other major bridges that all have the pointed arch form as a typical architectural feature of Seljuk's.

- Ottoman Period: There are more than 100 bridges in Anatolia and Thracia belonging to the Ottoman period. The most important ones can be listed as; Sultan Bayazid Veli Bridge, Mostar Bridge, Gazi Mihal Bridge, Murat River Bridge and Yantra Water Bridge in Bulgaria. Halil Rifat Paşa Bridge on the road from Kangal to Malatya with its 15 rows of voussoirs constituting from stones of 550 mm in width and 45 mm in thickness is another interesting masonry arch bridge stands currently.

  The master builder Sinan had built numerous works of art including various aqueducts and bridges. Twelve bridges were known to be built by him together with the repair and lengthening of the Kirkgöz Bridge in Afyon-Bolvadin. The most popular, beautiful and the highest bridge of Sinan is the Sinan (Mehmet Paşa) Bridge in Alpullu. There are some similarities in architectural features with the Sokullu Mehmet Paşa Bridge in Lüleburgaz, but the proficiency in its construction gives the idea of having been built later. The thickness of voussoirs is 580 mm on the lateral arches and 76 mm on the central arch. The length and width of the stones used in the central arch are of the ultimate dimensions with 2.5 m. and 0.60 m., respectively. The front part of the central pier is of a more pointed form than those of his other bridges.

There are probably no joints between the arch and the piers; the arch was directly set on the foundation. The span of 20.05 meters brings the idea to the mind that the ground is of rock [27, 28, 29].

The pier forms used by Sinan can not be strictly generated. Instead of applying the traditional forms, he studied on the intensity of water flow, so that the forms are seriously different from those of earlier centuries and possible erosion due to water flow was avoided [29, 30]. Silivri Bridge is the only one with shallow arches due to the less intensity of water flow.

Also, the water systems built by Sinan deserve a great importance. The Kırkceşme foundations, which were built to bring water from Belgrad Forest to Istanbul, are the most popular among all of them. According to some authors, it is suspicious that these systems were not at all built by the Ottomans, but it is certain that all the arches are of Ottoman [29].

The construction of arches by sound stones was completed in a short period of time. The most important arched aqueducts are Maglova, Kırkkemer, Uzunkemer and Güzelcekemer. Among them all, Uzunkemer is the longest with a total length of 711 meters (Figure 2.9). At its northern and southern ends, the water channel is supported by solid walls. The two-storey high middle part consists of archivolts spanning approximately 4.5- 5.35 meters. There are 47 arches in the lower and 50 arches in the upper level. The aqueduct changes direction at the pier between the twenty-third and twenty-fourth openings [12].

Figure 2.9. Uzunkemer Aqueduct, Turkey [31]

The Mağlova Aqueduct was a major utility in the water supply system of Istanbul during the 16th Century. The aqueduct is approximately 207.7 meters long and 32.4 meters high. The thickness of the structure varies between 2.65 meters and 7.7 meters getting thinner from bottom to top. Indeed, only very small cracks are visible on the structure and no external interventions seemed to be needed. The aqueduct is erected in two stories as seen in Figure 2.10. Main loads are resisted by the huge arch system. At the top of the structure, there is a hole from which water may flow [5].

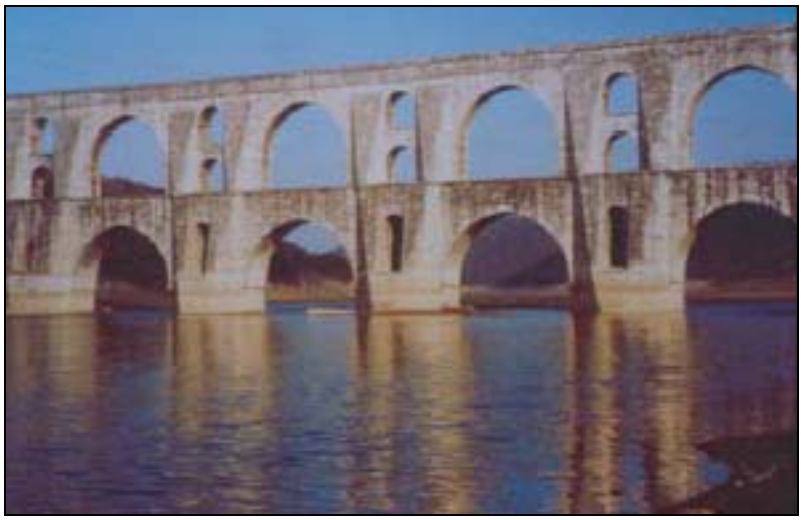

Figure 2.10. Mağlova Aqueduct, Turkey [5]

3. STRUCTURAL THEORY OF MASONRY ARCH BRIDGES

If one wants to deal with in more details how master builders achieved to built impressing bridges that survives till now, the first thing he or she has to do is to understand the structural criteria, *strength*, *stiffness* and *stability*, that should be satisfied. First of all, the structure must be strong enough to carry whatever loads are imposed, including its own weight. Secondly, it must not deflect unduly. Finally, it must not develop large unstable displacements, whether locally or overall. If these three criteria can be satisfied, then the designer can run through a check list of secondary limit states to make sure that the structure is otherwise serviceable.

Same procedure can be applied to masonry. Ancient structures seem naturally to be strong enough; they are still standing, without extreme deformations, and evidently the loading (self weight, wind, and earthquake) has not caused failure to occur by fracture of the material. It is a fact that the mean stresses are low in a typical masonry structure. Although cracking and local spalling may be seen, these seem hardly to affect the structural integrity of the whole.

Similarly, the designer is unlikely to worry about excessively large deflections. Therefore strength and stiffness do not lie in the foreground of the masonry design. Nevertheless, it is the third major criterion, that of *stability*, that is relevant for masonry in a curious form.

As an example, a masonry arch may be perfectly comfortable under the action of its own weight and at a certain intensity of the superimposed load P. The stresses are low and the deflections are negligible. However, at a certain value of P, a sudden change puts an end to this stability. As will be seen, a point is reached at which the structural forces can no longer be contained within the arch; the stresses are low but an unstable mechanism of collapse is formed. More clearly, collapse must be viewed as a geometrical problem rather than a problem in strength of materials; failure of an arch is not related to crushing of the material but only to its shape [1, 3, 32].

3.1. Line of Thrust

To begin with, let us consider the free-body equilibrium of the keystone. An each joint, there will exist a certain stress distribution. The stress resultant must be a compressive force, a *thrust*; the point of application is the *centre of thrust* and it must be contained within the plane of the joint. The two thrusts in the joints maintain the keystone in equilibrium. The same occurs with the other stones until we arrive at the springings of the arch. There the abutment must supply/resist a certain thrust. This is the *thrust of the arch* and the abutment must have adequate dimensions to resist it. The locus of the centre of thrust forms a line, namely the *line of thrust* [33].

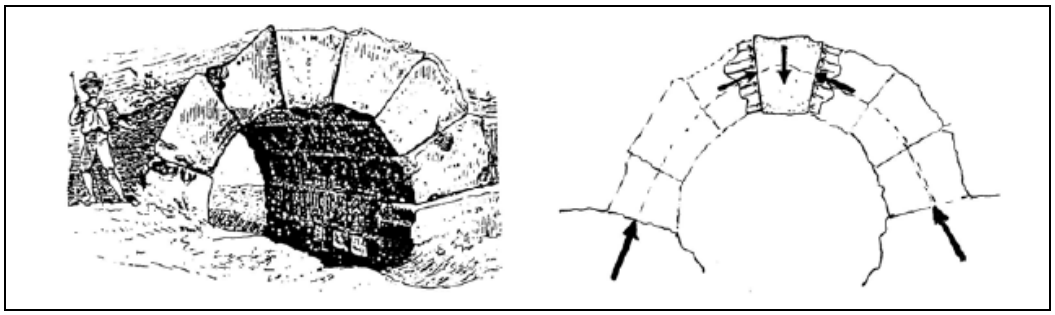

Figure 3.1. Thrust of massive voussoir arch [33]

Of course, to respect the main property of the masonry material, the line of thrust must be contained within the masonry arch. We may imagine one voussoir acting against the other two voussoirs only through the centers of thrust. If we now invert the arch, what was a force of compression will be a tension force: the voussoirs are hanging like a chain, as it appears in Figure 3.2 of Robison (1851).

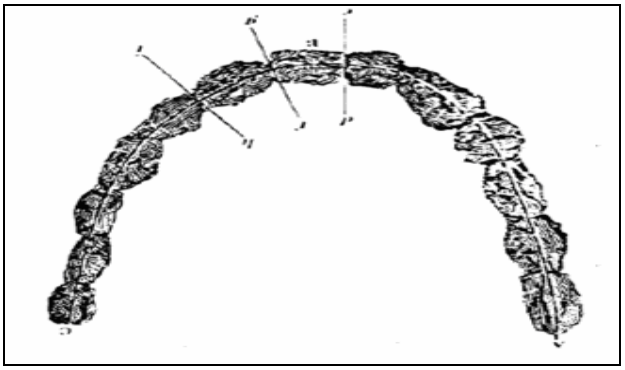

Figure 3.2. 'Hanging' masonry arch (Robison, 1851) [33]

This was Hooke's brilliant idea around 1670, when he was trying to solve the problem of the figure and thrust of the arches (Figure 3.3):

"As hangs the flexible line, so but inverted will stand the rigid arc"

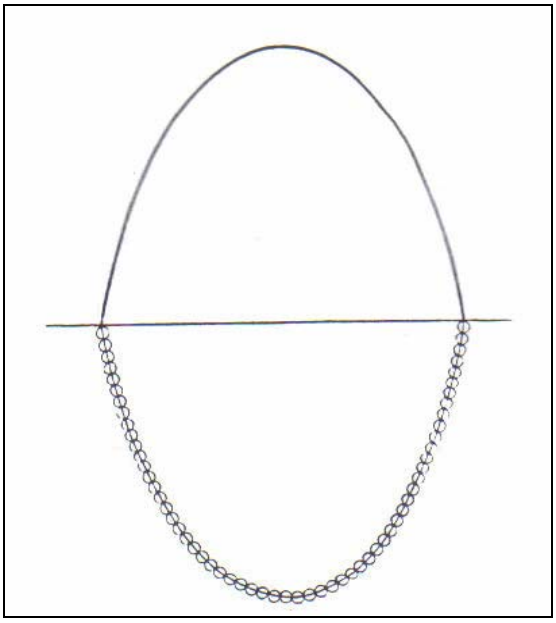

Figure 3.3. Hooke's Hanging Chain [1]

If the arch has all the voussoirs of the same size the line of thrust has very nearly the form of an inverted catenary. Some twenty years later Gregory (1697) completed Hooke's affirmation:

"none but the catenaria is the figure of a true or legitimate arch or fornix"

In Figure 3.3 the arch is in equilibrium with an internal stress distribution represented by the inverted catenary [1, 3, 33].

The geometry of this thrust line, that is, the actual shape of the ideal arch to carry the specified loads, will depend on the length of the equivalent chain and the distance apart of the supports. Thus a possible inverted chain is shown in Figure 3.3 lying within the boundaries of the semicircular arch; this represents one of the infinite numbers of ways in which the arch can carry its own weight. For masonry, thrusts must lie within the

boundaries of the construction which can be clearly understood from this spectacular picture.

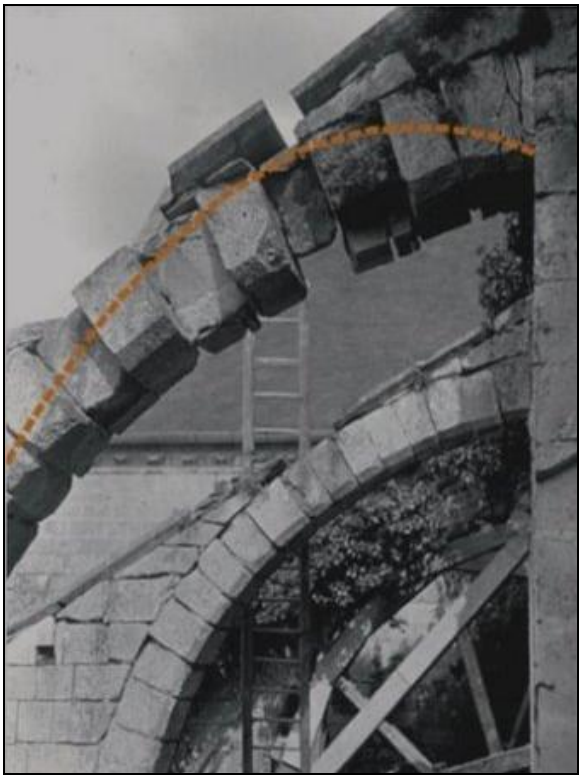

Figure 3.4. Possible location of line of thrust [34]

3.1.1. Actual Location of the Line of Thrust

Any line of thrust within the arch is a possible equilibrium solution. But this solution is not unique. It is evident that, in an arch of sufficient thickness, there are infinite possible inverted catenaries or lines of thrust. The arch is a statically indeterminate (hyperstatic) structure. The equations of equilibrium are not sufficient to obtain the inner forces [3, 33].

Though arch theory was well developed by the end of the VIIIth century (Heyman 1972), the question was posed for the first time by Moseley. And he tried to determine the position of the line of thrust. To do this he needs to make more affirmations, besides these of equilibrium. In the pre-history of elastic analysis he expressed *a new Theorem in Statics* with the purpose of obtaining the reactions of rigid hyperstatic structures: the Principle of

Least Pressure (formulation in Moseley 1833); application to arches in Moseley (1843). Applying this principle to arches he concluded that the actual thrust must be the minimum. Another approach was to design the arch with the profile of the line of thrust and, then, it was supposed it would coincide with the middle-line of the arch, Villarceau (1853). Other possibility was the physical insertions of hinges, which make the arch statically determinate, i.e., determine the position of the line of thrust [33].

Assume three hinges suggested by the analyst one of which is point A as shown in Figure 3.5. Since the arch is a statically determinate structure now, the reactions of the arch can be solved by statics. Hence, the reaction F_1 and the location of A (first point of thrust line) are known. Remaining points of the line of thrust, say the arch is to be divided into finite segments, are found by easily taking moments about unknown locations, B, C, D, E and F, of the imaginary thrust line. The line of thrust of the arch is originated by combining these points as shown below. This line of thrust will not be symmetrically placed within the arch. Some points in the thrust line will get very close to either extrados or intrados of the ring, whereas at other points, the thrust line will be seen in the kern of the ring.

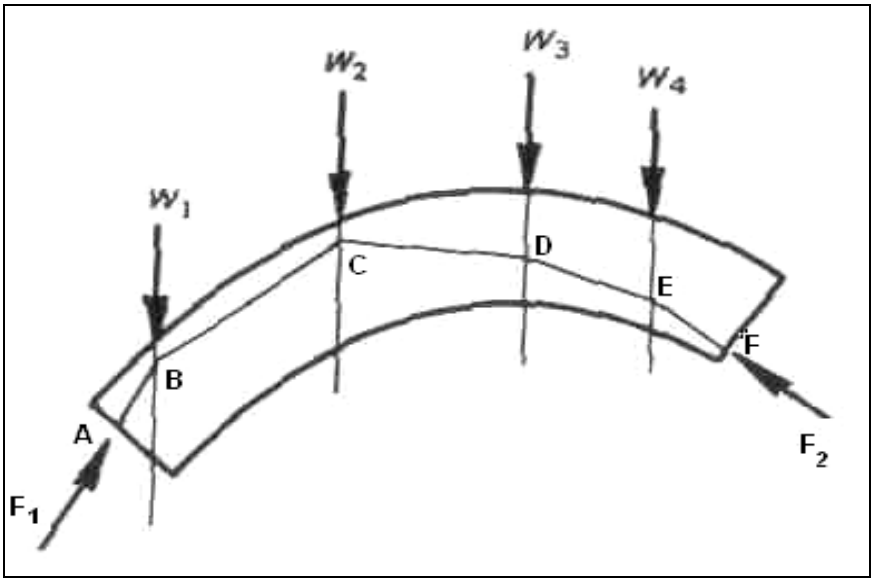

Figure 3.5. Construction of the thrust line

3.2. Middle Third Rule

Line of thrust, which is the action of the normal thrust of the arch, represents the resultants of the distributed loads on section through section. As indicated before, thrust line may be located at the middle of the section or very close to the edge of the section. If the stress distribution is assumed to be linear, then the response of this section changes dramatically according to the position of the normal thrust. In order that this last statement makes sense, a sketch will be used as shown below.

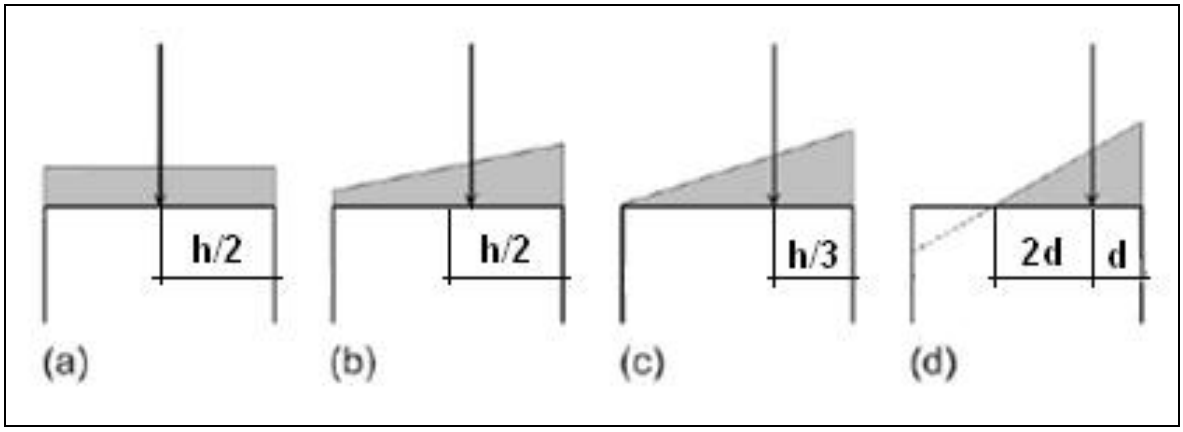

Figure 3.6. Response of the section caused by different load positions [34]

The section with a height of h is subjected to four different load schemes as it is seen in Figure 3.6. Four different responses of this section can be explained as follows:

a) When the normal force is located at $h/2$, σ_{max} and σ_{min} are equal and the whole section is in compression..

b) When the normal force is located at between $h/2$ and $h/3$, σ_{max} and σ_{min} are not equal but the whole section is again in compression.

c) When the normal force is located at $h/3$, σ_{min} comes out to be zero, the whole section is in compression.

d) When the normal force is located at a distance d, where $h/3 > d > 0$, the section undergoes tensile stresses. However, the part with a height of $3 \times d$ is again in compression.

In Figure 3.6, when the load has been moved to $h/3$, using simple elastic theory, the stress at one edge becomes zero; i.e., the section undergoes no tensile stresses. Going outside the middle third causes tensile stresses within the section. Assuming masonry has no tensile strength, the section of Figure 3.6.d is not contributing entirely. There may be some cracks where the thrust line lies out of this core, however there is no possibility to collapse as a consequence of these cracks. Therefore, the *middle third rule* is extremely safe approach in the determination of the collapse load.

3.3. Limit Analysis of Masonry Arch Bridges

If we can draw a line of thrust within the arch we know that this arch will have at least one possibility to stand. But, does this mean that the arch will stand? Will it not be possible to find, also, any way for the arch to collapse?

The solution of the problem came only in the XXth with the theory of *Limit Analysis* and the demonstration of the Fundamental Theorems by Gvozdev. There is no space here to explain the origins and development of Limit Analysis and the reader is directed to the books and articles of professor Heyman. In particular the *Safe Theorem* states that if it is possible to find an internal system of forces in equilibrium with the loads which does not violate certain material assumptions, the structures will not collapse; i.e., it is "safe". In the case of the masonry arch, any line of thrust compatible with the applied loads will satisfy the equilibrium conditions. As indicated, the main material requirement is the absence of any tensile forces. Therefore, if it is possible to draw a line of thrust (equilibrium) within the arch, this would be an absolute proof that the arch is stable and that collapse will never occur.

It is important point out two considerations. First of all, the thrust line of the safe theorem need not to be the actual thrust line: every thrust line in equilibrium with the external loads, lying within the arch profile, can be chosen to check the structure. Moreover, we do not know the actual stresses in the cross section. In fact, we did not make any assumption about the material constitutive relationship, but the fact that the thrust line

lies within the masonry ensures that there is only compressive action, which can be transmitted from one cross section to the next.

3.3.1. Basic Assumptions of Limit Analysis

The applicability of limit analysis to masonry structures modeled as assemblages of rigid blocks connected through joints depends on some basic assumptions. First of all, it is important to notice that friction between voussoirs is high enough to suppose that they cannot slide on one another, so that *sliding failure cannot occur*.

The assumption that stone has *no tensile strength* is almost exactly true in this kind of structures, made up of voussoir laid either dry or with very weak mortar: although stone itself may have some tensile strength, the joints will not, therefore no tensile forces can be transmitted from one voussoir to another.

As we can see from the analysis of existing bridges, stresses are low enough not to allow crushing of the material. This observation is equivalent to the assumption that *stone has an infinite compressive strength*.

The yield surface of a rectangular cross section which is subjected to a normal force, N , and a bending moment, M ,(see Figure 3.7) is formed by two parabolic arcs by ;

$$M = \pm \frac{bh^2}{2} \sigma_0 \frac{N}{N_0} (1 - \frac{N}{N_0}) \qquad (3.1)$$

where;

σ_0 = compressive strength of the masonry at yield state

$N_0 = bh\sigma_0$

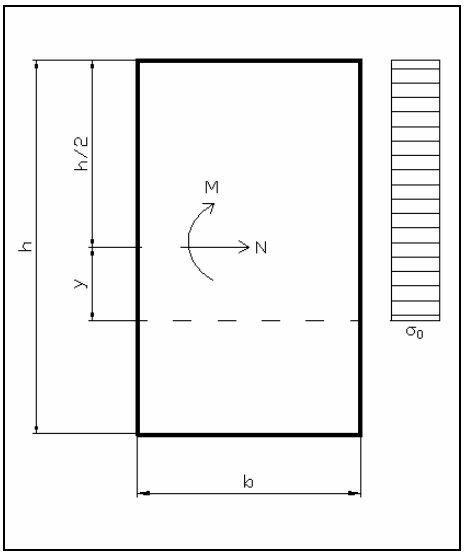

Figure 3.7. Forces on the masonry section

With the assumption that *stone has an infinite compressive strength* ($\sigma_0 \to \infty$), the two parabolic curves become two straight lines, tangential to parabolic ones at the origin;

$$M = \pm N(h/2) \qquad (3.2)$$

In order to clarify this assumption, the formula is put into practice with the below properties;

h = 0.711 m.

b = 1.0 m.

σ_0 = 5 MPa

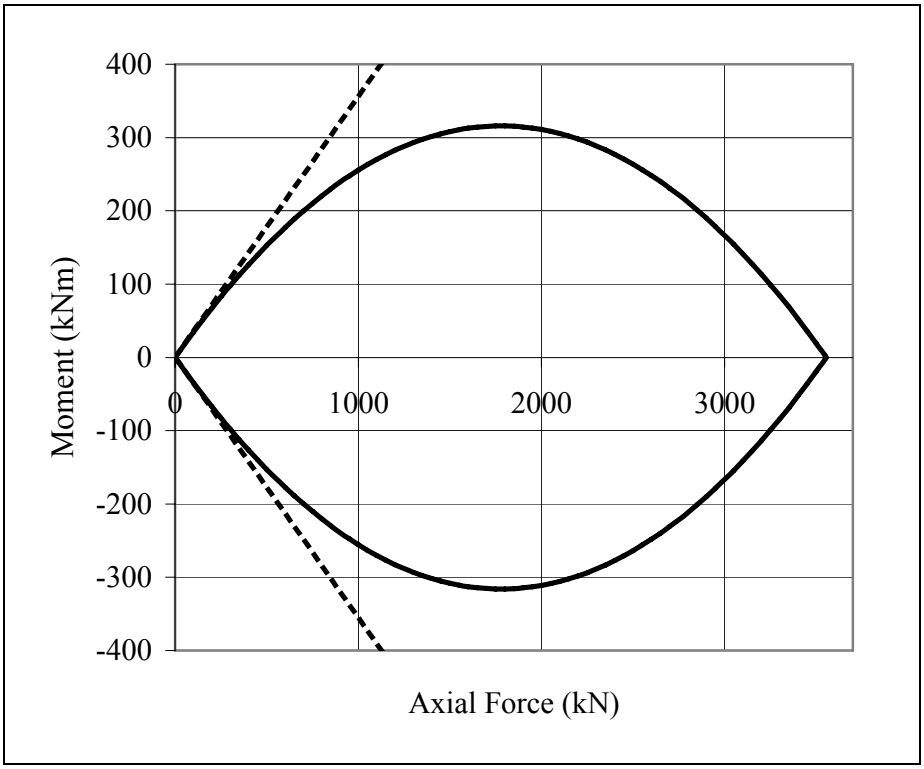

Figure 3.8. Yield surfaces for masonry

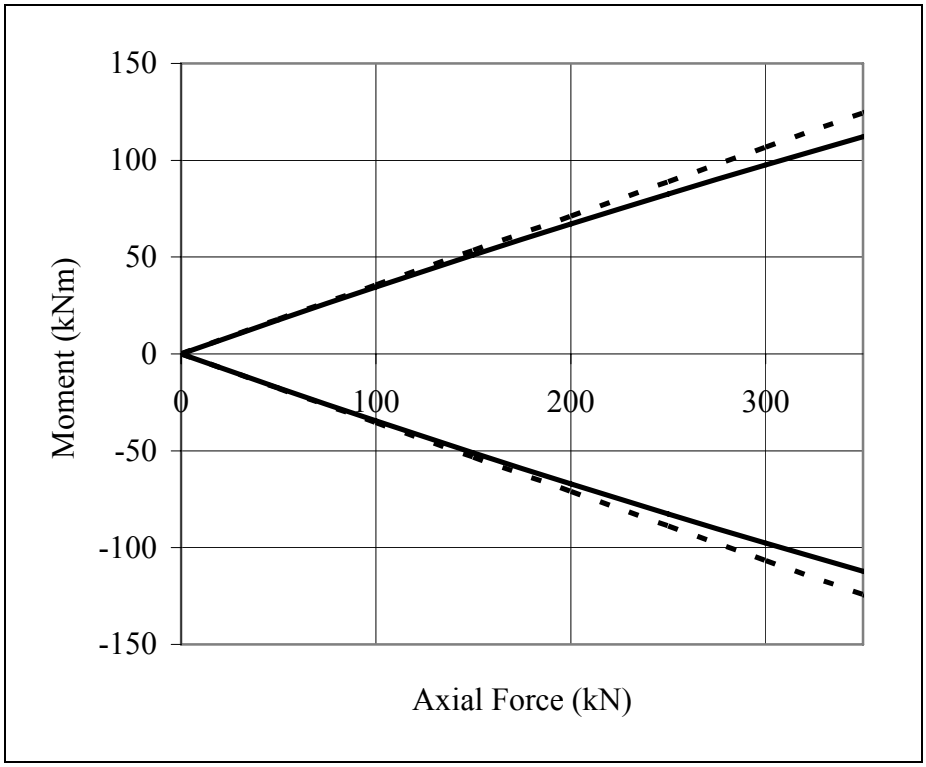

Figure 3.9. Yield surfaces for masonry at 10 per cent of axial load capacity

In Figure 3.8 and Figure 3.9, the smooth lines represent the actual yield surfaces of the given rectangular cross section, whereas the dashed line is for the yield surfaces of infinite compressive strength assumption. In the subject of the masonry structures, the mean compressive stresses are generally low, say 10 per cent of crushing strength. Therefore, the actual yield surface for this range is almost the same as the one that is formed by the assumption of stone having an infinite compressive strength as shown in Figure 3.9.

Each point of these lines represents a state of stress in which the axial force N lies in one of the masonry surfaces, its distance from the center point of the section being given by;

$$y = \frac{dM}{dN} = \pm\frac{h}{2} = \frac{M}{N} \qquad (3.3)$$

In this condition a hinge forms at a free edge as shown below.

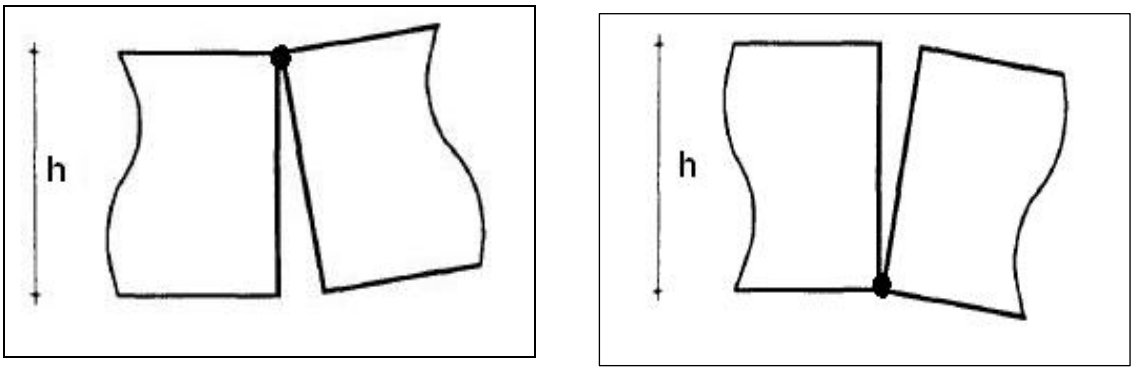

Figure 3.10. Hinge formation at free edges [32]

A general point (N, M) in Figure 3.9 which lies within the dashed open triangles represents thrust within the voussoirs at an eccentricity less than $(h/2)$. The line of thrust of Figure 3.5 lies indeed within the masonry at that point and no hinge is forming.

The hinge will form (see Figure 3.10) when the eccentricity, e, of the normal thrust has the value $h/2$, that is when $M = \pm N(h/2)$. The lines $M = \pm N(h/2)$ are shown as dashed lines in Figure 3.9 and they represent the condition that a hinge is existent.

Therefore if the line of thrust of Figure 3.5 touches either extrados or the intrados of the ring, a hinge is formed at this touching point.

In reality, the hinge will probably be formed at the weakest part of the ring; i.e. at the mortar. However in the case of limit analysis, the arch barrel is assumed to be monolithic and homogenous. Therefore, a hinge is formed anywhere at the point on the extrados or the intrados. More clearly; it is assumed that, the strength of the materials that constitute the arch, brick, stone or mortar, does not affect the likelihood of the formation of a hinge.

3.4. Failure Modes of Masonry Arch

In the literature, the masonry arch fails by a number of failure mechanisms which can be listed as; snap-through, shear, compression, longitudinal crack and mechanism. First four failure modes is out of the content of this thesis, therefore these failure modes are explained briefly.

- *Snap-through:* In snap-through, the hinges start to form but instead of the final gradual formation and rotation of the hinges, a rapid change of the local geometry occurs with the section of arch under the load snapping through. The arch barrel can be viewed as a shell having a large axial thrust and with the effective load-carrying area becoming increasingly small as hinges develop.

- *Shear:* There are few examples of the failure of masonry arches from shear. Known examples include the testing of an arch without fill using a simulated wheel load which resulted in punching shear failure of the arch ring. In a well-proportioned and well-maintained arch shear failure is difficult to see, although punching failure can occur where loss of mortar leaves individual blocks unsupported by axial thrust.

- *Compression:* Arch forms which are more likely to suffer compression failures are short stocky arches where the line of thrust tends to form more direct paths (within the voussoirs) to the abutments.

- *Longitudinal crack:* In reality, most loads are applied to part of the width of the arch. In many cases loads will pass in opposing directions on two lanes and the result is sometimes longitudinal crack through the arch. These cracks have rarely caused the failure of the arch, therefore the arch can be considered as an idealized 2-dimensional form.

- *Mechanism:* The failure of masonry arches comes mostly from mechanism type failure. The arch is exposed to its own weight and an additional point load P as shown in Figure 3.11.a. Referring back to the Hooke's hanging chain; the chain will be deformed from the catenary to the shape shown in Figure 3.11.b. As P is increased, the inverted chain (that is, the line of thrust) will fit less and less comfortably within the arch, and at a certain value of P, the thrust line can only just be contained. This limiting stage is shown in Figure 3.11.c, and it will be seen that the thrust line reaches the surface (either the extrados or the intrados) at four locations. At each of these locations a hinge will form, and four hinges transform the stable arch structure into a mechanism of collapse: the four-bar chain of Figure 3.11.d. It will be appreciated that, if the black dots in Figure 3.11.d represent frictionless hinges, then the configuration shown would correspond to a real mechanism.

In fact, collapse only occurs finally at the point when it is no longer possible to fit the thrust line within the boundaries of the arch. This is a geometrical constraint, not related to any initial state of the arch (its initial crack pattern), the final mode of collapse is represented by Figure 3.11.c [3].

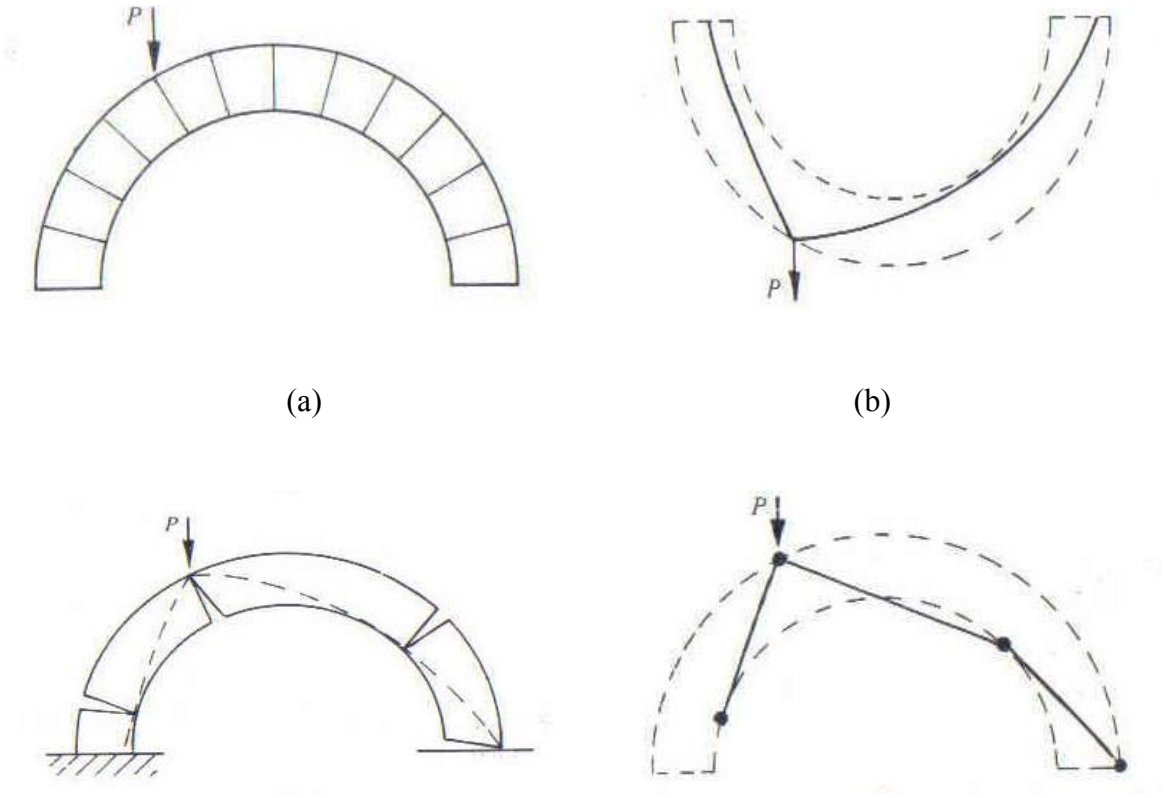

(a) (b)

(c) (d)

Figure 3.11. Collapse of arches under a point load [3]

In order to investigate the behavior of a real arch, Prestwood Bridge, a singe span bridge, is tested to collapse within the experimental research on masonry bridges supported by the British Transport Research Laboratory (TRL). The experimental collapse mechanism of the bridge is shown in Figure 3.12. The collapse mechanism exhibits four hinges that are clearly visible in the picture. Incidentally, the mechanism developed with negligible material crushing. The arch mechanism causes the fill region under the applied load (right hand side) to move downward and the fill at the other side of the bridge to move upward [35].

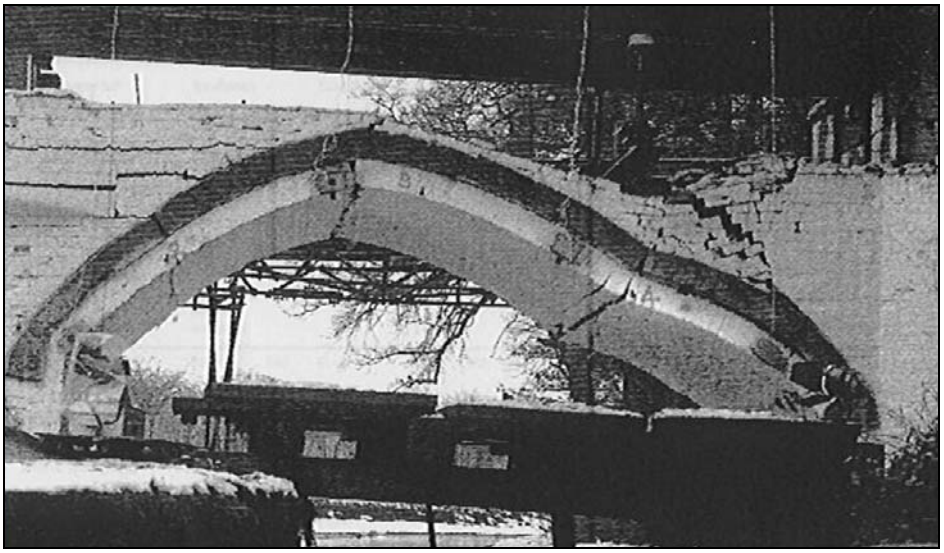

Figure 3.12. Collapse of Prestwood Bridge [35]

4. ARCH ASSESSMENT METHODS

Arches have been used for bridging for at least 4000 years. Once successfully erected, arch bridges usually carry the ever-increasing loads imposed without collapse or distress. Material degradation, intensified by abuse or neglect, may eventually lead to failure, but the deterioration is slow and can be arrested easily.

Masonry arches are rarely constructed now. The reasons given for this usually emphasize the assumed economic disadvantages, particularly where first cost is the main criterion. However, there will always be a need for strengthening the old bridges. In order to select an appropriate strengthening method, the first thing that the engineer should do is to calculate the critical load that causes collapse.

Attempts at calculating the strength of arches date back many centuries. Most important arch assessment methods can be given as MEXE, Pinned-elastic, Finite Element and Mechanism Methods.

4.1. MEXE Method

This arch capacity assessment method is a very popular one since it is extremely simple. During the early 1950s a military load classification was introduced by the Military Engineering Experimental Establishment (MEXE), England. MEXE is based on an unknown blend of classic elastic arch theory devised by Pippard coupled with the results of series of tests.

The basic assumption are that the arch is parabolic, pinned at both ends, soundly built, symmetrically loaded at the crown with a transverse load distribution, has a span/rise ratio of four and specified density. These assumptions allow a closed form solution for the stresses and by limiting the tensile and compressive strength of the masonry, a nomogram was developed. Unknown provisional axle load (PAL) is dependent only on the span and the depth of the arch ring plus the fill [36].

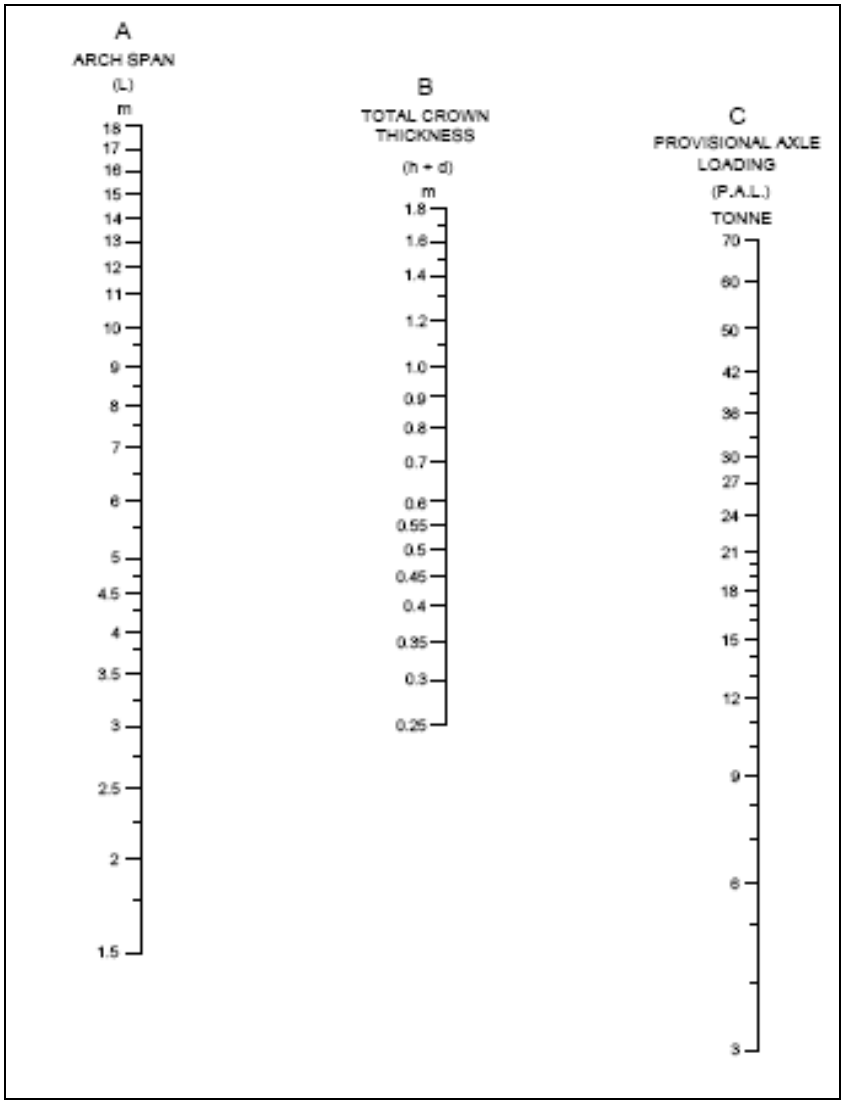

Figure 4.1. Nomogram for determining the provisional axle loading (PAL) of masonry arch bridges before factoring [36]

The PAL is then factored according to the geometry, materials and bridge condition. The factors in Table 4.1 are used to determine the modified axle load with the range of factors for which identified values are known. The modified axle load is subsequently multiplied by axle factors to give allowable single and multiple axle loads.

Table 4.1. Factors used to determine the modified axle load

Factor		Value
Span / rise factor	F_{sr}	0.6 – 1.0
Profile factor	F_p	0.0 – 1.0
Material factor	F_m	
e) Barrel factor		0.7 – 1.5
f) Fill factor		0.5 – 1.0
Joint factor	F_j	
a) Width factor		0.8 – 1.0
b) Mortar factor		0.8 – 0.9
c) Depth factor		0.9 – 1.0
Condition factor	F_c	0.3 – 1.0

Full scale models show that this method predicts the load carrying capacity far below the test results. Moreover, there are lots of factors that the engineer should decide. In this method, the failure mode is out of concern. Nevertheless, it is so quick and easy to apply. That is why this method is very widespread.

4.2. Pinned – Elastic Analysis

In this method, firstly Castigliano, secondly Pippard and then Hughes, assume that a small induced spread of the abutments makes the arch barrel (which is pinned to the abutments) form three hinges between certain voussoirs making it a statically determinate structure. However, the calculation assumes a two pinned centre line, parabolic arch with a concentrated load placed at the crown. Using virtual work it is possible to calculate expressions for the horizontal thrust at the abutments, the bending moment and the strain energy, which can be used to determine the maximum value of concentrated load required to produce failure [37].

The most critical limitations of this approach are the following. Commonly accepted arch theory dictates that an arch is not weakest under the action of a point load at the crown. Furthermore, the stone, mortar and fill material do not show elastic behavior as opposed to the assumption of this method. In addition, the tensile strength of the masonry is negligibly small and cracks can form under excessive loadings due to this lack. However, in this method since the material is assumed to be linear elastic, it does not

account for these cracks. All through the analysis, the section is considered to fully contribute to capacity, which is obviously not the case for a section with cracks.

4.3. Finite Element Method (FEM)

In this method loads are applied to the arch ring and the resulting member forces are determined. These are used to determine the stress states and deformations. The stresses are used to identify the areas of tension and the deformations are used to modify the geometry, which enables the modeling of snap-through behavior. The arch ring properties, area – stiffness – geometry, and loads are updated and reapplied with the process cycled to convergence. The incremental – iterative solution procedure has been applied by external programming into the Finite Element Analysis (FEA) commercial programs.

Towler [38] and Crisfield [39] appear to have been the first researchers to experiment with FEA in this area. Both went on to simulate the effect of fill using horizontal springs to model passive pressure from the soil. In these works and later research [40] macroscopic modeling is used where voussoirs are not modeled individually but a single constitutive formulation is used to model masonry called “smeared crack technique” or macro-modeling. While these pieces of research and others use FEA, they have not transferred widely to industry perhaps because they were developed outside the confines of commercial FEA packages.

More recently, however, Ng et al. [41] describes analysis of masonry arch bridges using general-purpose FEA software (LUSAS) and reports close agreement between predictions from FEA and the results of the full-scale tests carried out under the TRL program.

A FE approach allows the compressive response of masonry to be introduced into one-dimensional, two-dimensional or three-dimensional models. They may give detailed information on local phenomena, such as stress concentrations in some structural element or in some part of it, but the mechanical parameters affecting the overall response can be

identified only if simple models are formulated; one-dimensional models (e.g. [42]) are the only ones that have been reported to be efficient for multi-span bridge analysis.

Collapse mechanisms and crack genesis with large displacements are not easy to simulate using finite element analysis. Setting up a model with correct parameters, interpreting the results and checking if the initial assumptions were valid, requires the very meticulous and conscientious work of a specialist in non-linear finite element methods. To achieve more realistic and accurate results with finite elements, a great level of detail for the model is necessary, but most of the parameters are highly uncertain. For example, the material properties; density, compressive strength, tensile strength, angle of shear resistance, Young's modulus, Shear modulus, load dispersal angle and so on; of the ancient stone, mortar and also back fill material are very inhomogeneous and do not have constant and predictable mechanical properties. Moreover, the interaction of blocks in the ring is another uncertain phenomenon. If the bridge is a multi-span one, the effect of the arch action nearby (say arch # 2) on the investigated arch (say arch # 1) is hard to explain and put into the mathematical model. Another uncertainty can be the arch – fill interaction together with the stone - mortar interaction. All these parameters that affect the strength of the arch are always very problematic to determine. Therefore, assessment of the bridge with this method, FEM, cannot be realized at reasonable costs.

The chosen FE analysis can model the load-deflection behavior extremely well in cases where the material properties are well known. Unfortunately, this is often only the case for bridges where, for research purposes, tests to collapse have been undertaken, with associated material testing [41].

4.4. Mechanism Method

Another way of calculating the collapse load of any masonry arch bridge is originated from plastic analysis which has been examined by Heyman. The theory of engineering plasticity incorporates two theorems: a lower bound (safe theorem) and an upper bound (unsafe theorem). The lower bound theorem states that if, for a given load, a statically admissible distribution of internal forces can be found such that the entire arch satisfies the yield condition, then this load is said to be a lower bound on the collapse load.

According to the upper bound theorem, a load for which the virtual work of the loads is equal to the virtual work of the internal forces as the structure works through a kinematically admissible mechanism forms an upper bound on the collapse load. A uniqueness theorem shows that if both conditions are satisfied by a given load, then this must be the collapse load.

4.4.1. Assessment of the Arch Capacity by Mechanism Method

The 'line of thrust' of an arch may be described as the line at which a flexible member of infinite strength would be in equilibrium with the load system imposed. In fact, most arches can contain an infinite number of such thrust lines in equilibrium with any one set of loads. Only when the arch is on the point of collapse is the line of thrust defined explicitly, because at that stage the line just fits within the arch. If the arch material is strong and stiff, which is the case for most of the time, the line of thrust may approach close to the intrados or extrados without causing crushing. In this case the position of the line of thrust is defined at these points. There are usually four such points, and they form the hinge locations in the collapse mechanism, *A* to *D* in Figure 4.2.

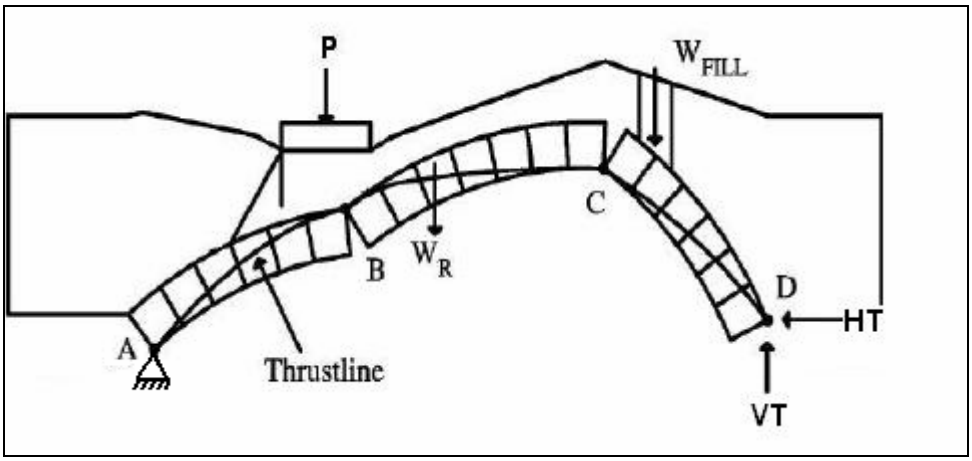

Figure 4.2. Failure mechanism of a masonry arch [43]

Until the solution is found, the location of the hinges is not known. We may say only that *A* and *C* lie on the intrados and *B* and *D* on the extrados. There are three further unknowns in this case *HT* (horizontal abutment thrust), *VT* (horizontal abutment thrust) and the failure load *P*. If we guess the position of the hinges and equate the moments to the

right of each to zero, we are left with three equations in three unknowns which can be evaluated explicitly. Once these are solved the implied line of thrust may be drawn. If it passes outside the arch at any point, the wrong hinge positions have been chosen and a new attempt must be made.

Thus, a 'mechanism' (or '*upper bound*') limit analysis involves an assumed hinge configuration with the lowest upper bound solution being the correct one since in this case the thrust line between the hinges will lie entirely within the arch. Therefore, in this case the 'safe' (or '*lower bound*') theorem is also satisfied (the latter states that if a thrust line can be found for the complete arch which is in equilibrium with the external self weight and which lies every where within the masonry of the arch ring, then the arch is 'safe').

If the hinge positions are chosen with complete freedom on the extrados and intrados calculating the moments may be difficult. If the arch is divided into segments, the choice of hinge positions may be limited to the nodes between these segments, and calculations can be applied more successfully. This method is admirably set out by Heyman [3].

Although mechanism method has a powerful way of predicting the strength of arches, it has several restrictions that can be important as follows:

- Displacements cannot be calculated as the solution is derived from force equilibrium calculations alone. Therefore, second order effects are not taken into consideration.
- The arch ring is assumed to be monolithic and, therefore, the behavior of multi-ring arches cannot be represented if shearing between rings occurs or rings are separated.
- Failure is based on four hinges developing. Other types of failure cannot be identified.

4.5. Difficulties in Computations on Masonry Arch Bridges

As it is seen, there are many arch assessment methods. In every analysis type, there are obviously some vague points. Therefore, the analysis of historic masonry arch bridges

is a complex task. First, limited resources have been allocated to the study of the mechanical behavior of masonry, which includes non-destructive in situ testing and adequate laboratory testing. Second, and most important, the difficulties in using the existing knowledge are inherent to the analysis of historic structures. Usually, salient aspects are;

- Information about the inner core of the structural elements is missing.
- Characterization of the mechanical properties of the materials used is difficult and expensive.
- There is a large variability in mechanical properties.
- Significant changes have occurred in the core and constitution of structural elements, associated with long construction periods.
- Existing damage in the structure is unknown.
- Regulations and codes are not applicable.

In some bridges, the apparent ring thickness is not the correct one, but it is a bit smaller that the actual (Figure 4.3). Actual thickness which takes part in the fill is somehow different than what we see from the face. In these bridges, actual collapse load is greater than the calculated one. Therefore, the analyst is on the safe side.

Characterization and variability of the mechanical properties for the fill and the ring are the complicated points for finite element models. 3-D analysis makes the model more sophisticated; therefore analyst should avoid making 3-D models. In other methods, these effects are limited.

Existing damage is another problematic issue. For MEXE, there are some factors in order to take these effects into the calculation. For finite element analysis, modeling these damages, such as cracks, is a very hard task.

Figure 4.3. Changing in the thickness of voussoir [44]

Regulations and code are indeed insufficient not only in Turkey but all over the world. MEXE is the only codified masonry arch assessment method which is indeed an unsatisfactory method of analysis. , there is no consistent description for defects in the codes.

5. COLLAPSE ANALYSIS OF MASONRY ARCH BRIDGES BY MECHANISM METHOD

The plastic analysis for masonry structures is relied on either lower bound or upper bound theory as explained in Chapter 4. In the context of masonry gravity structures; masonry piers, masonry dams or masonry arches, there are fundamentally three main considerations. Firstly, the structure should satisfy the basic *equilibrium considerations*. Secondly, the *yield conditions* for masonry structures should be fulfilled. Finally, the structure should confirm the *mechanism condition*.

The thrust line, explained in Chapter 3, can be easily drawn for statically determinate structures such as masonry piers (Figure 5.1). Statics alone is enough to determine the location of the line of thrust which is the *equilibrium part* of the three main considerations that the masonry structure should satisfy. Unlike masonry piers, masonry arches are indeed statically indeterminate structures. There are many positions for the thrust line prior to failure. Its position may uniquely be determined if the masonry arch is on the point of collapse as indicated earlier in Figure 4.1.

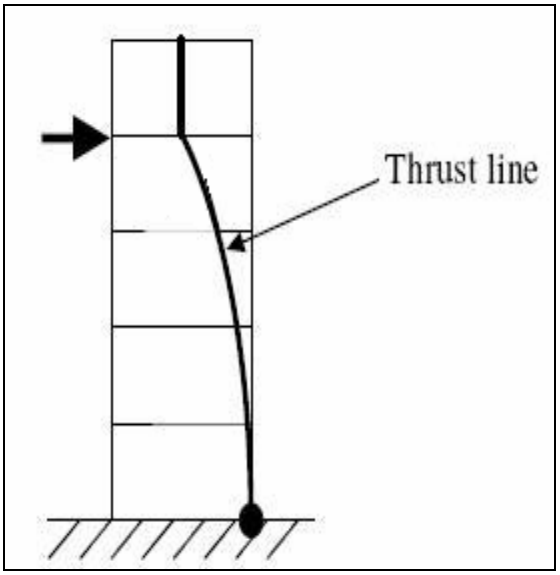

Figure 5.1. Thrust line for masonry pier [45]

The second consideration, *yield condition*, states that the line of thrust both lies entirely within the masonry.

The *mechanism consideration* states that the line of thrust, which should remain in the ring for the masonry arch, touches either the extrados or the intrados of the masonry blocks.

For the *lower bound theorem* of the plastic analysis, the applied load will be the lower bound on the true plastic collapse load if the thrust line satisfies the equilibrium and yield conditions. Whereas, the *upper bound theorem* of plastic analysis states that; if a line of thrust satisfies the equilibrium and mechanism conditions, then the applied load will be an upper bound on the true plastic collapse load.

Using the mechanism method with an upper bound theory, an algorithm and corresponding computer program is designed to predict the ultimate load carrying capacities of single span masonry arch bridges. The program has been written in MATLAB 6.5., a computer software developed by *The Mathhworks Inc.* for numeric computations.

5.1. Program Algorithm

General steps for calculating the ultimate load carrying capacities of a single span masonry arch by the mechanism method are introduced in Chapter 4.4. Explicitly, the algorithm performs the Mechanism Method in the following three main stages; choosing possible hinge locations, calculating the collapse load by equilibrium equations and controlling the mechanism considerations.

5.1.1. Choosing Possible Hinge Locations

As explained before, the basic assumption of the Mechanism Method is the formation of the four hinges. The locations of these hinges are not known with the exception that two of them lie on the extrados and remaining two on the intrados as seen in Figure 5.2. In the algorithm, the first hinge, Hinge *A*, is located at any segment on the

intrados between the abutment and the segment placed at quarter span starting from the first point on the intrados. The second hinge, Hinge *B*, is located on the extrados between Hinge *A* and, third hinge, Hinge *C*. Similarly, Hinge *C* is located on the intrados between Hinge *B* and the final hinge. Hinge *D* is located at any segment on the extrados between $3L/4$ and the other abutment.

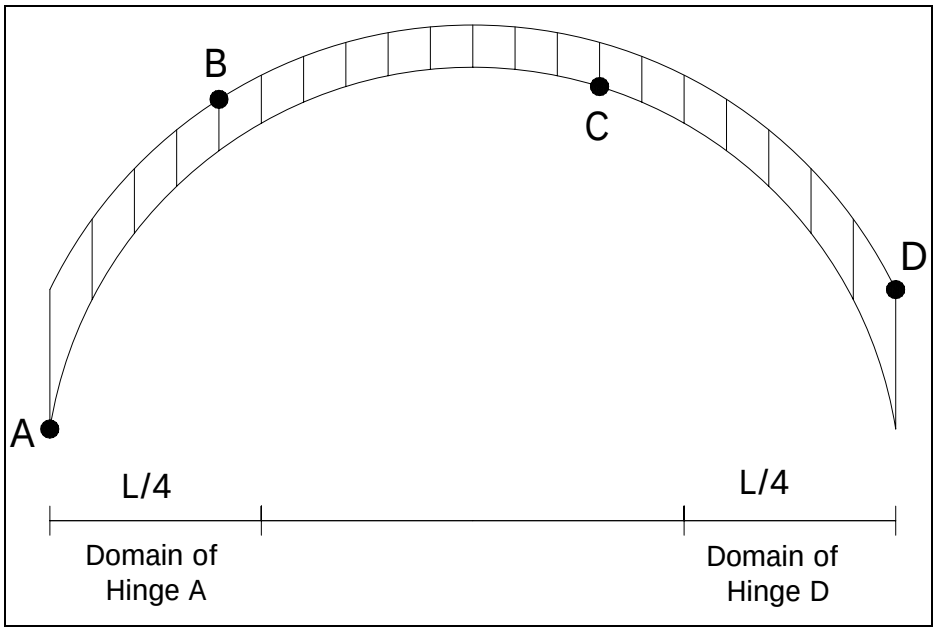

Figure 5.2. Hinge location for the masonry arch

The arch shown Figure 5.2 is to be formed by (n) segments and there are $(n+1)$ distinct points for originating the intrados and extrados of the arch. The program firstly locates Hinge *A* to the first point of intrados. Hinge *B* is then set to the second point of the extrados whereas Hinge *C* to the third point of the intrados. The final hinge, Hinge *D*, then moves the points in the extrados one by one in its domain; that is, between the points corresponding to $3L/4$ and the left abutment (the $(n+1)^{th}$ point in the extrados). As a result; the first cycle has been completed.

After the conclusion of the first cycle, the position of Hinge *C* is changed to the nearest point as the fourth point in the intrados. Hinge *D* now takes another tour in its domain. Subsequently, Hinge *C* goes to the fifth point in the intrados and Hinge *D* makes one more cycle. In this way, by keeping the Hinges *A* and *B* fixed, the Hinges *C* and *D* can be located at all possible points by these tours.

Now, it is Hinge *B*'s turn; the position of Hinge *B* is modified to the next point, say the third point, in the extrados. Similarly, Hinges *C* and *D* make their original tours while Hinge *B* travels point by point, where the position of Hinge *A* is still the same.

As Hinge *A* is located at the first point of the intrados, the whole tours explained before are the possible hinge locations which are then used in the calculation of the collapse load. Since the domain for the first hinge is limited between the first point of the extrados and the point corresponding to $L/4$, there are extra positions that the hinges can be located. Therefore, Hinge *A*, secondly, moves to the second point, and then to the third point and so on as Hinges *B*, *C* and *D* visit the possible locations indicated before. The point that coincides to $L/4$ is the final point that Hinge *A* passes through. For the arch with $(n+1)$ points, possible locations of the hinges end with;

- Hinge A: The point coincides to $L/4$
- Hinge B: $(n-1)^{\text{th}}$ point in the extrados
- Hinge C: $(n)^{\text{th}}$ point in the intrados
- Hinge D: $(n+1)^{\text{th}}$ (last) point in the extrados.

5.1.2. Calculating the Collapse Load

The hinge locations are therefore found in a systematic fashion. For any set of hinge locations, the collapse load P is applied $n/2$ times starting from the second segment up to the crown. Since the arches are mostly symmetric, there is no need to take any load positions beyond crown. Thus, critical load position with corresponding hinge locations can be found without any assumption. Coming back to Chapter 4.4., there are three unknowns in the Mechanism Method:

- Vertical abutment thrust (VT) which is actually located at Hinge *D*
- Horizontal abutment thrusts (HT) which is also located at Hinge *D*
- The collapse load, P

For any set of hinge locations and collapse load P, one should find three equations in order to solve the unknowns. These three equations can be attained by taking moments about the hinge locations, *A*, *B* and *C*. In the calculation of the moments, the program uses some parameters which are shown in Table 5.1 with appropriate units, variable names and forms.

Table 5.1. Parameters used in the program

Parameters	**Variable Name**	**Variable Form**	**Appropriate Unit**
Geometry of the Intrados	coordint	$\left[(X's)\ (Y's)\right]_{(n+1)x2}$	m
Geometry of the Extrados	coordext	$\left[(X's)\ (Y's)\right]_{(n+1)x2}$	m
Specific Weight of Fill	gfill	scalar	$\frac{kN}{m^3}$
Specific Weight of Ring	gring	scalar	$\frac{kN}{m^3}$
The Thickness of Fill at the Crown	H	scalar	m

First of all, the program calculates the area of the fill and the ring for each segment approximating each segment as a trapezoid. Taking the width of the arch as unity, weight of the fill and weight of the ring can be found easily by multiplication of areas with related specific weights. Calculated weights are applied to the model at the midpoints of each segment as shown in Figure 5.3

For any arrangement of hinge locations, the program should calculate necessary moment arms. As an example, (see Figure 5.4), in order to take moment about Hinge C, X_{C-D} as the moment arm for VT, Y_{C-D} as the moment arm for HT, r_i as the moment arms for W_i and l_i as the moment arm for the fraction of the collapse load, P_i, are calculated. Subsequently, first equation can be written as;

$$VT \times X_{C-D} - HT \times Y_{C-D} - W^{C-D}{}_i \times r^{C-D}{}_i - P^{C-D}{}_i \times l_i^{C-D} = 0 \qquad (5.1)$$

In Equation 5.1 superscript term $C-D$ used in W_i , r_i , P_i and l_i signifies that these factors are taken just in the region between Hinge *C* and Hinge *D*. P_i, on the other hand, indicates the fraction of the collapse load found by the Boussinesq (1885) Equation.

Other two equations can also be written in a similar fashion by taking moments about Hinges A and B. Three equations can now be used to find unknowns P , HT and VT .

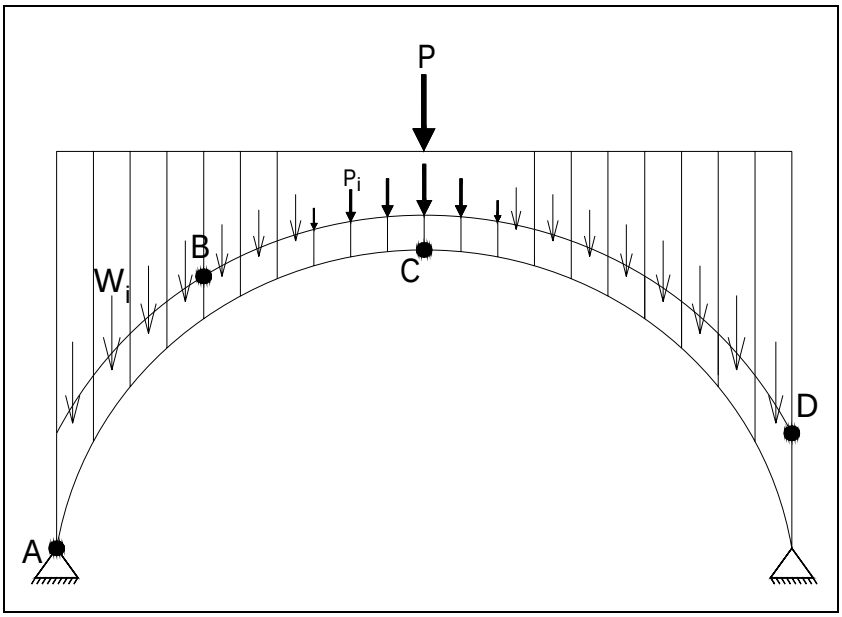

Figure 5.3. Model of masonry arch bridge

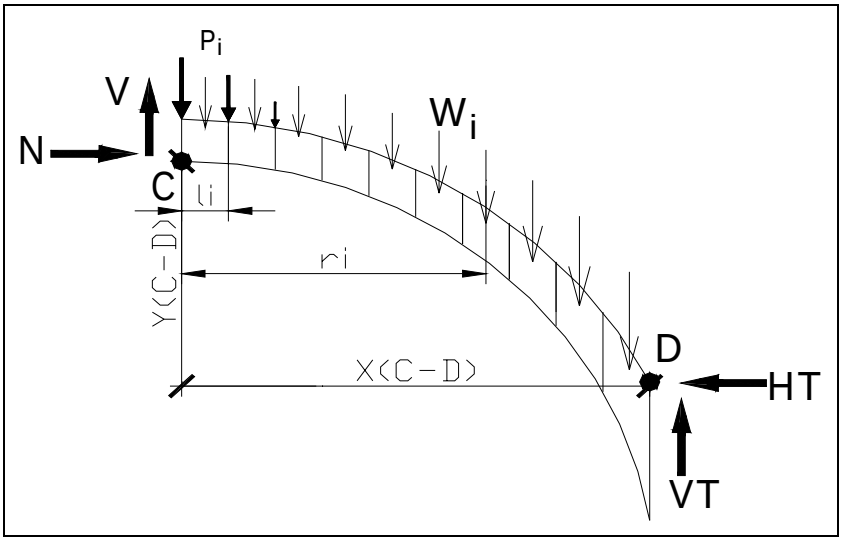

Figure 5.4. Free body diagram of the arch that is cut from Hinge C

5.1.3. Controlling the Mechanism Considerations

In order to find the collapse load, the algorithm begins with firstly choosing the hinge locations and continues with calculating the unknowns. However, the potential risk here is that the results may offer incorrect solutions. In order to avoid such situations, the algorithm eliminates wrong sets of hinge locations and correspondingly wrong collapse loads.

As explained before, *mechanism consideration* states that the line of thrust, which should remain in the ring for the masonry arch, touches either extrados or intrados of the masonry blocks. For that reason, the program draws the thrust line for each set of hinge locations. The construction of thrust line is described in Chapter 3.2.1. Therefore, there is no need to explain again here. After drawing it, the program checks whether the thrust line lies within the domain or not.

In order to make this point more clear, let us assume an illogical set of hinge locations as seen in Figure 5.5:

- Hinge *A*: 1st point in the intrados
- Hinge *B*: 2nd point in the extrados
- Hinge *C*: 3rd point in the intrados
- Hinge *D*: $(n+1)^{th}$ (last) point in the extrados

One can easily observe that given hinge location is a wrong one. But the algorithm firstly calculates the collapse load for this set of hinge locations and then draws the thrust line and finally checks the orientation of the thrust line and discards if it does not lie within the masonry block.

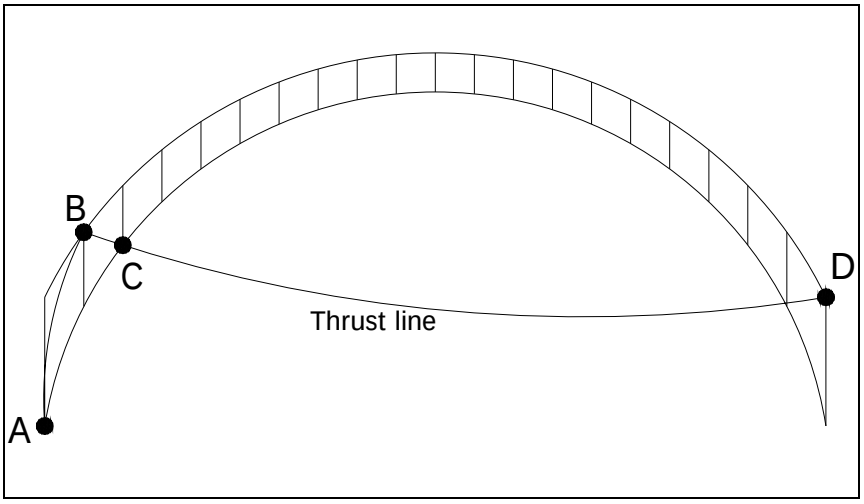

Figure 5.5. Wrong set of hinge locations

By performing these three main stages, the program finds the maximum loads corresponding to different load positions that the masonry arch bridge can carry for any individual set of hinge locations. Generally, in the program, the worst load position is found to be between $L/3$ and $L/4$ as stated many times by a number of authors. As an illustration, consider a bridge with a point live load P, at some general position. The whole analysis is carried out and a figure (Figure 5.6) of 'Limit Load vs. Loading Position' is drawn in the program. From this sketch, the worst position of the concentrated live load P is not the central one, but is located about $1/3$ of the span. Hence, for developing assessment analysis, FEM or Mechanism Method, the live load should be affected at $1/3-1/4$ of the span which is the worst position for the masonry arch bridges.

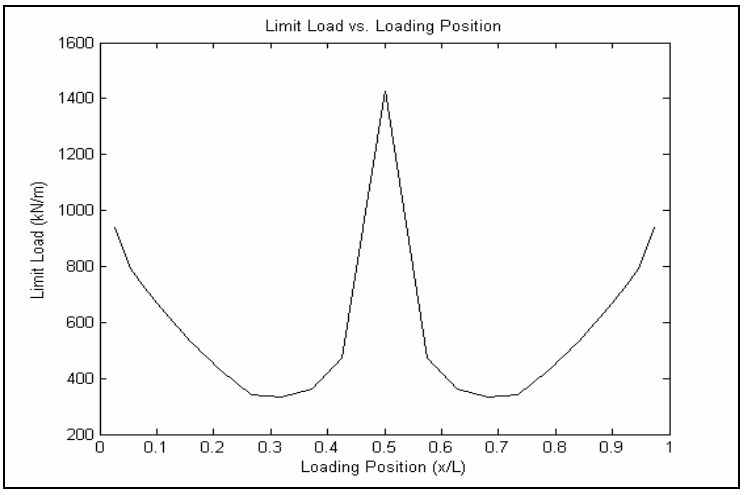

Figure 5.6. Limit load vs. loading position

5.2. Dispersion of Load

The user can run the program by two different load dispersion types, namely line load or strip load (see Figure 5.7 and Figure 5.8). In the program, in order to specify the width that the load is to be distributed over, an indicator, w, is utilized with an appropriate unit as m.

If a line load is to be considered in the program, w should be taken as zero.

Live loads shown in Figure 5.7 and Figure 5.8 should be distributed logically over the ring in order to get more accurate results. Assuming back fill as a semi-infinite, homogeneous, isotropic mass, with a linear stress-strain relationship, the stresses over the ring can be determined by Boussinesq Equations.

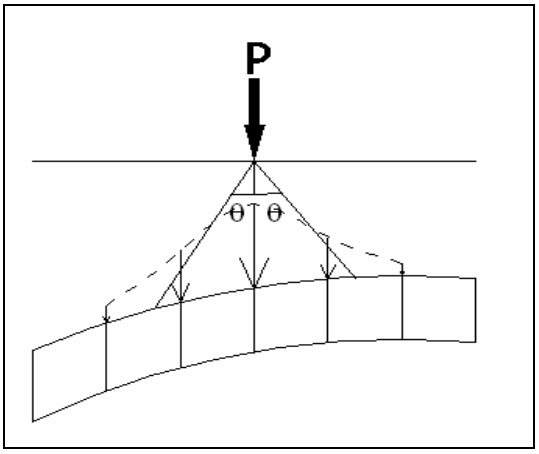

Figure 5.7. Dispersion of line load

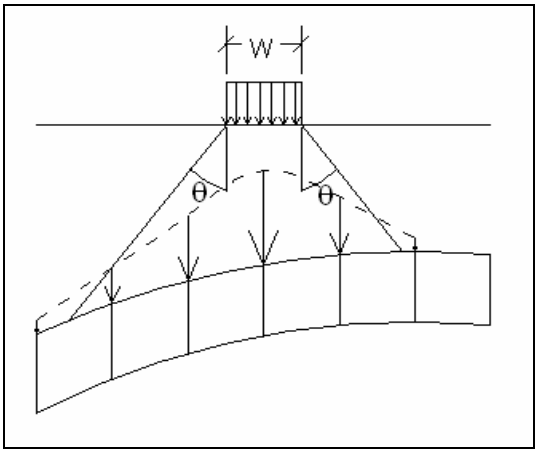

Figure 5.8. Dispersion of uniform pressure

The dispersion angle, θ, is the limiting angle that the load can diffuse. In the program, the corresponding variable name is *disperselangle* and its appropriate unit is *degree*. The dispersion angle may change from 0^0 to 45^0. However, experimental studies show that, choosing the limiting distribution angle as 30^0 is reasonable.

5.2.1. Dispersion of Line Load

The magnitude of the pressure on the back of the arch originated from a point line load P (see Figure 5.7 and Figure 5.9) can be obtained by a formula determined by Boussinesq:

$$\sigma_z = \frac{2P}{\pi} \times \frac{z^3}{\left(x^2 + z^2\right)^2} \qquad (5.2)$$

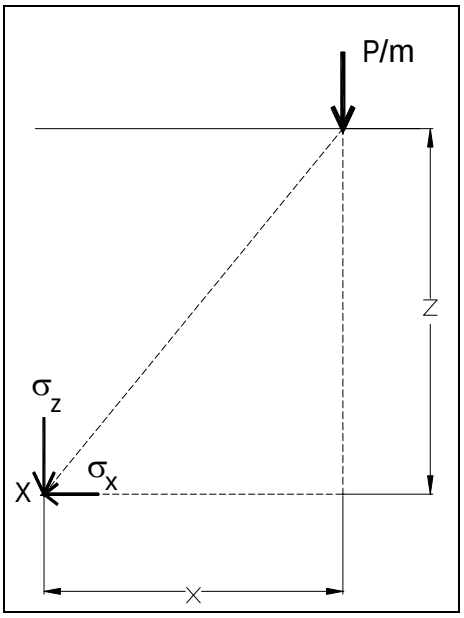

Figure 5.9. Stress distribution due to line load

The Boussinesq equation gives the magnitude of pressure using a known line load of P. However, in the calculation of collapse load, the magnitude of P is an unknown. When a limiting dispersion angle is specified, the magnitudes of the pressures calculated using the Boussinesq equation are scaled up so that that the integral of the vertical

pressures acting on a length of arch equals the magnitude of the applied force. Therefore, the fraction instead of the magnitude of pressure is found and this fraction is used in the rest of the program. The effects of σ_x and σ_{xz} are not taken into consideration.

5.2.2. Dispersion of Strip Load

Similarly the fraction of stresses at point X due to a uniform pressure on a strip area of width w and infinite length are given in terms of the angles α and β defined in Figure 5.10 and can be found by the formula below;

$$\sigma_z = \frac{Q}{\pi} \times \{\alpha + \sin\alpha \times \cos(\alpha + 2\beta)\} \qquad (5.3)$$

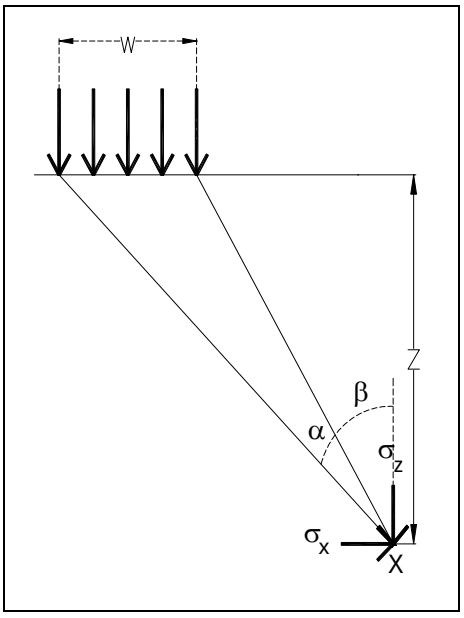

Figure 5.10. Stress distribution due to uniform pressure

In the Boussinesq Equations, the fractions, say σ_i and σ_j, are found in terms of stresses whether line load or strip load is to be used. In order to denote these fractions of stresses as nodal fraction of forces, they should be converted into the equivalent forces by:

$$F_i = \frac{\sigma_i \times l}{2} + \frac{\left(\sigma_j - \sigma_i\right) \times l}{6} \qquad (5.4)$$

$$F_j = \frac{\sigma_i \times l}{2} + \frac{\left(\sigma_j - \sigma_i\right) \times l}{3} \qquad (5.5)$$

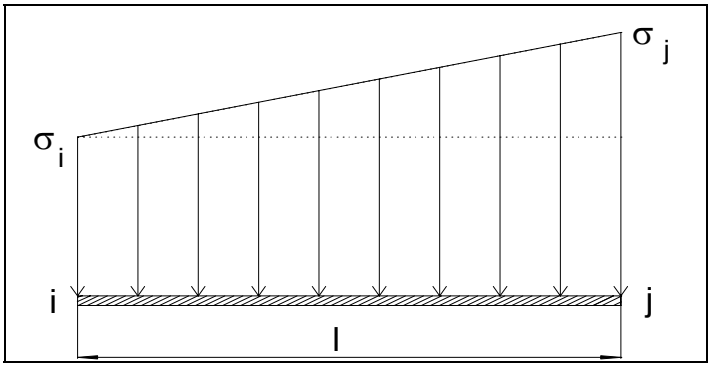

Figure 5.11. Pressure exerted at the back of the arch

5.3. Performing an Analysis

In order to show how the program can be run, an analysis is performed in details. A hypothetical elliptic arch with the dimensions shown below is to be analyzed step by step.

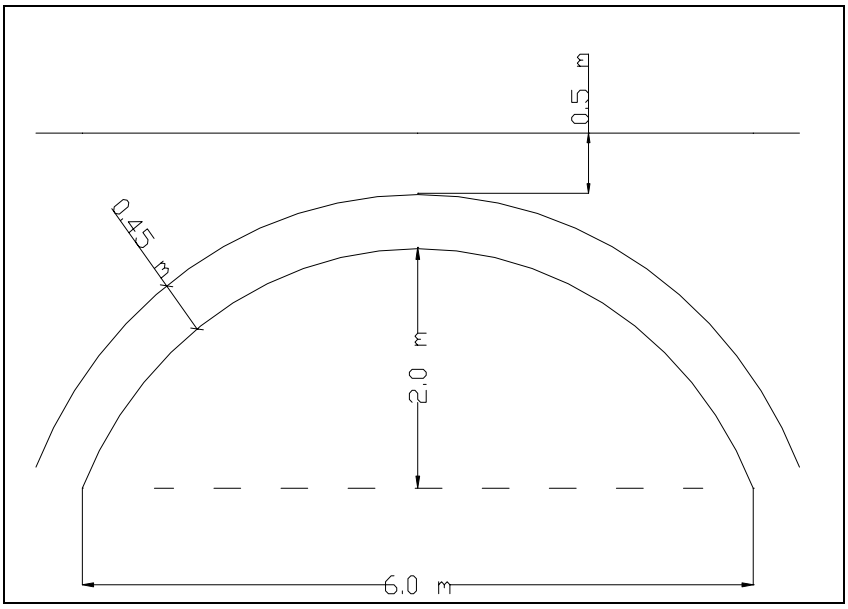

Figure 5.12. Hypothetical arch geometry

5.3.1. Defining the Properties of the Bridge

In order introduce the geometry to the program; the bridge is divided into 20 equal segments.

The geometries of the extrados and the intrados of the arch bridge can now be specified in the matrix form as $\left[(X's)\ (Y's)\right]_{21x2}$ with an appropriate unit as m as it is seen in the
Table 5.2.

There is a fundamental point in this part while introducing the geometry. *The* $[X]$ *coordinates of extrados should be the same as the ones used in the intrados*.

Table 5.2. Coordinates of the intrados and the extrados

coordint (m)		**coordext (m)**	
[X]	[Y]	[X]	[Y]
0.0	0.000	0.0	1.210
0.3	0.872	0.3	1.525
0.6	1.200	0.6	1.760
0.9	1.428	0.9	1.944
1.2	1.600	1.2	2.090
1.5	1.732	1.5	2.206
1.8	1.833	1.8	2.297
2.1	1.908	2.1	2.365
2.4	1.960	2.4	2.413
2.7	1.990	2.7	2.441
3.0	2.000	3.0	2.450
3.3	1.990	3.3	2.441
3.6	1.960	3.6	2.413
3.9	1.908	3.9	2.365
4.2	1.833	4.2	2.297
4.5	1.732	4.5	2.206
4.8	1.600	4.8	2.090
5.1	1.428	5.1	1.944
5.4	1.200	5.4	1.760
5.7	0.872	5.7	1.525
6.0	0.000	6.0	1.210

Other properties are indicated below:

- The thickness of the fill at the crown, H, is specified as $0.5m$ in a scalar form.
- Specific weight of the fill, *gfill*, is taken as $20\frac{kN}{m^3}$.
- Specific weight of the ring, *gring*, is taken as $24\frac{kN}{m^3}$.
- The dispersion angle, *disperselangle*, is given as 30^0.
- The width w that the bridge is loaded over is chosen as $0.75m$.
- Hypothetical arch ratio: Historic masonry arch bridge structures are generally very old and have been subjected to long term historical loadings and movements. These bridges have deteriorated, resulting in some structural damage such as loss of some mortar and/or cracking. In order to include such deficiencies, an indicator, *har*, is utilized in the program. The estimation of this factor is based on quantitative information obtained from a close inspection of the structure. For bridges that are in good condition, without any significant cracks in the vault, *har* can be chosen as $0.85-0.9$. Correspondingly, *har* should be reduced if the bridge is in a bad condition. With existing longitudinal or transversal cracks in the arch ring and mortar loss, *har* will be decreased up to 0.7. Therefore, hypothetical arch ratio is nothing but the reduction of the weak zone. $har = 0.9$ means that 10 per cent outer part of the ring is to be discarded and remaining inner 90 per cent part is taken as a hypothetical total ring. In this illustrative analysis *har* is chosen as 0.85.

5.3.2. Analysis Results

The program completes the solution in less than a minute for this example; i.e. for 20 segments. The program generates two figures as output:

- Worst Load Position & Possible Line of Thrust: From this figure, Figure 5.13, the analyst can go over the geometry and see whether there is a problem related with the geometry. The small triangle on the road level indicates the location of the load that

has the worst effect on the collapse mechanism. The small circles point to 4-hinges and the dotted lines in the ring show the hypothetical ring. On the other hand, the solid line which lies within the hypothetical ring is the line of thrust for the loading that causes collapse

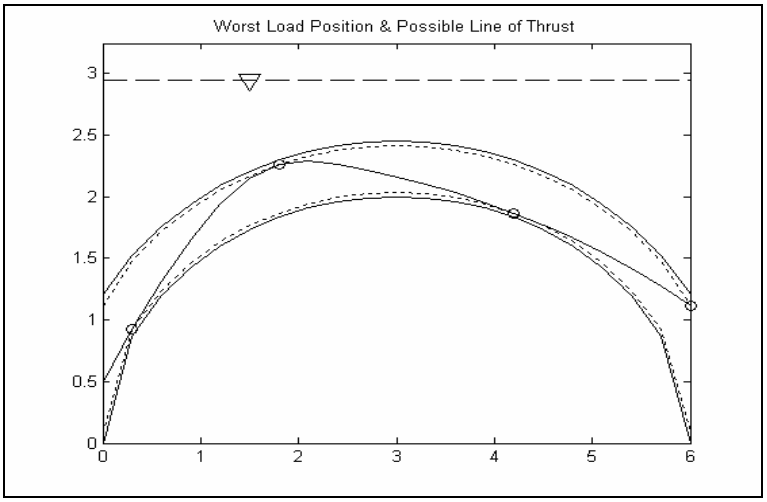

Figure 5.13. Worst Load Position & Possible Line of Thrust

- Limit Load vs. Loading Position: This figure, Figure 5.14, represents the limit load of the sample arch as a function of the load position. The lowest load, collapse load, is found as 297 kN/m width for a position located nearby $1/4$ of the arch span for this illustrative analysis. If the load moves beyond this location (say 0.4 times the arch span), the maximum load that the bridge can carry increases.

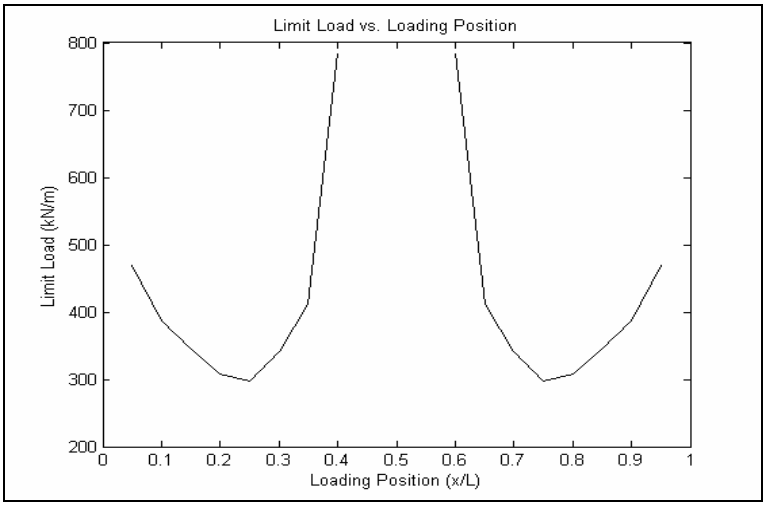

Figure 5.14. Limit Load vs. Loading Position

In some bridges as it can be exactly seen from this specific geometry, the limit load for central or near-central loading comes as infinite. There may be two reasons for this behavior. Loading the bridge from the crown makes the bridge exactly symmetric about $1/2$ of the span. This causes changing of the collapse mechanism from 4-hinge mechanism to 5-hinge one as can be seen from Figure 5.15.

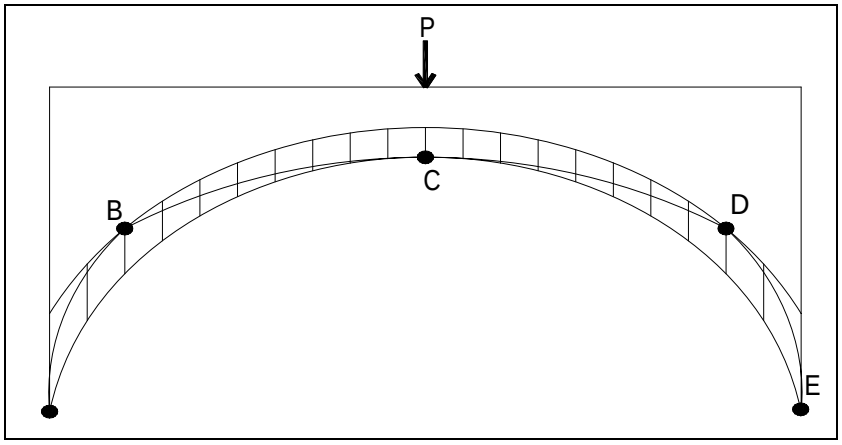

Figure 5.15. Collapse mechanism at central loading

Another reason can be the formation of the compressed spars (Figure 5.16). These spars may form inside the ring thickness and transmit the compression force, coming from the live load and the weight of the bridge, directly to the stiff abutments. Referring back to Chapter 3.3.1, the assumptions of limit analysis states that masonry has infinite strength and sliding does not occur. Therefore, the limit load may be infinite if the loading acts at the centre.

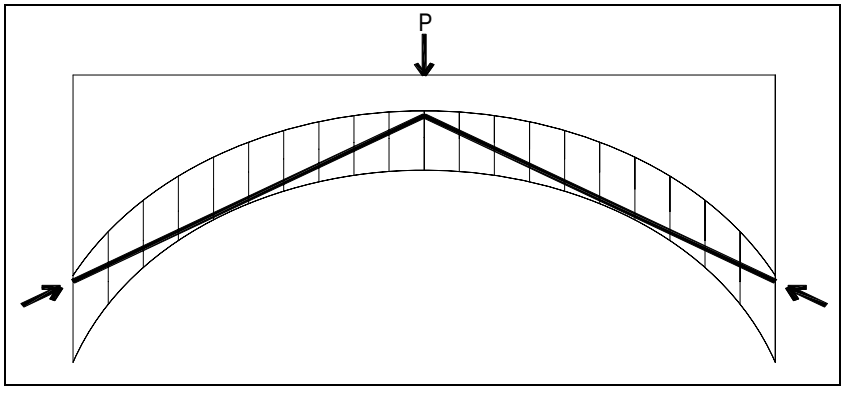

Figure 5.16. Resistant mechanism at central loading

The accuracy of the program is highly affected by the number of segments that constitutes the arch. However, it should not be too sensitive to the number of segments when a reasonable number of segments is used. For an elliptic arch with the same bridge dimensions as shown in Figure 5.12, the relationship between the predicted collapse load and the number of segments used in the program is shown in Figure 5.17. When only 10 segments are used, the predicted collapse load is too high; however, convergence is fairly achieved when 20 segments are used. If the number of segments exceeds 20, the time duration for the solution will become long but the change in the predicted collapse load is not drastically different than that of the 20 segments case. Therefore, dividing the bridge into 20 segments is reasonable when both accuracy and run time are considered.

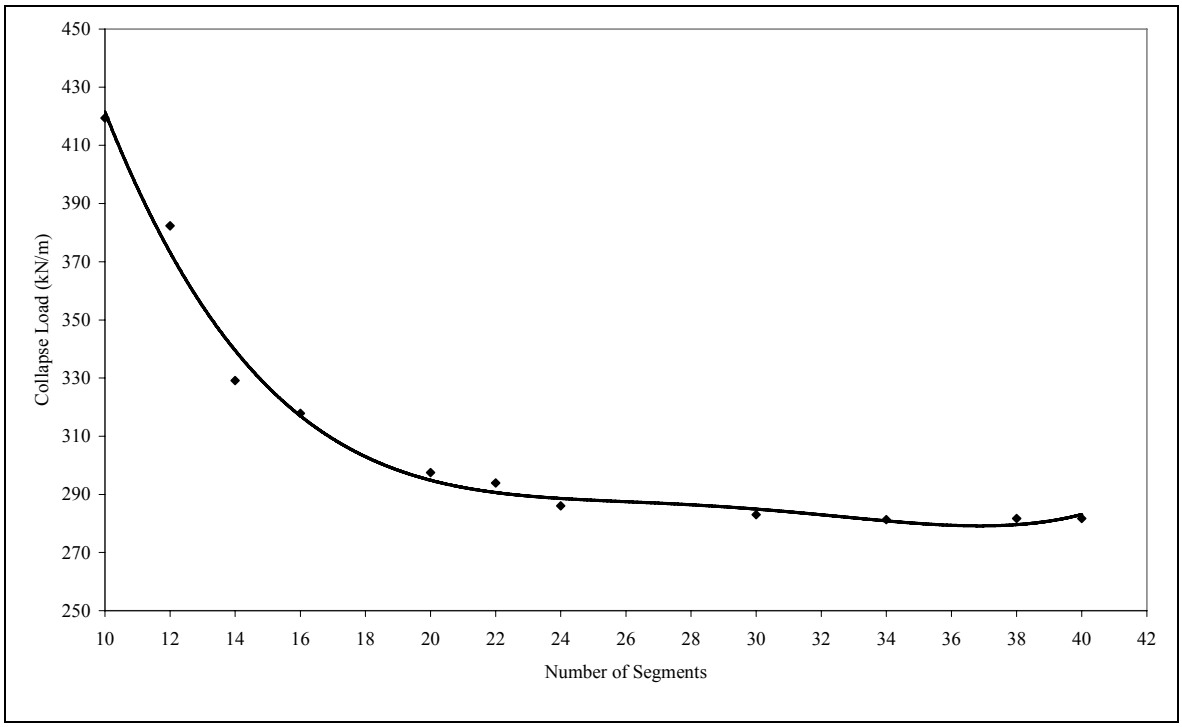

Figure 5.17. Convergence of the program

5.4. Validation of the Program

In the late 1980's and early 1990's, the British Transport and Road Research Laboratory (TRL) carried out a series of load tests to collapse on arch bridges on the field. By these tests, TRL examined the behavior of the arch bridges and their assessment

analysis. In these tests, most bridges failed in four hinge mechanisms, although some of the bridges were reported as failing by snap through or in compression.

In order to validate the predicted collapse load, the program was performed on four arch bridges which were loaded to collapse by TRL. Comparisons are made for four masonry arch bridges using the geometrical properties given in Table 5.3.

Table 5.3. Bridges tested under the TRL program

	Barlea	Stratmashie	Preston	Bridgemill
Span (m) (L)	9.865	9.425	5.18	18.29
Rise at the crown (m) (f)	1.695	2.99	1.64	2.85
Ring thickness (m) (r)	0.45	0.6	0.36	0.711
Fill depth at the crown (m) (H)	0.295	0.41	0.38	0.203

- *Barlea Bridge:* The bridge was loaded to collapse using a transverse line load of $750mm$ width located at $1/4$ of the span. The bridge was in good condition and there were no major defects found on the bridge. The ultimate load recorded was $296\,kN/m$ width.
- The result of the proposed program using $har = 0.9$ is $247\,kN/m$ width. The worst location of the load is found to be at $2.656m$ (0.27 of the span) which was indeed very close to the application of load.

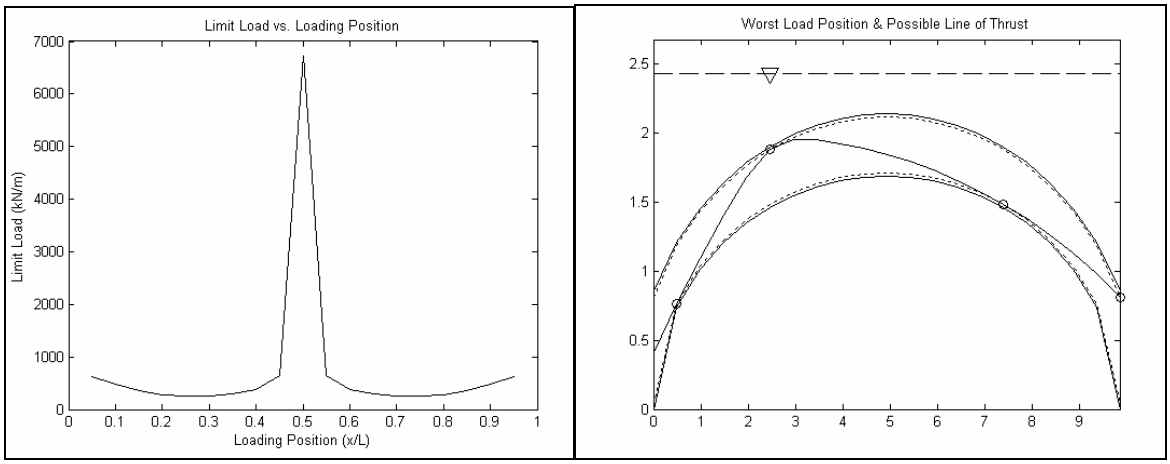

Figure 5.18. Program results for Barlea Bridge

- *Stratmashie Bridge:* The bridge was loaded to collapse using a transverse line load of $750mm$ width located at $1/4$ of the span. Dimensionally, it was in good condition but there was only a little mortar in parts of the arch and a serious longitudinal crack in the arch ring as mentioned in the report on its testing. The ultimate load recorded was $228\,kN/m$ width perpendicular to the span.
- *har* is chosen as 0.75 due to the abovementioned loss of mortar and longitudinal crack in the arch ring. The collapse load is found to be $218\,kN/m$ width which was actually very close to the test result. The location of the load that has the worst effect is found to be at 0.3 of span. When the live load is affected at 1/4 of the span, the load that causes collapse is found to be $246\,kN/m$ width.

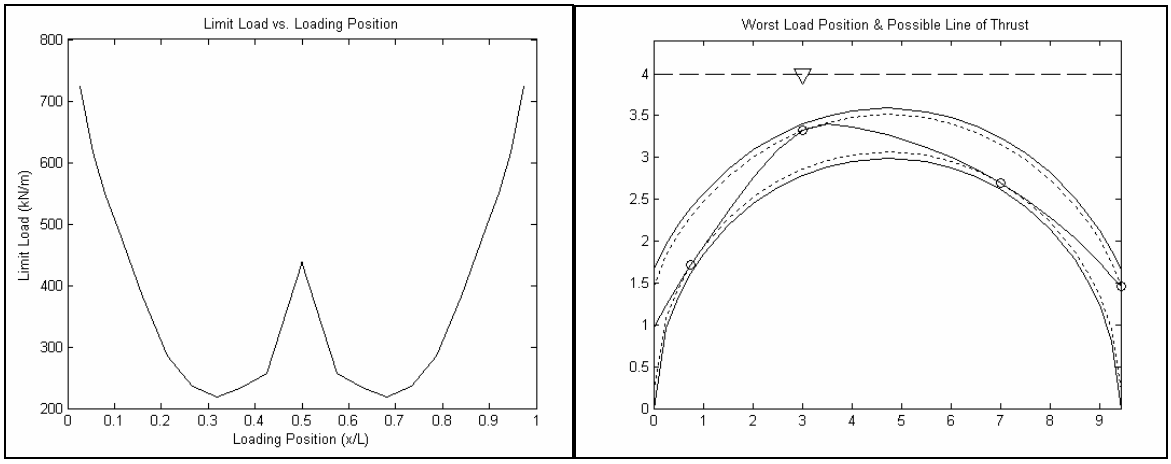

Figure 5.19. Program results for Stratmashie Bridge

- *Preston Bridge:* The bridge was loaded to collapse using a transverse line load of $750mm$ width located at $1/3$ of the span. No measured values regarding the health of the Preston Bridge were found. The ultimate load recorded was $241\,kN/m$ width.
- Choosing *har* as 0.85 which is an appropriate guess for a bridge with inadequate data gives the predicted collapse load as $191\,kN/m$ width. The location of the load that has the critical effect is found to be at 0.27 of the span.

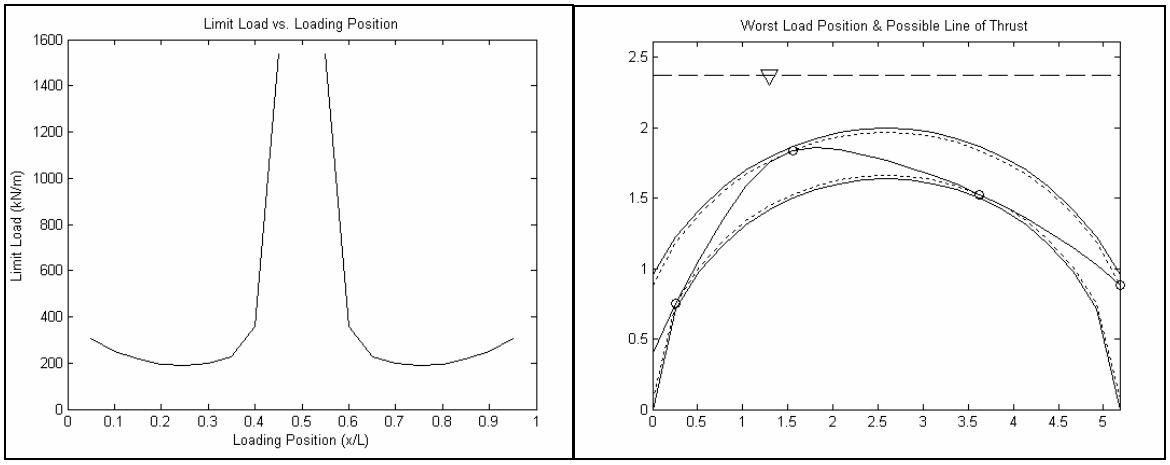

Figure 5.20. Program results for Preston Bridge

- *Bridgemill:* The bridge was loaded to collapse using a transverse line load of $750mm$ width located at $1/4$ of the span. Being the stone arch with the longest span to be experimentally tested, it was chosen by the several different researchers. The whole structure was in good condition, without any significant cracks in the vault. The ultimate load recorded was $361kN/m$ width.
- If the analyst goes over the geometrical properties of the arch meticulously, there will be two striking points that decrease the numerical quantity of *har*. Firstly, the bridge comprises a long span of $18.29m$. Secondly, the arch is particularly flat with a $span/rise$ ratio of 6.42. It can be expected for such geometrical properties that the elastic deformations prior to collapse will significantly change the arch geometry. In order to take such effects into account, *har* should be decreased minimally 10 per cent for bridges with a span greater than $12m$ and $span/rise \geq 6$ after considering the condition of the bridge. If this caution is not put into practice, the predicted collapse load will be found above than the accurate one. In this case, the program can provide an invaluable upper bound prediction, which can be used as an alternative arch assessment technique. In the view of this clarification, choosing *har* as 0.8 yields the predicted collapse load as $397kN/m$ width which is not a bad estimate. The location of the load that has the worst effect is found to be 0.22 of the span.

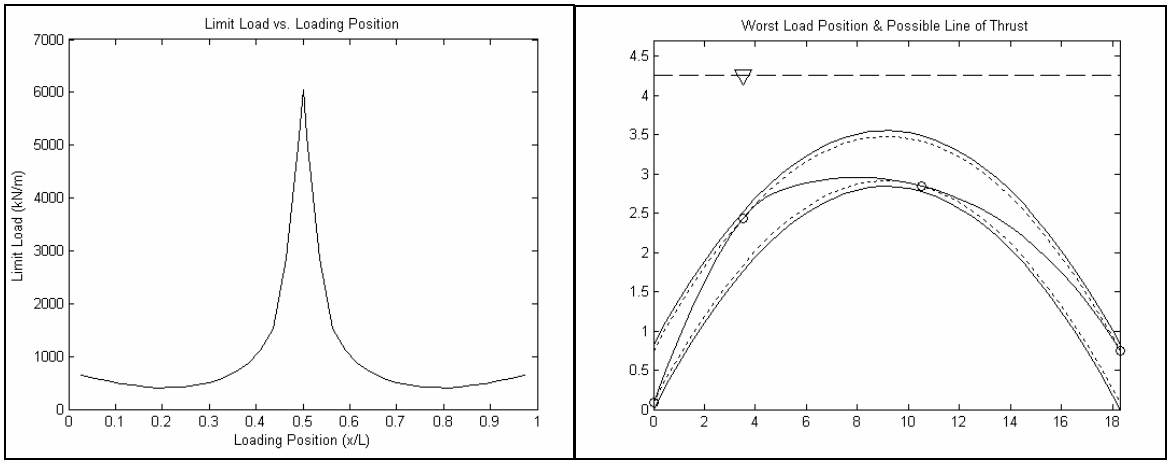

Figure 5.21. Program results for Bridgemill

The results are summarized in table below. As it can be seen, there is a close correlation between the actual collapse loads and the predicted ones. For that reason, it can be concluded that the proposed program which is designed to predict the ultimate load carrying capacities of single span masonry arch bridges can be used with confidence if the analyst selects a suitable value for the indicator *har* considering the above-mentioned effects.

Table 5.4. Correlation between experimentally collapse loads and predicted collapse loads

Bridge	Experimentally Collapse Load (kN/m) width	Predicted Collapse Load (kN/m) width	Predicted / Experimentally Collapse Load
Barlea	296	250	85%
Stratmashie	228	218	96%
Preston	241	191	79%
Bridgemill	361	397	110%

6. A NON-DIMENSIONAL PARAMETRIC STUDY OF MASONRY ARCH BRIDGES

The influence of the change in arch geometry on the collapse load considered in the proposed program-based parametric study is discussed in this chapter. Fundamentally, there are four parameters (Figure 6.1) that describe the geometry of an elliptic arch:

- Span of the bridge (L)
- Rise at the crown (f)
- Ring thickness (r)
- Fill depth at the crown (H)

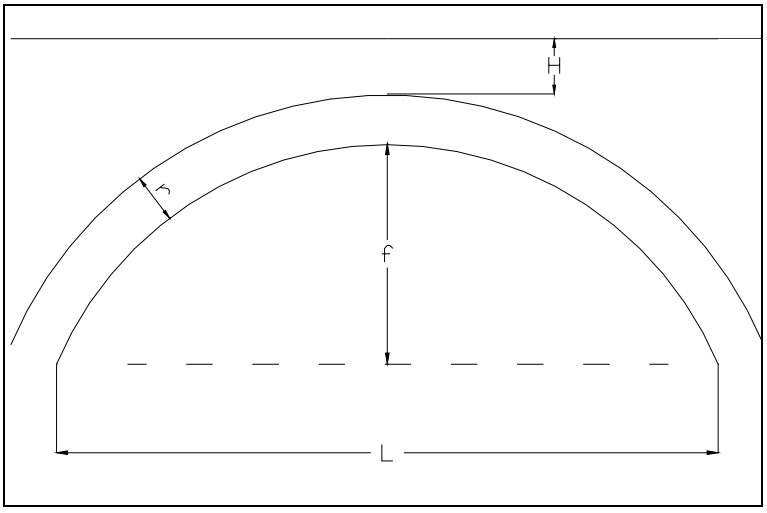

Figure 6.1. Parameters that describe the geometry of an elliptic arch

In order to identify the effects of these parameters on the collapse load, these parameters should be converted into non-dimensional forms. To begin with, if one is asked to select any two parameters in order to convert them into a non-dimensional form, first answer is probably like this: f should be certainly related with L, therefore f/L can be the first non-dimensional variable.

Referring back to Chapter 3.3.1. 'Basic Assumptions of Limit Analysis', the hinge will form when the eccentricity, e, of the normal thrust has the value of $h/2$, that is when $M = N \times (h/2)$ where h is the height of a rectangular section. Therefore, the formation of a hinge is completely related with r; i.e., the likelihood of the formation of any hinge decreases with increasing r. If the formation of a hinge becomes difficult with increasing r, corresponding collapse load will turn out to be higher as expected. Therefore, the capacity of an arch is highly dependent on the ring thickness, r. If we assume the collapse load, P, as zero, the capacity of the arch will be nothing but its own weight. The most important parameters that affect the weight of the structure are absolutely L and f. Consequently, r, L and f give the impression of being highly interrelated.

Consider a triangular plane which exerts pressure to the solid plate shown below. Let the task be to calculate the minimum thickness of the solid plate, r, so that the plate carries the exerted pressure safely.

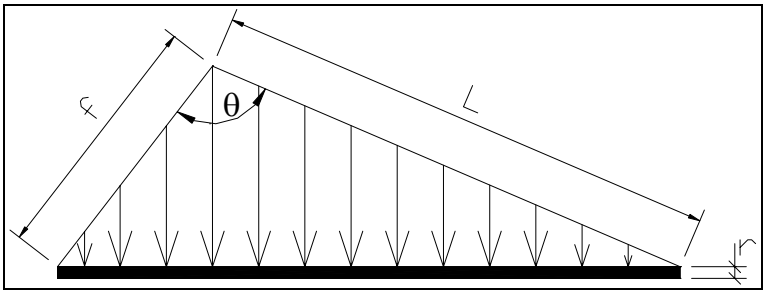

Figure 6.2. Triangular plane carried by a solid plate with thickness, r

The solution for this problem is straightforward. The minimum thickness, r, can be written as a function of stress and the magnitude of the stress exerted to the solid plate is proportional to the enclosed area which is given by the following equation:

$$A = \frac{1}{2} \times \sin\theta \times f \times L = c \times f \times L$$

where c is a constant.

Hence it can be concluded that, r is absolutely proportional to $f \times L$.

Applying the same problem to a new geometry, a semi-circular cylinder (Figure 6.3), yields similar behavior. The thickness, r, is related with the enclosed area where $f = L = R$ this time:

$$A = \frac{\pi}{2} \times R^2 = c \times f \times L$$

where c is a constant.

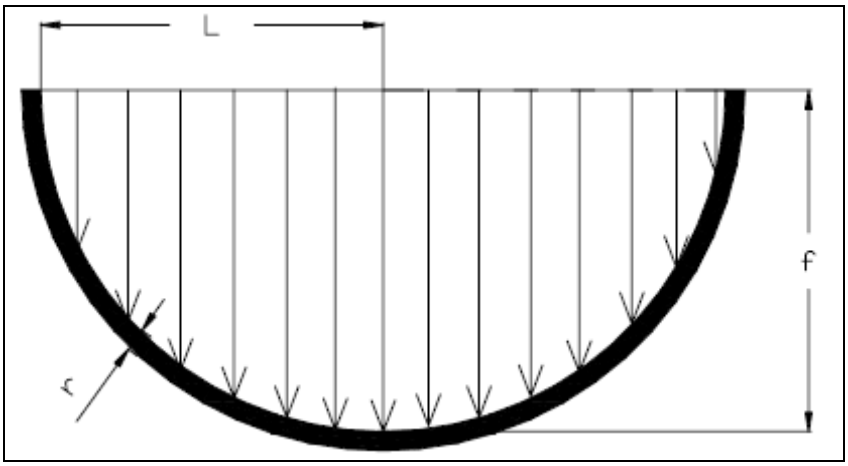

Figure 6.3. A semi-circular cylinder carried by a solid plate with thickness

In this geometry, r seems to be again proportional to $f \times L$.

If one is to extend these results to the masonry arches, it can be concluded that the weight which has the proportionality of $f \times L$ is carried by a ring with a thickness of r which shows the similar behavior to given samples. It brings a conclusion of the above-mentioned relations between r, L and f: r is not only affected by L or f alone but changes with $f \times L$. One way of converting these three parameters to a non-dimensional form is squaring the thickness, r. Correspondingly, the second non-dimensional term is chosen as $\frac{r^2}{f \times L}$.

Finally, in order to investigate the effect of the fill depth at the crown, H, it should be converted into a non-dimensional form as well. If one selects H/L as a final non-dimensional form, L appears as a common denominator. Therefore, the individual effect

of these three non-dimensional forms on the collapse load can be investigated by taking L constant.

Geometrical properties of three real arch bridges, Stratmashie, Barlea and Preston, are used in this parametric study. Except for the geometry, the parameters used in the program are taken constant for all samples as indicated in the table below.

Table 6.1. Parameters used in the parametric study

gfill $\left(\frac{kN}{m^3}\right)$	*gring* $\left(\frac{kN}{m^3}\right)$	*disperselangle* $(\deg ree)$	*w* (m)	*har*
20	24	30	0.75	0.85

6.1. The Effect of f/L on the Predicted Collapse Load

The effect of this parameter is investigated in the region of $0.15 \le f/L < 0.45$ for all sample bridges. By taking span constant, the rise at the crown is increased and/or decreased in a manner that there are enough data on this region. The critical thing is that the effect of f/L is investigated only, so other two non-dimensional parameters, $\frac{r^2}{f \times L}$ and H/L, should be constant during the study.

H is not changed during this part of the parametric study, therefore H/L is already constant, whereas, the change in f/L alters the value of $f \times L$, and consequently $\frac{r^2}{f \times L}$ is affected by the change in f/L. The ring thickness, r, should be modified so as to prevent any change in $\frac{r^2}{f \times L}$. As an illustration, the geometrical properties used in the calculation of the collapse load for Stratmashie Bridge are tabled below. It can be seen that the non-dimensional parameters $\frac{r^2}{f \times L}$ and H/L are constant.

Table 6.2. Geometrical properties of Stratmashie Bridge used in the investigation of f/L

	New L (m)	New f (m)	actual r (m)	New H (m)	Modified r (m)	$\frac{f}{L}$	Modified r^2/fL	$\frac{H}{L}$
actual	9.425	2.990	0.600	0.410	0.600	0.317	0.013	0.0435
trial1	9.425	2.828	0.600	0.410	0.583	0.300	0.013	0.0435
trial2	9.425	2.592	0.600	0.410	0.559	0.275	0.013	0.0435
trial3	9.425	2.356	0.600	0.410	0.533	0.250	0.013	0.0435
trial4	9.425	2.121	0.600	0.410	0.505	0.225	0.013	0.0435
trial5	9.425	1.885	0.600	0.410	0.476	0.200	0.013	0.0435
trial6	9.425	1.649	0.600	0.410	0.446	0.175	0.013	0.0435
trial7	9.425	1.414	0.600	0.410	0.413	0.150	0.013	0.0435
trial8	9.425	3.299	0.600	0.410	0.630	0.350	0.013	0.0435
trial9	9.425	3.534	0.600	0.410	0.652	0.375	0.013	0.0435
trial10	9.425	3.770	0.600	0.410	0.674	0.400	0.013	0.0435
trial11	9.425	3.063	0.600	0.410	0.607	0.325	0.013	0.0435

In the figures, Figure 6.5, Figure 6.6 and Figure 6.7, the solid lines show the predicted collapse load which is found from the program versus f/L. In order to see the relationship between the predicted collapse load and f/L, a trend line is fitted to the data points. The equation of the trend line together with the correlation coefficient, R^2, can be obtained from this least squares solution.

It is apparent from Figures 6.5., 6.6. and 6.7. that the predicted collapse load increases with increasing f/L. In the equations, the collapse load is found to be related to f/L as follows:

- $(f/L)^{0.40}$ for Stratmashie Bridge
- $(f/L)^{0.36}$ for Preston Bridge
- $(f/L)^{0.40}$ for Barlea Bridge

The effect of f/L on the collapse load seems to be similar for all bridges. Therefore, it can be concluded that the collapse load is proportional to, by averaging the three powers in the above equations, $(f/L)^{0.39}$.

During the trials, horizontal abutment thrust, HT, is found to increase with decreasing f/L although there is a decrease in the collapse load. Therefore, especially for shallow bridges, the horizontal abutment thrust can be a problem. The designer, if any, should concern such a thrust that should be resisted by the soil.

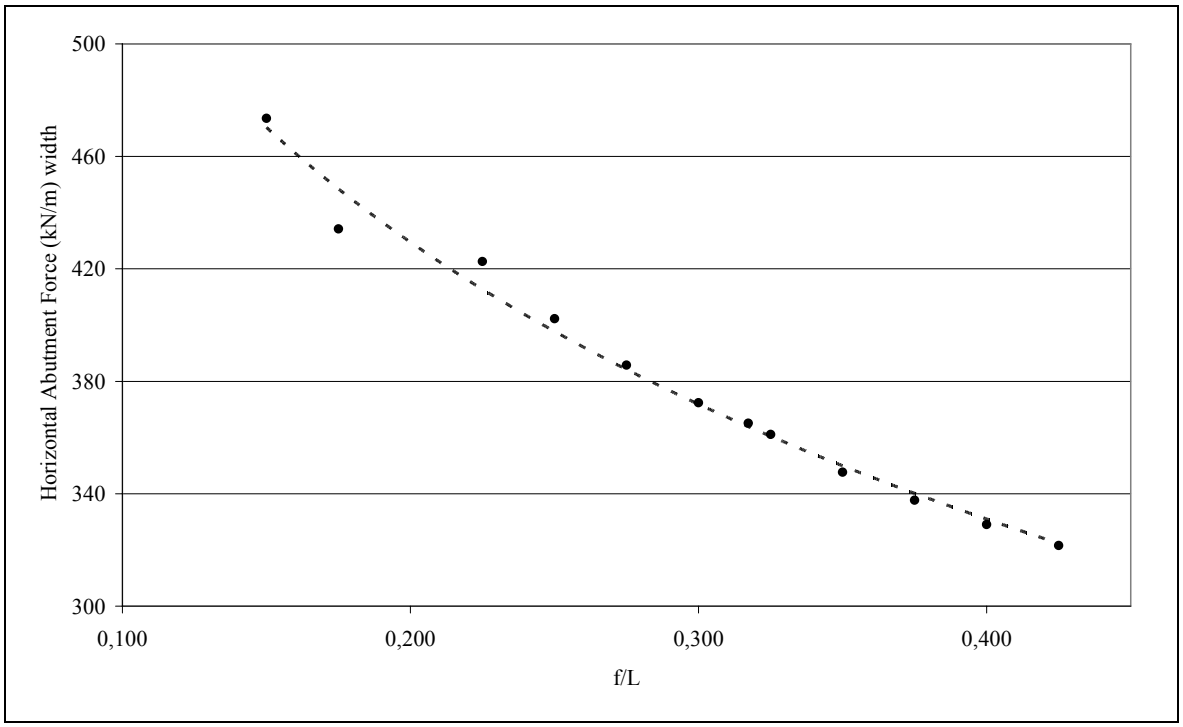

Figure 6.4. Horizontal abutment thrust vs. f/L for Stratmashie Bridge

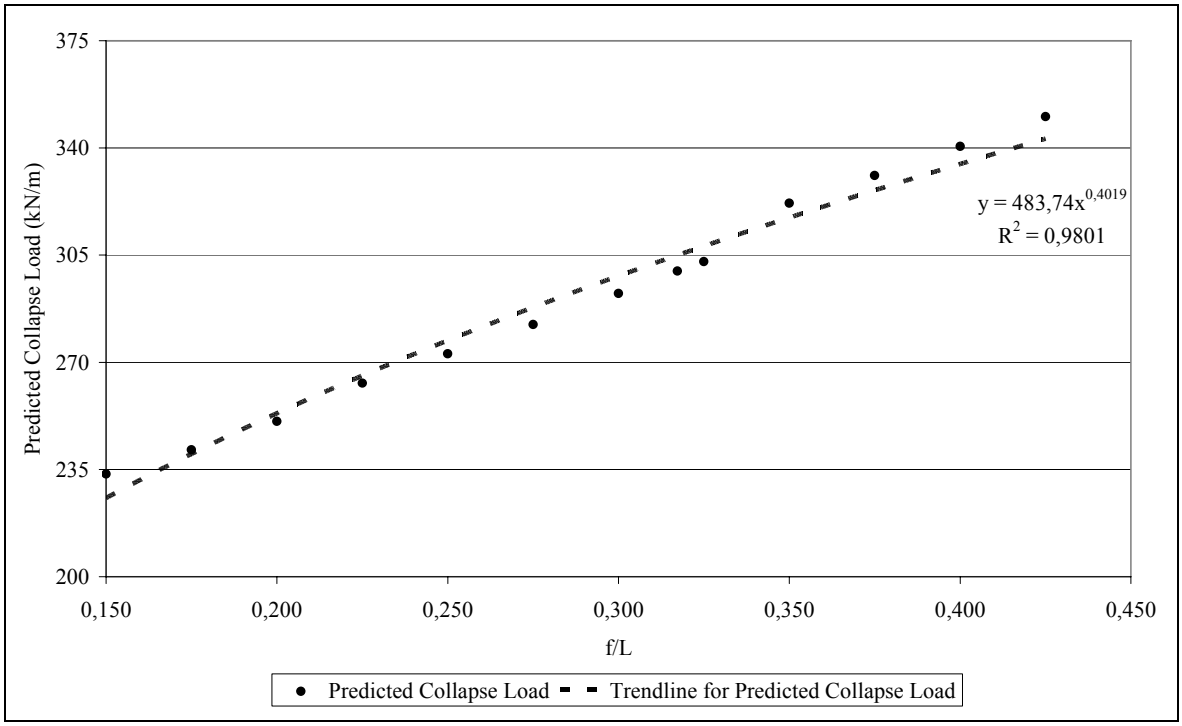

Figure 6.5. The effect of f/L for Stratmashie Bridge

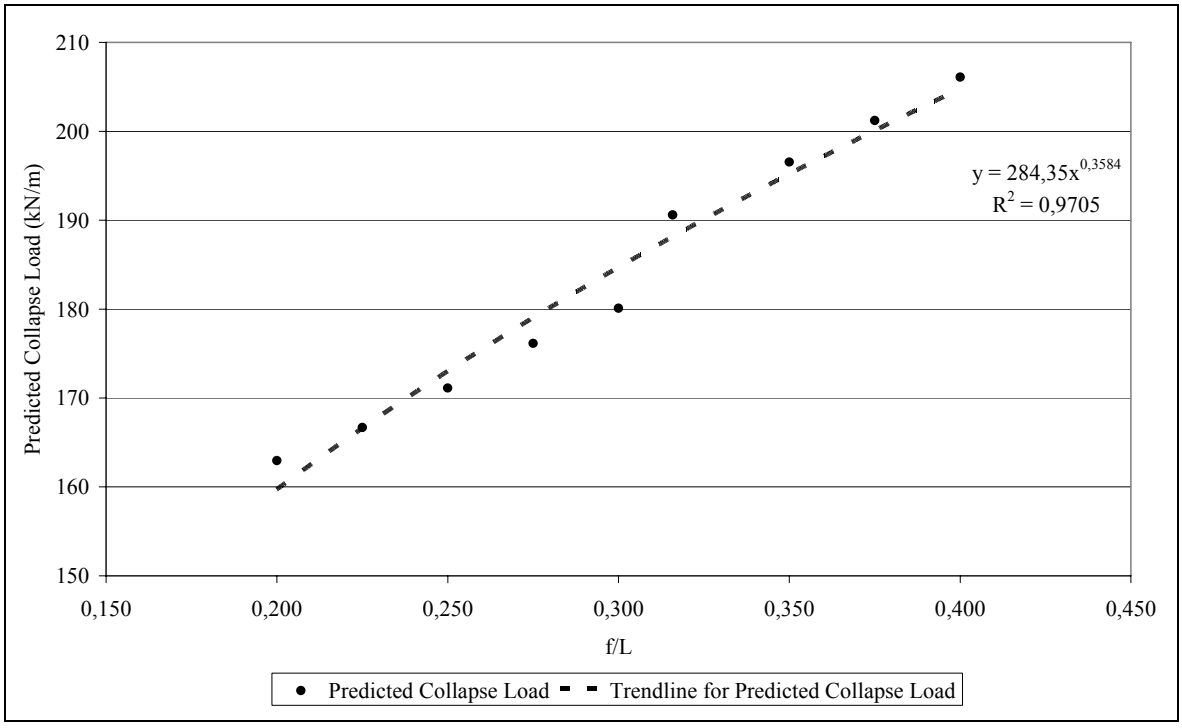

Figure 6.6. The effect of f/L for Preston Bridge

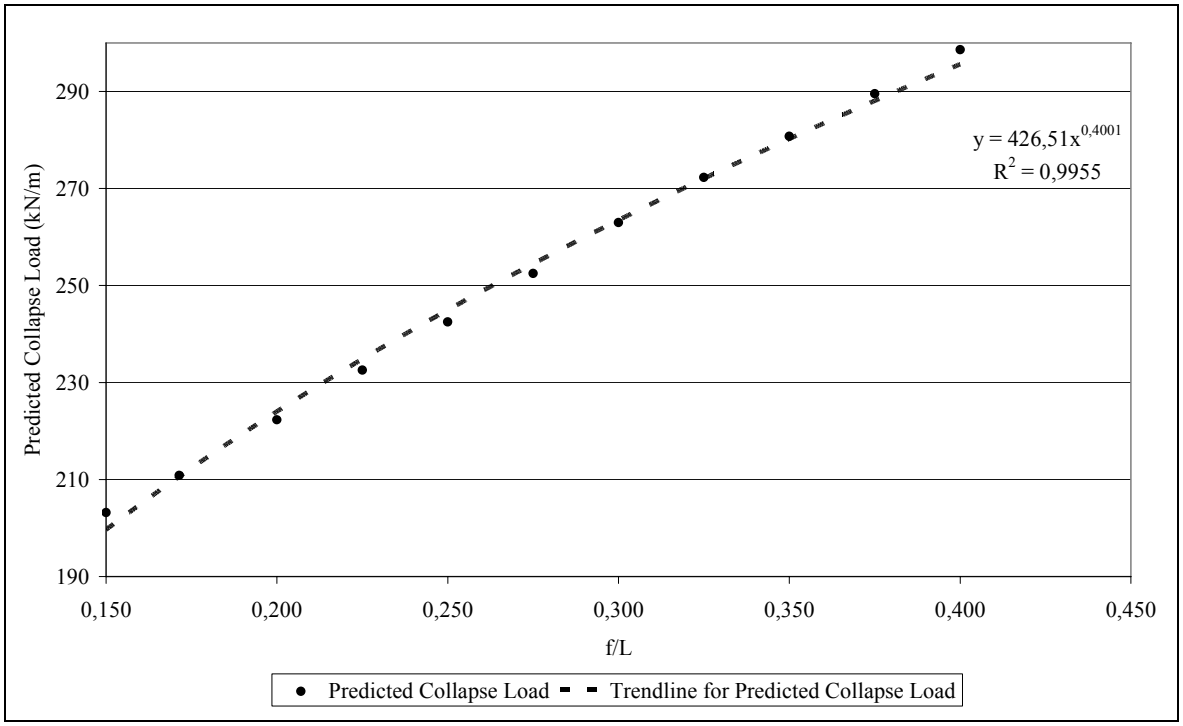

Figure 6.7. The effect of f/L for Barlea Bridge

6.2. The Effect of $\frac{r^2}{f \times L}$ on the Predicted Collapse Load

The effect of this parameter is investigated in the region of $0.006 < \frac{r^2}{f \times L} < 0.02$. By taking span, rise and fill thickness constant, the ring thickness is increased and/or decreased in a manner that there are enough data on this region. Since L, f and H are all taken constant, there is no change in other non-dimensional parameters, f/L and H/L.

As an illustration, while investigating the effect of $\frac{r^2}{f \times L}$ on the capacity, the geometrical properties used in the calculation of the collapse load for Stratmashie Bridge are tabulated below. It can be seen that only variable non-dimensional parameter is $\frac{r^2}{f \times L}$.

Table 6.3. Geometrical properties of Stratmashie Bridge used in the investigation of $\frac{r^2}{f \times L}$

	New L (m)	New f (m)	New H (m)	New r (m)	$\frac{f}{L}$	$\frac{H}{L}$	$\frac{r^2}{f \times L}$
actual	9.425	2.990	0.410	0.600	0.317	0.0435	0.013
trial1	9.425	2.990	0.410	0.566	0.317	0.0435	0.011
trial2	9.425	2.990	0.410	0.518	0.317	0.0435	0.001
trial3	9.425	2.990	0.410	0.471	0.317	0.0435	0.008
trial4	9.425	2.990	0.410	0.613	0.317	0.0435	0.013
trial5	9.425	2.990	0.410	0.630	0.317	0.0435	0.014
trial6	9.425	2.990	0.410	0.660	0.317	0.0435	0.015
trial7	9.425	2.990	0.410	0.680	0.317	0.0435	0.016
trial8	9.425	2.990	0.410	0.692	0.317	0.0435	0.017
trial9	9.425	2.990	0.410	0.700	0.317	0.0435	0.017
trial10	9.425	2.990	0.410	0.720	0.317	0.0435	0.018

It is apparent from, Figure 6.8, Figure 6.9 and Figure 6.10 that the predicted collapse load increases with increasing $\frac{r^2}{f \times L}$. In the figures, the solid lines show the predicted collapse load which is found from the program versus $\frac{r^2}{f \times L}$. In order to see the relationship between the predicted collapse load and $\frac{r^2}{f \times L}$, a trend line is fitted to the data points. The equation of the trend line together with the correlation coefficient, R^2, can be obtained from this least squares solution.

Indeed, the equation fits well to the data points for all three graphs with $R^2 > 0.998$. In the equations, collapse load is found to be a function of;

- $\left(\frac{r^2}{f \times L}\right)^{1.67}$ for Stratmashie Bridge
- $\left(\frac{r^2}{f \times L}\right)^{1.67}$ for Preston Bridge
- $\left(\frac{r^2}{f \times L}\right)^{1.68}$ for Barlea Bridge

The effect of $\frac{r^2}{f \times L}$ on the collapse load seems to be similar for all bridges. Therefore it can be concluded that collapse load is proportional to, by averaging the three powers in the above equations, $\left(\frac{r^2}{f \times L}\right)^{1.67}$.

In the graphs, it is observed that $\frac{r^2}{f \times L}$ has a great effect on the collapse load. Therefore, $\frac{r^2}{f \times L} < 0.013$ is not recommended for design purposes by the author.

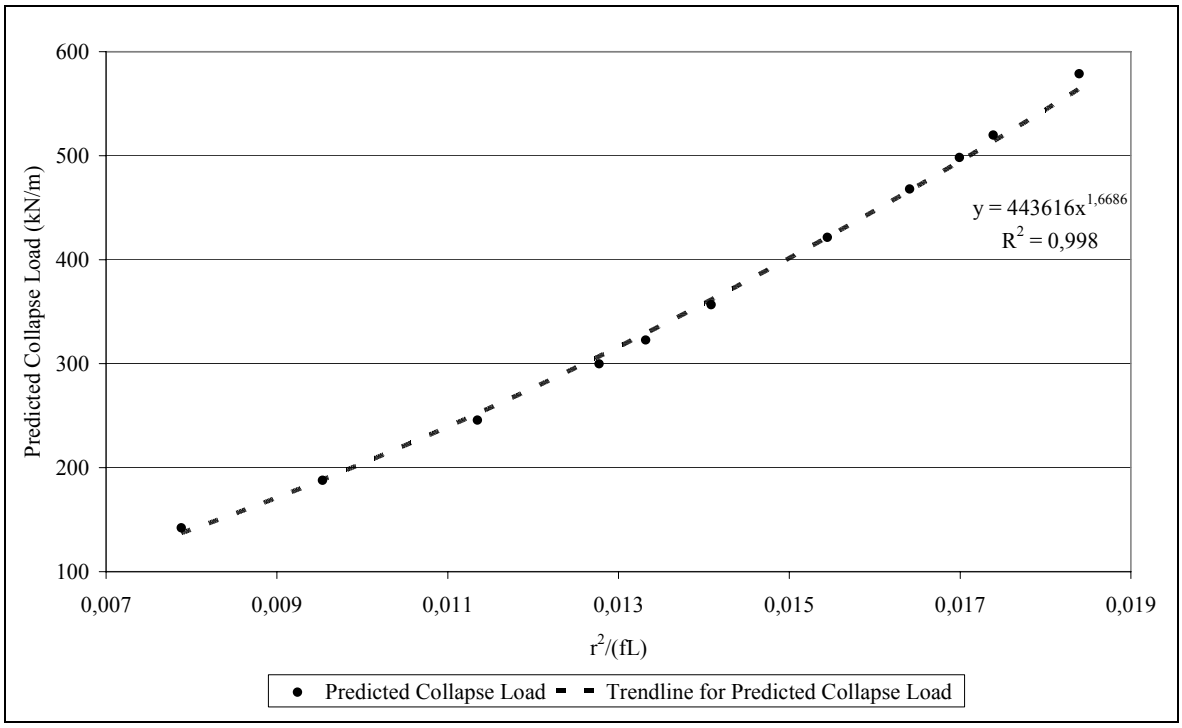

Figure 6.8. The effect of $\frac{r^2}{f \times L}$ for Stratmashie Bridge

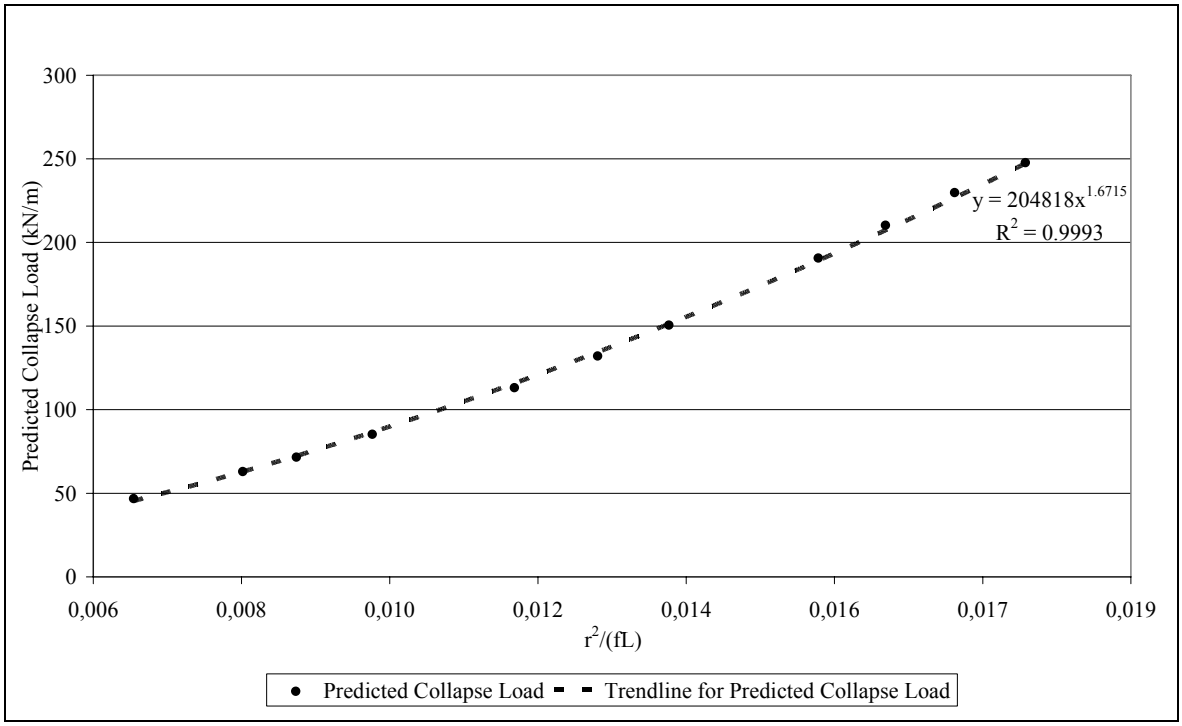

Figure 6.9. The effect of $\frac{r^2}{f \times L}$ for Preston Bridge

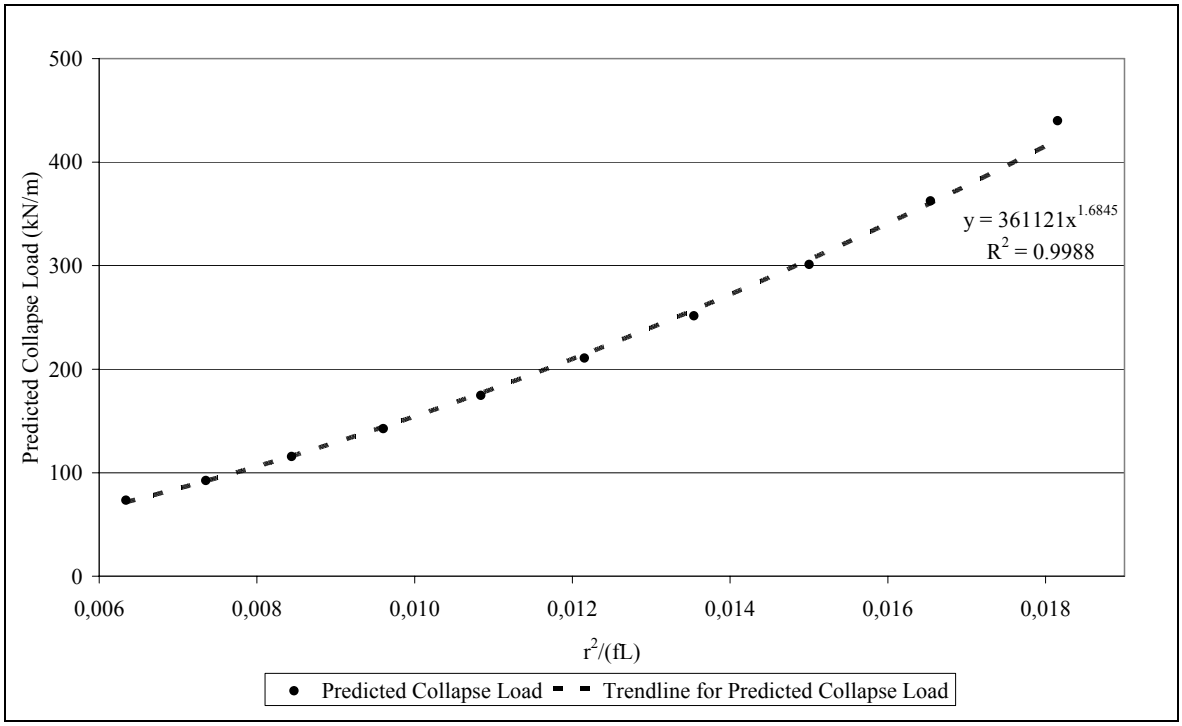

Figure 6.10. The effect of $\frac{r^2}{f \times L}$ for Barlea Bridge

6.3. The Effect of H/L on the Predicted Collapse Load

The effect of this parameter is investigated in the region of $0.025 < H/L < 0.075$. By taking span, rise and ring thickness constant, the fill at crown is increased and/or decreased in a manner that there are enough data on this region. Since L, f and r are all taken constant, there is no change in other two non-dimensional parameters, f/L and $\frac{r^2}{f \times L}$.

As an illustration, while investigating the effect of H/L on the predicted collapse load, the geometrical properties used in the calculation of the collapse load for Stratmashie Bridge are tabulated below. It can be seen that only variable non-dimensional parameter is H/L.

Table 6.4. Geometrical properties of Stratmashie Bridge used in the investigation of H/L

	New L (m)	New f (m)	New r (m)	New H (m)	$\frac{f}{L}$	$\frac{r^2}{f \times L}$	$\frac{H}{L}$
actual	9.425	2.990	0.600	0.410	0.317	0.013	0.044
trial1	9.425	2.990	0.600	0.226	0.317	0.013	0.040
trial2	9.425	2.990	0.600	0.198	0.317	0.013	0.035
trial3	9.425	2.990	0.600	0.170	0.317	0.013	0.030
trial4	9.425	2.990	0.600	0.254	0.317	0.013	0.045
trial5	9.425	2.990	0.600	0.283	0.317	0.013	0.050
trial6	9.425	2.990	0.600	0.311	0.317	0.013	0.055
trial7	9.425	2.990	0.600	0.339	0.317	0.013	0.060
trial8	9.425	2.990	0.600	0.368	0.317	0.013	0.065

It is apparent from Figure 6.11, Figure 6.12 and Figure 6.13, that the predicted collapse load increases with increasing H/L. In the figures above, the solid lines show the predicted collapse load which is found from the program versus H/L. In order to see the relationship between the predicted collapse load and H/L, a trend line is fitted to the data points. The equation of the trend line together with the correlation coefficient, R^2, can be obtained from this least squares solution.

Indeed, the equation fits well to the data points for all three graphs with $R^2 > 0.978$. In the equations, collapse load is found to be a function of H/L as follows:

- $(H/L)^{0.39}$ for Stratmashie Bridge
- $(H/L)^{0.44}$ for Preston Bridge
- $(H/L)^{0.37}$ for Barlea Bridge.

There is not a coherent parallelism in this non-dimensional parameter. The power of the proportionality increases with increasing H/L as seen in the table below.

Table 6.5. The effect of H/L on the power of proportionality

	H/L	Power of Proportionality
Stratmashie Bridge	0.046	$(H/L)^{0.39}$
Preston Bridge	0.073	$(H/L)^{0.44}$
Barlea Bridge.	0.030	$(H/L)^{0.37}$

In addition to such deviations, there is another problem related with this non-dimensional parameter. The lateral earth pressures, active-pressure and passive-pressure, are not included in the program. Without considering lateral earth pressure, the effect of H/L on the collapse is limited. For further developments, it is recommended that the H/L effect including such lateral pressure effects together with the abovementioned deviation should be reviewed. Omitting these effects, collapse load is proportional to, by averaging these three factors, $(H/L)^{0.40}$.

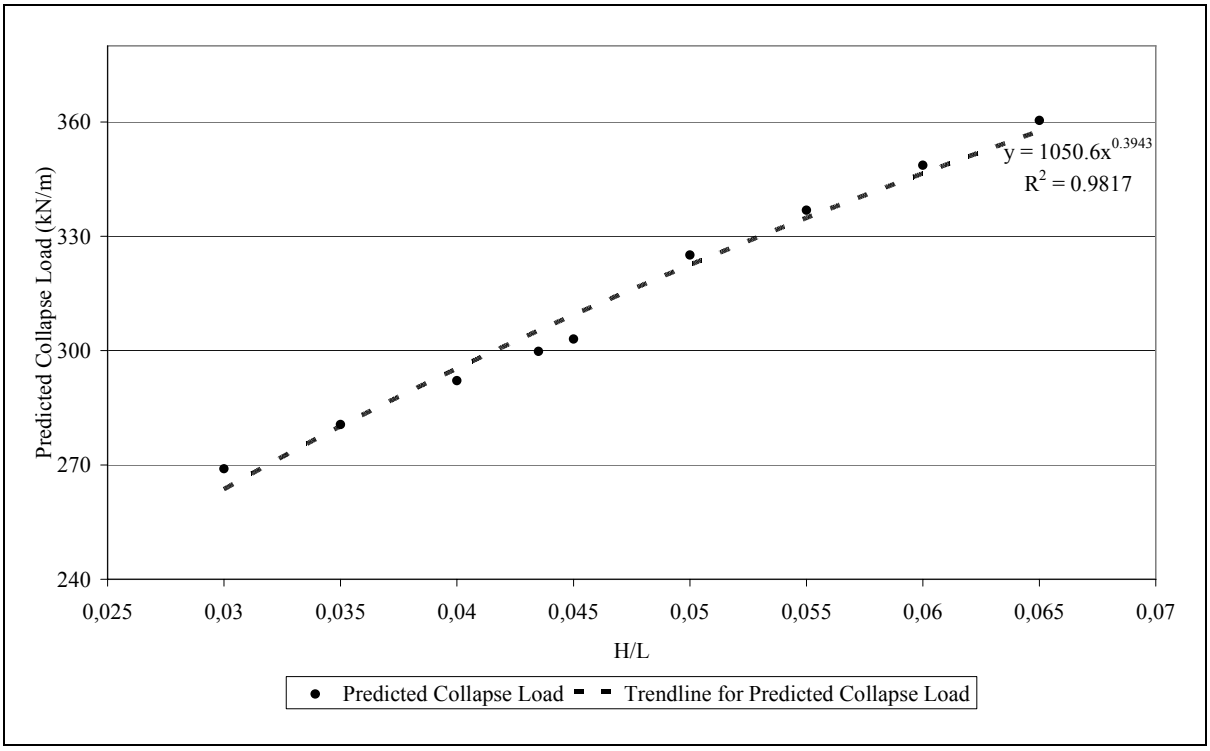

Figure 6.11. The effect of H/L for Stratmashie Bridge

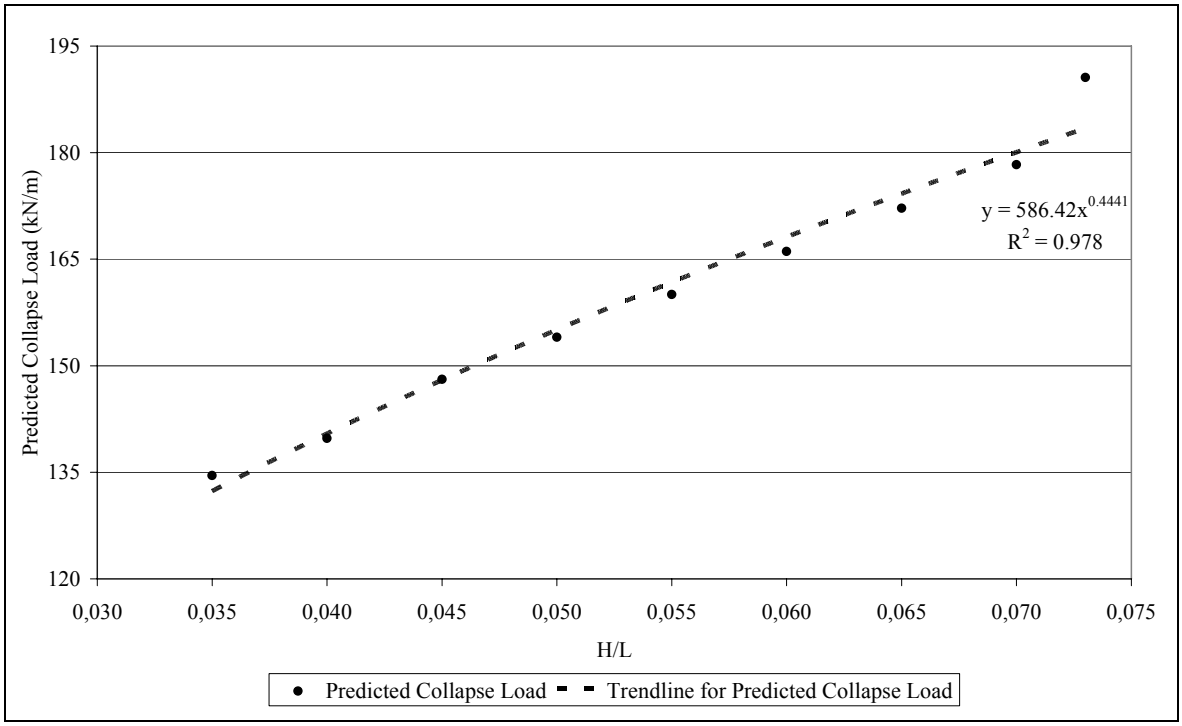

Figure 6.12. The effect of H/L for Preston Bridge

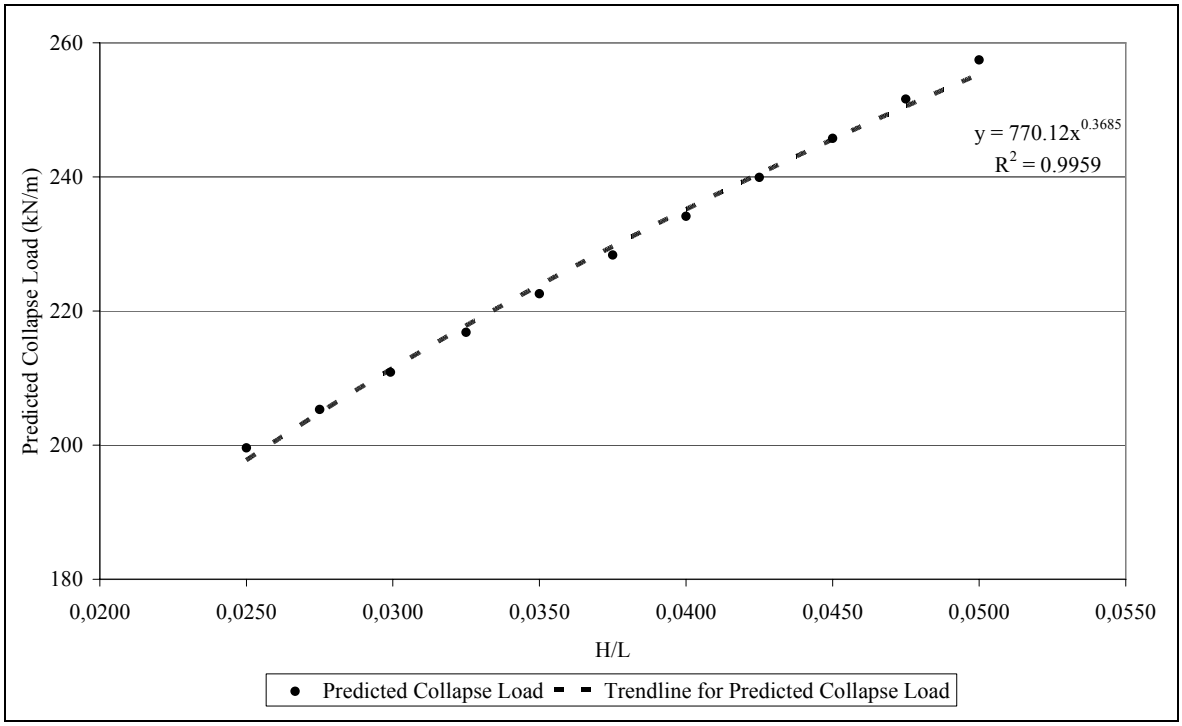

Figure 6.13. The effect of H/L for Barlea Bridge

7. PROPOSED ARCH ASSESSMENT METHOD

7.1. Method Description

Heyman states that any estimate of the bridge's safety will not depend (at least not markedly) on the strength of the material. Rather the safety of an arch could perhaps be expressed in terms of its shape; the matter will be one of geometry, and not of the 'stress and strains' of a modern theory of structures.

On this basis, the individual effects of the non-dimensional parameters f/L, $\frac{r^2}{f \times L}$ and H/L are studied and the relationship between these parameters and the predicted collapse load is proven previously. In this part, a new and very simple arch assessment technique is offered to predict the collapse load of existing masonry arch bridges by using the geometrical properties of the tested ones.

An existing bridge is going to be assessed by means of a tested bridge. Let the geometrical properties of existing bridge be

- Span of the existing bridge, L_E
- Rise of the existing bridge, f_E
- Ring thickness of the existing bridge, r_E
- Fill depth of the existing bridge, H_E

where subscript E means *Existing*. Similarly, the geometrical properties of the tested bridge are L_T, f_T, r_T and H_T, where subscript T means *Tested*. Tested bridge was previously loaded to collapse and an ultimate load, P_T, was recorded.

It is easy to convert the geometrical properties of the tested and existing bridges into non-dimensional forms as follows:

- f_T/L_T, $\frac{r_T^{\,2}}{f_T \times L_T}$ and H_T/L_T for tested bridge
- f_E/L_E, $\frac{r_E^{\,2}}{f_E \times L_E}$ and H_E/L_E for existing bridge

These non-dimensional parameters can be compared by

- $\frac{(f/L)_E}{(f/L)_T}$
- $\frac{\left(\frac{r^2}{f \times L}\right)_E}{\left(\frac{r^2}{f \times L}\right)_T}$
- $\frac{(H/L)_E}{(H/L)_T}$.

It may be possible to determine the strength of the existing masonry arch bridges by this analogy. However, while investigating the individual effect of the abovementioned non-dimensional parameters, the span, L, is taken constant. Therefore, comparing these non-dimensional parameters give the comparison between f_E and f_T, r_E and r_T, H_E and H_T. There should be a missing point related with the spans on the condition that L_E is not equal to L_T. In order to adjust L_E relative to L_T, there should be another factor related with the geometry.

7.1.1. Scaling Factor

As depicted, when $L_E \neq L_T$, the comparisons between the abovementioned three non-dimensional parameters seem to be inadequate. There should be one more comparison

between L_E and L_T so that the given technique works. Such a relationship is to be found out on the condition that while investigating the effect of this relationship, other non-dimensional parameters, f/L, $\frac{r^2}{f \times L}$ and H/L should stay constant. It is only possible when the geometry scales up or down entirely.

Let the geometry of a masonry arch bridge be scaled 10 per cent up entirely. New geometrical properties come out as follows:

- New span of the bridge $1.1 \times L$
- New rise at the crown $1.1 \times f$
- New ring thickness $1.1 \times r$
- New fill depth at the crown $1.1 \times H$

New non-dimensional parameters for this geometry can, therefore, be calculated as

- $\frac{1.1 \times f}{1.1 \times L} = \frac{f}{L}$
- $\frac{(1.1 \times r)^2}{(1.1 \times f) \times (1.1 \times L)} = \frac{r^2}{f \times L}$
- $\frac{(1.1 \times H)}{(1.1 \times L)} = \frac{H}{L}$

As can be seen, scaling the geometry up or down entirely does not cause any change in the non-dimensional parameters.

In order to investigate the effect of scaling factor, two tested bridges, namely Stratmashie and Barlea Bridge, are going to be analyzed. The non-geometrical parameters used in this part are the ones that are used in the parametric study (Table 6.1). The whole geometry is scaled up and/or down in a manner that there are enough data to get a logical relationship between amount of scaling and predicted collapse load.

In the figures, the solid lines show the predicted collapse load which is found from the program versus the amount of scaling by which the geometrical properties of the bridge are modified. In order to see the relationship between the predicted collapse load and the amount of scaling, a trend line is added across the data points. The equation of this best fit curve together with the correlation coefficient, R^2, is obtained in a least squares sense.

Indeed, the equation fits very well to the data points for the graphs with $R^2 > 0.9997$. It is apparent from Figure 7.1 and Figure 7.2 that the predicted collapse load increases with increasing scale factor (SF). In the equations, collapse load is found to be a function of

- $(SF)^{1.89}$ for Stratmashie Bridge
- $(SF)^{1.86}$ for Barlea Bridge.

There is a coherent parallelism between two samples. Therefore, it can be concluded as collapse load is proportional to, by averaging the powers of the above equations, $(SF)^{1.88}$.

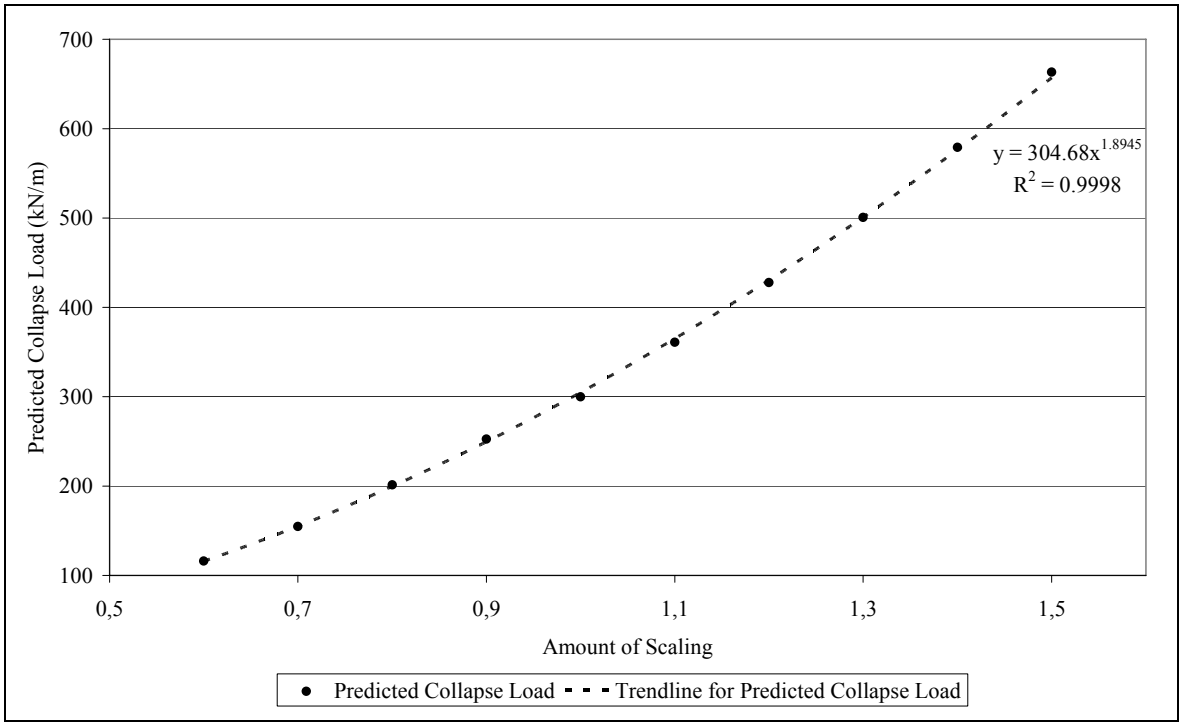

Figure 7.1. The effect of scaling factor for Stratmashie Bridge

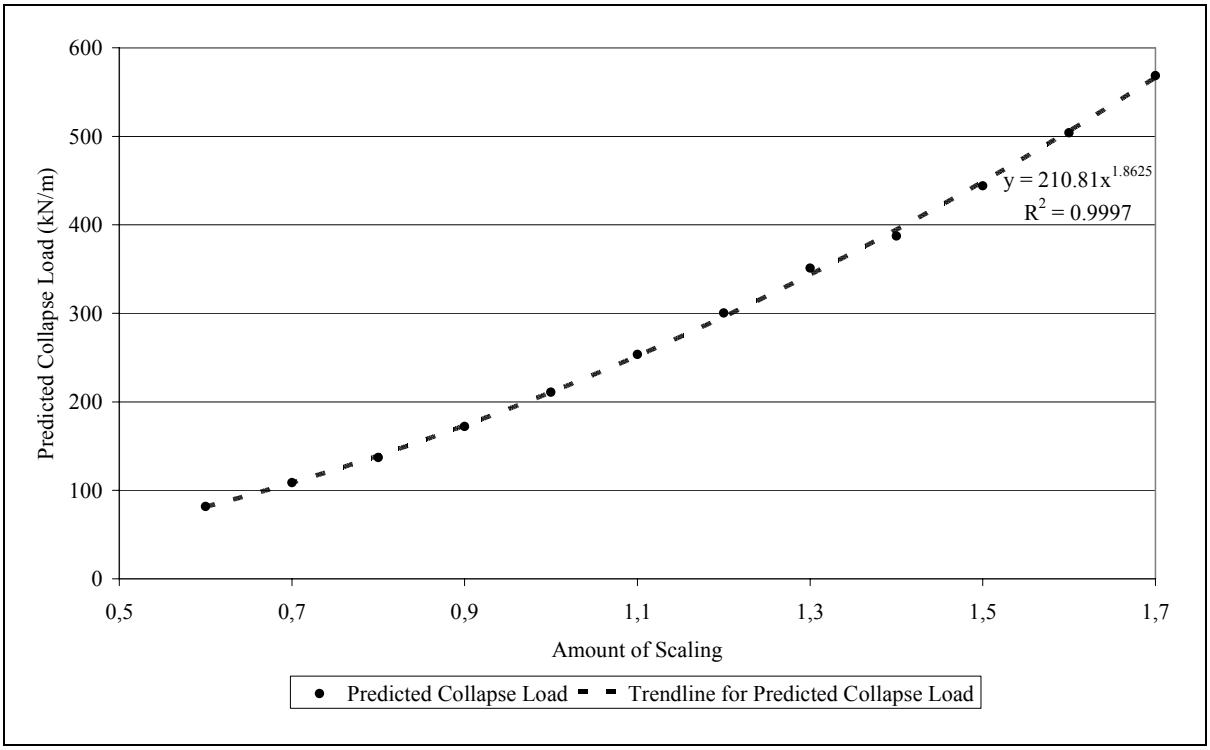

Figure 7.2. The effect of scaling factor for Barlea Bridge

7.1.2. Analytical Formula of the Method

It is now possible to determine the capacity of existing masonry arch bridges by means of tested ones. The idea behind the offered method is very simple: The proportion of the non-dimensional parameters between existing and tested masonry arch bridges gives the proportion of their strengths. In order to perform this understanding, the effect of each non-dimensional parameter is investigated and concluded that the predicted collapse load changes with the power of:

- 0.39 for $\left(f/L\right)$
- 1.67 for $\left(\frac{r^2}{f\times L}\right)$
- 0.40 for $\left(H/L\right)$
- 1.88 for $\left(SF\right)$.

The comparison of the first three parameters has been undertaken. The final parameter, scaling factor, is nothing but the ratio of L_E to L_T. By comparing these four parameters, the probable limit load for an existing masonry arch bridge can be found from the below formula:

$$P_E = \left[\frac{\left(f/L\right)_E}{\left(f/L\right)_T}\right]^{0.39} \times \left[\frac{\left(\frac{r^2}{f\times L}\right)_E}{\left(\frac{r^2}{f\times L}\right)_T}\right]^{1.67} \times \left[\frac{\left(H/L\right)_E}{\left(H/L\right)_T}\right]^{0.40} \times \left[\frac{L_E}{L_T}\right]^{1.88} \times P_T \qquad (7.1)$$

7.2. Validation of the Method

In order to use this method in a safe manner, it should be validated. To check whether the method is acceptable or not, the predictions obtained from the method are compared with the predictions of fictitious masonry arch bridges obtained from the program. The predictions of this method are also validated by means of the tested bridges.

7.2.1. Validation of the Method by Means of Fictitious Masonry Arch Bridges

The method was practiced on several fictitious arch geometries. The predictions are approximated from two tested masonry arch bridges, Stratmashie and Barlea. The reader can access the geometrical properties of the fictitious masonry arch bridges and the summary of the results from Appendix B. Same bridges are analyzed using the program and a comparison is made between the program results and the offered method.

It is apparent from Figure 7.3 that offered method predicts the collapse load below the program result. The reason behind this can be the fact that there were a loss of mortar and a serious longitudinal crack in the arch ring. Therefore, applying the method which is approximated from Stratmashie Bridge gives a lower limit in the prediction of the undamaged arch capacity.

On the other hand, the predictions of the method that was approximated from Barlea Bridge (Figure 7.4) are close to the program results. In this approximation, the offered method gives a bit higher predictions. The program results are in between these two approximations as it is seen from Figure 7.5. Therefore, the predictions by the offered method are more reliable when the number of tested bridges is increased.

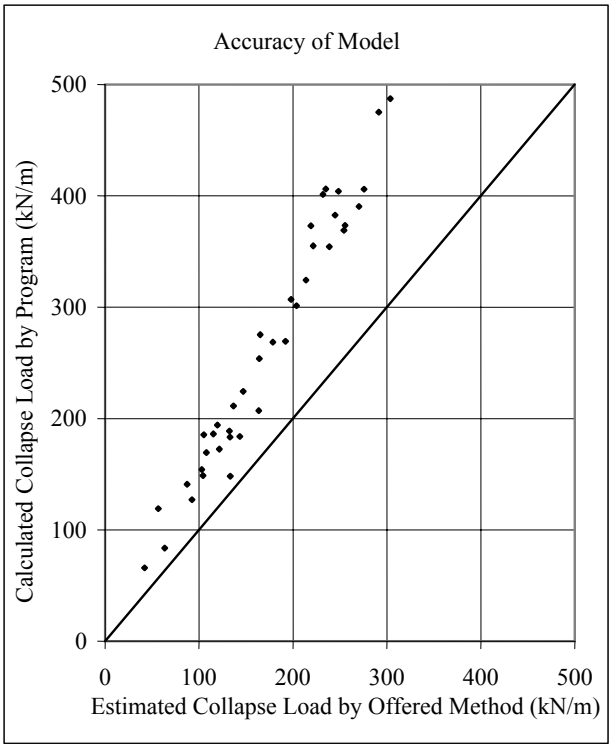

Figure 7.3. Accuracy of the method approximated from Stratmashie Bridge

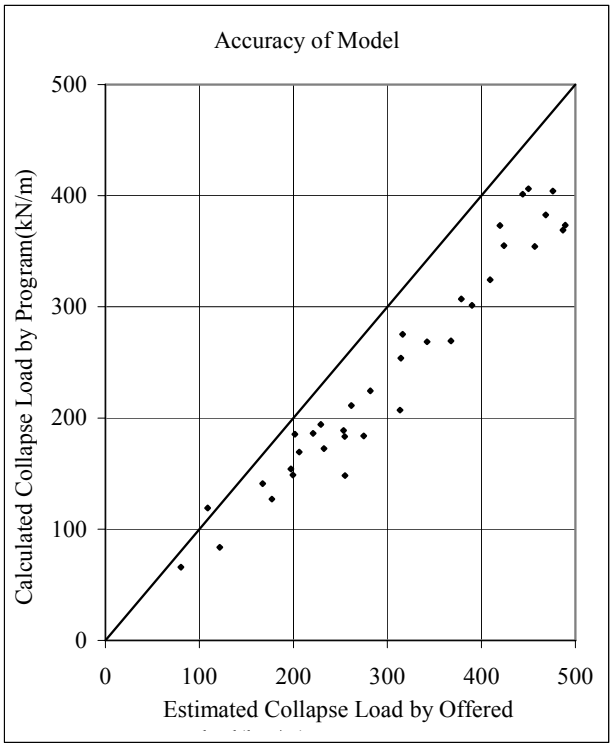

Figure 7.4. Accuracy of the method approximated from Barlea Bridge

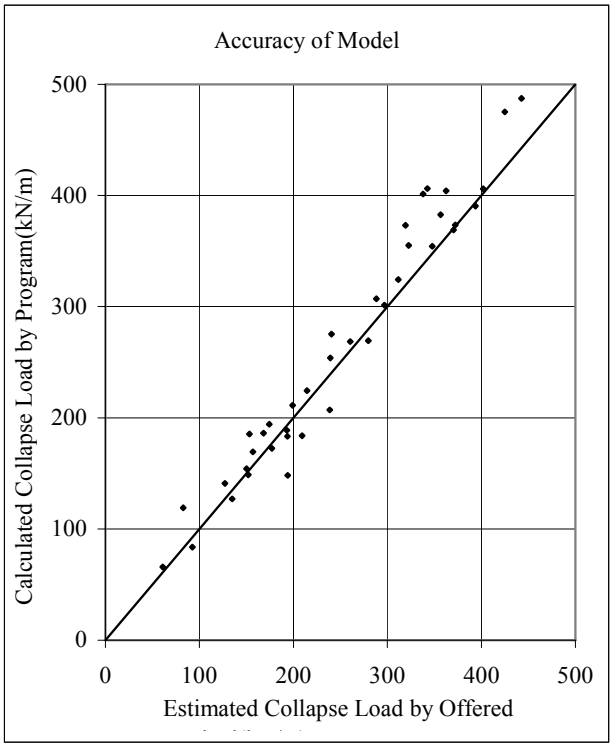

Figure 7.5. Accuracy of the method when two approximations are used

7.2.2. Validation of the Method by Means of Tested Bridges

In order to validate the method, an experimentally tested bridge, Barlea Bridge, is going to be analyzed by means of two tested bridges, Bridgemill and Preston. The geometrical properties, non-dimensional parameters and collapse load for each bridge are tabulated in Table 7.1.

Table 7.1. Properties of the bridges that were tested previously

Bridges	L (m)	f (m)	r (m)	H (m)	$\frac{f}{L}$	$\frac{r^2}{f \times L}$	$\frac{H}{L}$	Experimental Collapse Load (kN/m) width
Bridgemill	18.3	2.850	0.711	0.203	0.156	0.010	0.011	361
Preston	5.18	1.640	0.36	0.38	0.317	0.015	0.073	241
Barlea	9.86	1.690	0.45	0.295	0.171	0.012	0.030	295

Applying the formula

$$P_E = \left[\frac{(f/L)_E}{(f/L)_T}\right]^{0.39} \times \left[\frac{\left(\frac{r^2}{f \times L}\right)_E}{\left(\frac{r^2}{f \times L}\right)_T}\right]^{1.67} \times \left[\frac{(H/L)_E}{(H/L)_T}\right]^{0.40} \times \left[\frac{L_E}{L_T}\right]^{1.88} \times P_T \qquad (7.1)$$

- The prediction that is approximated from Bridgemill gives:

$$P_E = \left[\frac{0.171}{0.156}\right]^{0.39} \times \left[\frac{0.012}{0.010}\right]^{1.67} \times \left[\frac{0.030}{0.011}\right]^{0.40} \times \left[\frac{9.86}{18.3}\right]^{1.88} \times 361$$

$P_E = 255 kN/m$ width (86.5 per cent of actual collapse load)

- The prediction that is approximated from Preston gives:

$$P_E = \left[\frac{0.171}{0.317}\right]^{0.39} \times \left[\frac{0.012}{0.015}\right]^{1.67} \times \left[\frac{0.030}{0.073}\right]^{0.40} \times \left[\frac{9.86}{5.18}\right]^{1.88} \times 241$$

$P_E = 304 kN/m$ width (103 per cent of actual collapse load)

As it can be seen, predicted collapse loads are very close to the exact one. Besides, averaging these two predictions give 94.4 per cent of the test result with $P_E = 280 kN/m$ width.

If this method is applied to an existing masonry arch bridge, the tested bridges used in the method should be chosen in a manner such that the condition of the tested bridges is well-matched to the bridge that is assessed. For example, while applying this method to a bridge with cracks and a loss of mortar, like in the Stratmashie Bridge, choosing Barlea Bridge which was in a good condition as a tested bridge can give inaccurate results. Namely; the prediction for Stratmashie Bridge, with an experimentally determined collapse load of $228 kN/m$ width, is found to be $437 kN/m$ width when Barlea Bridge is used as a

tested bridge. Taking the ring thickness smaller than the original one can be a sensible suggestion for this kind incompatibly. That is to say, for Stratmashie Bridge, taking the arch thickness 0.5 m instead of the 0.6 m changes the predicted collapse load from $437 kN/m$ width to $237 kN/m$ width which is 104 per cent of the test result.

Equation 7.1 can be cast into a more compact form by using the geometric properties and corresponding collapse loads of available tested bridges, Bridgemill, Preston and Barlea. The numerical values of the non-dimensional terms, span length and experimental collapse load can be inserted into Equation 7.1 as *Geometric Multiplication Factor* (*GMF*):

Bridgemill:

$$GMF = \left[\frac{1}{0.156}\right]^{0.39} \times \left[\frac{1}{0.010}\right]^{1.67} \times \left[\frac{1}{0.011}\right]^{0.40} \times \left[\frac{1}{18.3}\right]^{1.88} \times 361$$

$$GMF = 44024 \text{ kN/m}$$

Barlea Bridge

$$GMF = \left[\frac{1}{0.171}\right]^{0.39} \times \left[\frac{1}{0.012}\right]^{1.67} \times \left[\frac{1}{0.030}\right]^{0.40} \times \left[\frac{1}{9.86}\right]^{1.88} \times 296$$

$$GMF = 51246 \text{ kN/m}$$

Preston Bridge:

$$GMF = \left[\frac{1}{0.317}\right]^{0.39} \times \left[\frac{1}{0.015}\right]^{1.67} \times \left[\frac{1}{0.073}\right]^{0.40} \times \left[\frac{1}{5.18}\right]^{1.88} \times 241$$

$$GMF = 52729 \text{ kN/m}$$

There is a coherent parallelism between calculated *Geometric Multiplication Factors*. Therefore, it can be concluded as collapse load is proportional to, by averaging *GMFs*:

$$GMF = 49333 \text{ kN/m}$$

A new formula that predicts the probable limit load for an existing masonry arch bridge can be rewritten as:

$$P_E = \left(f/L\right)_E^{0.39} \times \left(\frac{r^2}{f \times L}\right)_E^{1.67} \times \left(H/L\right)_E^{0.40} \times \left(L_E\right)^{1.88} \times GMT \qquad (7.2)$$

For an upper limit, *GMF* can be taken as 50000 kN/m. However, *GMF* should be decreased according to the condition of the bridge. For bridges in bad condition, with cracks and loss of mortar, *GMF* can be taken as 25000 kN/m. *GMF* = 45000 kN/m generally serves very close predictions to the exact ones for bridges that are in good condition.

This new and compact formula can be used to predict the ultimate load capacities of existing masonry arc bridges. In order to validate this analytical formula, experimentally tested bridges, Bridgemill, Barlea and Stratmashie Bridges, are going to be analyzed. The geometrical properties, non-dimensional parameters and collapse load for each bridge are tabulated in Table 7.1.

- The prediction for Bridgemill gives:

$$P_E = \left(0.156\right)^{0.39} \times \left(0.010\right)^{1.67} \times \left(0.011\right)^{0.40} \times \left(18.3\right)^{1.88} \times 45000$$

$$P_E = 387 kN/m \text{ width} \quad (107 \text{ per cent of actual collapse load})$$

- The prediction for Barlea Bridge gives:

$$P_E = \left(0.171\right)^{0.39} \times \left(0.012\right)^{1.67} \times \left(0.030\right)^{0.40} \times \left(9.86\right)^{1.88} \times 45000$$

$$P_E = 260 kN/m \text{ width (88 per cent of actual collapse load)}$$

- The prediction for Preston Bridge gives:

$$P_E = (0.317)^{0.39} \times (0.015)^{1.67} \times (0.073)^{0.40} \times (5.18)^{1.88} \times 45000$$

$P_E = 206 kN/m$ width (86 per cent of actual collapse load)

8. CONCLUDING REMARKS

Using Mechanism Method which is a powerful and efficient masonry arch assessment approach, a computer program is designed to predict the capacity of single span masonry arch bridges. This program has been used successfully to study the behavior of masonry arch bridges. Following conclusions about the program can be drawn:

- First of all, the analysis of masonry arch bridges is a field of research in which satisfactory analytical tools are hard to develop. However a reasonable accuracy for the predicted collapse load has been achieved by the program. The program seems to be more valid in the analysis of medium span single masonry arch bridges. For spans longer than 20 m, the elastic deformations prior to collapse will significantly change the arch geometry. Since the Mechanism Method does not consider such second order effects, the program may give inaccurate predictions for these bridges.

- There are uncertainties in many of the factors which influence the load capacity. However the program can be adopted to avoid guessing critical unknown parameters.

- The strength of the masonry arch bridges highly depends on their health conditions. The cracks on the ring significantly decrease the capacity of the arch. In order to include such deficiencies, an indicator, har, is utilized in the program. Appropriate selection of this indicator gives close predictions to the actual behavior.

Using the designed program, a non-dimensional parametric study is undertaken and the findings of this study can be summarized as follows:

- The capacity of the masonry arch bridges increases with increasing f/L. Additionally, horizontal abutment thrust, HT, is found to increase with decreasing f/L although there is a decrease in the collapse load. In a real arch, especially for shallow arches, it is likely that abutments will move depending on the value of this thrust. Since abutment movement is totally ignored in the mechanism method, the

capacity of the shallow arches may not be predicted accurately. In the assessment of such bridges, *har* should be selected appropriately after a close inspection of the abutments where the main considerations should be the condition, location and size of the abutments.

- The ring thickness has a great effect on the capacity of the arch. Therefore, for design purposes, $\frac{r^2}{f \times L} < 0.013$ is not recommended.

In the last part of the study, a simple and useful arch assessment method is offered. The method predicts the capacity of an existing bridge by using the geometric properties and corresponding collapse loads of the tested bridges. The motivation for this part of the study is that the proportion of the non-dimensional parameters between existing and tested masonry arch bridges gives the proportion of their strengths. The validation of the proposed method shows that the capacity of the masonry arch bridge is highly affected by its geometry. Material strength is a secondary concern.

For further studies, some additional tests on the proposed method could be useful to validate it again. In the current study, the capacity of a tested bridge is predicted by approximation over two tested bridges. The consistency of the predictions against the number of tested bridges used could be investigated by increasing the number of tested bridges in this method.

Moreover, in this study, no lateral earth pressure is included in the program. Therefore, the effect of the non-dimensional parameter, H/L, can be reviewed considering active and passive pressures of the fill. After that, the effect of H/L on the offered method can be modified.

APPENDIX A: MATLAB PROGRAMS

A.1. Limit Load Prediction Code

```
function [collapseload,limitload] =
mechanismmethod(coordext,coordint,gfill,gring,H,har,disperselangle,w)
%%%%%%%%%%%%%%%%%%%%%%%%%%%%%%%%%%%%%%%%%%%%%%%% %
%     This program predicts the maximum load that the masonry arch can cary      %
%     using The Mechanism Method (by Heyman, 1980).                              %
%     The collapse load is calculated by the upper bound (kinematic) theory.     %
%     Critical hinge location and location of force can also be found by the program.%
%%%%%%%%%%%%%%%%%%%%%%%%%%%%%%%%%%%%%%%%%%%%%%%% %%%
%                              INPUTS                                            %
%                                                                                %
%    coordext       :   Extrados Geometry            [X's Y's]   (m)             %
%    coorint        :   Intrados Geometry            [X's Y's]   (m)             %
%    gfill          :   Specific Weight of Rill                  (kN/m^3)        %
%    gring          :   Specific Weight of Ring                  (kN/m^3)        %
%    H              :   Crown Thickness                          (m)             %
%    har            :   Hypothetical Arch Ratio                  (~0.85)         %
%    disperselangle :   maximum spread angle of load             (degree)(~0.30) %
%                                                                                %
%%%%%%%%%%%%%%%%%%%%%%%%%%%%%%%%%%%%%%%%%%%%%%%% %
%                              BASIC OUTPUTS                                     %
%                                                                                %
%    collapseload   :   Collapse Load                            (kN/m)          %
%    limitload      :   Force location        limitload(:,1)     (kN/m)          %
%                   :   Collapse Load         limitload(:,2)     (m)             %
%                                                                                %
%%%%%%%%%%%%%%%%%%%%%%%%%%%%%%%%%%%%%%%%%%%%%%%% %
```

```
n = size(coordext,1)-1;
index = n+1;
Htotal = H+max(coordext(:,2));
maxHlocation=find(coordext(:,2)-max(coordext(:,2))==0);
weightfill = zeros(n,1);
weightring = zeros(n,1);
r = zeros(n,1);
for i = 1:n
   weightfill(i,:) = (Htotal-((coordext(i,2)+coordext(i+1,2))/2))*...
      (coordext(i+1,1)-coordext(i,1))*gfill;
   weightring(i,:) = ((coordext(i,2)-coordint(i,2))+(coordext(i+1,2)-coordint(i+1,2)))/2*...
      (coordext(i+1,1)-coordext(i,1))*gring;
   r(i,:) = (coordext(i+1,1)+coordext(i,1))/2;
end
weighttotal = weightfill+weightring;
%safe region (middle third rule)
for i=1:n+1
   middlethird(i,:)=(coordext(i,2)-coordint(i,2))/6;
   safeext(i,:)=(coordext(i,2)+coordint(i,2))/2+middlethird(i,:);
   safeint(i,:)=(coordext(i,2)+coordint(i,2))/2-middlethird(i,:);
end
safeext=[coordint(:,1) safeext];
safeint=[coordint(:,1) safeint];
% Replaced hinge location surfaces %
coordrint=[];
coordrext=[];
Htot=[];
for i=1:n+1
   a=(coordext(i,2)-coordint(i,2))/2*har+(coordext(i,2)+coordint(i,2))/2;
   b=(coordext(i,2)+coordint(i,2))/2-(coordext(i,2)-coordint(i,2))/2*har;
   coordrint=[coordrint;b];
   coordrext=[coordrext;a];
   Htot(i)=Htotal;
```

```
end
coordrint=[coordint(:,1) coordrint];
coordrext=[coordint(:,1) coordrext];
%
label1 = 1:n+1;
label2 = 1:ceil(n/4)+1;
label3 = floor(3*n/4)+1:n+1;
%
hingeforcepattern = [];
forces = [];
A=[];
for i = label2
   for j = label3
      index1 = find(label1 > i & label1 < j);
      for k = 2:length(index1)-1
         index2 = find(index1 > index1(k));
         for t = 2:length(index2)
            for x = 2:maxHlocation
               Forcelocation=coordext(x,1);
               h1=coordrint(i,:);
               h2=coordrext(index1(k),:);
               h3=coordrint(index1(index2(t)),:);
               h4=coordrext(j,:);
               h5=coordrext(x,:);
               coord = [h1; h2; h3; h4 ; h5];
               [Forcefactors] = forcedispersion(coordext,H,coord(5,1),disperselangle,w);
               i2=size(Forcefactors);
               f=i2(1,1);
               coefficient = zeros(3,3);
               RHS = zeros(3,1);
               % Moment about Point #3
               index3 = find(coordint(:,1)-coord(3,1) == 0);
               index4 = find(coordint(:,1)-coord(4,1) == 0);
```

```
M = 0;
for y = index3+1:index4
   M = M+weighttotal(y-1,1)*(r(y-1,1)-coord(3,1));
end
coefficient(1,1) = coord(4,1)-coord(3,1);
coefficient(1,2) = coord(4,2)-coord(3,2);
coefficient(1,3) = 0;
c1=0;
for m=1:f
   if Forcefactors(m,1)>coord(3,1)
   c1 = Forcefactors(m,3)*(coord(3,1)-Forcefactors(m,1));
   end
coefficient(1,3)=coefficient(1,3)+ c1;
end
RHS(1,1) = M;
% Moment about Point #2
index3 = find(coordint(:,1)-coord(2,1) == 0);
index4 = find(coordint(:,1)-coord(4,1) == 0);
M = 0;
for y = index3+1:index4
   M = M+weighttotal(y-1,1)*(r(y-1,1)-coord(2,1));
end
coefficient(2,1) = coord(4,1)-coord(2,1);
coefficient(2,2) = coord(4,2)-coord(2,2);
coefficient(2,3) = 0;
c2=0;
for m=1:f
   if Forcefactors(m,1)>coord(2,1)
   c2 = Forcefactors(m,3)*(coord(2,1)-Forcefactors(m,1));
   end
coefficient(2,3) = coefficient(2,3) + c2;
end
RHS(2,1) = M;
```

```
            % Moment about Point #1
            index3 = find(coordint(:,1)-coord(1,1) == 0);
            index4 = find(coordint(:,1)-coord(4,1) == 0);
            M = 0;
            for y = index3+1:index4
               M = M+weighttotal(y-1,1)*(r(y-1,1)-coord(1,1));
            end
            coefficient(3,1) = coord(4,1)-coord(1,1);
            coefficient(3,2) = coord(4,2)-coord(1,2);
            coefficient(3,3) = 0;
            c3=0;
            for m=1:f
               if Forcefactors(m,1)>coord(1,1)
               c3 = Forcefactors(m,3)*(coord(1,1)-Forcefactors(m,1));
               end
            coefficient(3,3)= coefficient(3,3) + c3;
            end
            RHS(3,1) = M;
            %
            % Computation of the unknowns
            VHP = inv(coefficient)*RHS;
            %
            % Elimination of meaningless terms
            if VHP(3,1) > 0 & VHP(3,1) < 999000000000 & VHP(1,1) > 0 & VHP(2,1) >
0
               L=[coord(5,1) VHP(3,1)];
               A=[A; L];
               forces = [forces VHP];
               hingeforcepattern = [hingeforcepattern coord];
            end
         end
      end
   end
```

```
    end
end
forcest=[];
hingeforcepatternt=[];
thrustline=[];
for i=1:length(forces);
    vf=forces(1,i);
    hf=forces(2,i);
    p=forces(3,i);
    h4=[hingeforcepattern(4,2*i-1) hingeforcepattern(4,2*i)];
    h5=[hingeforcepattern(5,2*i-1) hingeforcepattern(5,2*i)];
    %Thrust line
    tl = zeros(n+1,1);
    index6 = find(coordint(:,1)-h4(1,1) == 0);
    tl(index6,1)=h4(1,2);
    [Forcefactors] = forcedispersion(coordext,H,h5(1,1),disperselangle,w);
    Effectedforces=p.*Forcefactors(:,3);
    for m = 1:index6-1;
        M1 = 0;
        for  j = m:index6-1
            M1 = M1+weighttotal(j,1)*(r(j,1)-coordint(m,1));
        end
        M2=0;
        for k=1:length(Effectedforces)
            if  coordint(m,1) <= Forcefactors(k,1)
            M2 = M2+ Effectedforces(k)*(Forcefactors(k,1) - coordint(m,1));
            end
        end
              tl(m,1) = (vf*(h4(1,1)-coordint(m,1))-...
              M1 + hf* h4(1,2)-M2)/hf;
    end
    if index6 -(n+1)<0
        for m = index6+1:n+1;
```

```
            M = 0;
            for j = index6:m-1;
                M = M+weighttotal(j,1)*(coordint(m,1)-r(j,1));
            end
            tl(m,1) = (vf*(coordint(m,1)-h4(1,1))-...
            M - hf* h4(1,2))/-hf;
        end
    end
    if tl > coordrint(:,2)-0.001 & tl < coordrext(:,2) + 0.001
        forcest=[forcest forces(:,i)];
        hingeforcepatternt=[hingeforcepatternt hingeforcepattern(:,2*i-1)
hingeforcepattern(:,2*i)];
        thrustline=[thrustline tl];
    end
end
collapseload = min(forcest(3,:));
index7=find(forcest(3,:)-collapseload==0);
plot(coordint(:,1),coordrint(:,2),'k:',coordint(:,1),coordrext(:,2),'k:')
title('Worst Load Position & Possible Line of Thrust')
xlim([0 max(coordint(:,1))])
ylim([0 1.1*Htotal])
hold on
plot(coordint(:,1),coordint(:,2),'k',coordint(:,1),coordext(:,2),'k',coordint(:,1),thrustline(:,ind
ex7),'k',coordint(:,1),Htot,'k--')
hold on
plot(hingeforcepatternt(1,2*index7-1),hingeforcepatternt(1,2*index7),'ko',...
    hingeforcepatternt(2,2*index7-1),hingeforcepatternt(2,2*index7),'ko',...
    hingeforcepatternt(3,2*index7-1),hingeforcepatternt(3,2*index7),'ko',...
    hingeforcepatternt(4,2*index7-1),hingeforcepatternt(4,2*index7),'ko','markersize',7)
hold on
plot(hingeforcepatternt(5,2*index7-1),Htotal,'kv','markersize',11)
figure
limitload=[];
```

```
for i=1:length(forcest)-1
   if hingeforcepatternt(5,2*i-1)- hingeforcepatternt(5,2*i)==0
      forcest(3,i+1)=max(forcest(3,i),forcest(3,i+1));
      forcest(3,i)=max(forcest(3,i),forcest(3,i+1));
   end
   limitload=[limitload; hingeforcepatternt(5,2*i-1) forcest(3,i)];
end
limitload=[limitload;hingeforcepatternt(5,2*length(forcest)-1) forcest(3,length(forcest))];
plot(limitload(:,1)/max(coordint(:,1)),limitload(:,2),'k',(max(coordint(:,1))-
limitload(:,1))/max(coordint(:,1)),limitload(:,2),'k')
title('Limit Load vs. Loading Position')
xlabel('Loading Position (x/L)')
ylabel('Limit Load (kN/m)')
```

A.2. Force Dispersion Code (Utilizing Boussinesq Equation)

```
function [Forcefactor] = forcedispersion(coordext,H,forcelocation,disperselangle,w)
%                                                                                %
%%%%%%%%%%%%%%%%%%%%%%%%%%%%%%%%%%%%%%%%%%%%%%%%%%%%%%%%%%%%%%%%%%%%%%% %%
%                                                                                %
%       This program calculates the distribution of point and distributed loads  %
%       on the arch ring using Boussinesq (1885) equations.                      %
%                                                                                %
%%%%%%%%%%%%%%%%%%%%%%%%%%%%%%%%%%%%%%%%%%%%%%%%%%%%%%%%%%%%%%%%%%%%%%%%%%%%%%
                                                                                 %
%                                    INPUTS                                      %
%                                                                                %
%     coordext        :  Extrados Geometry          [X's Y's]     (m)            %
%     H               :  Crown Thickness                          (m)            %
%     forcelocation   :  The location of force      [X]           (m)            %
%     disperselangle  :  maximum spread angle of the load         (degree)       %
%     w               :  Strip width                Use 0 "zero" for Point load cases %
%                                                                                %
%%%%%%%%%%%%%%%%%%%%%%%%%%%%%%%%%%%%%%%%%%%%%%%%%%%%%%%%%%%%%%%%%%%%%%%%%%%%%%%
%                                                                                %
%                                    OUTPUTS                                     %
%                                                                                %
%     Forcefactors    :  X coordinate of related nodes    Forcefactor(:,1)       %
%                     :  Y coordinate of related nodes    Forcefactor(:,2)       %
%                     :  Load factors                     Forcefactor(:,3)       %
%                                                                                %
%%%%%%%%%%%%%%%%%%%%%%%%%%%%%%%%%%%%%%%%%%%%%%%%%%%%%%%%%%%%%%%%%%%%%%%%%%%%%%%
%                                                                                %
```

```
n = size(coordext,1)-1;
Htotal = H+max(coordext(:,2));
if w==0
  Ang=[];
% angle between the load and the points at the extrados%
   for i=1:n+1
      ai = atan(abs((coordext(i,1)-forcelocation(1,1))/(Htotal-coordext(i,2))));
      aidegree=angledim(ai,'radians','degrees');
      Ang = [Ang aidegree];
   end
   index1 = find(coordext(:,1)-forcelocation(:,1) ==0);
   a=find(Ang- disperselangle <= 0);
   index3=[a(1)-1 a a(length(a))+1];
   if  index3(1)==0
      index3(1)=[];
   end
   if  index3(length(index3))>n+1
      index3(length(index3))=[];
   end
   Stressfactor=[];
   for i=1:length(index3)
      x=abs(coordext(index3(i),1)-forcelocation(1,1));
      z=Htotal-coordext(index3(i),2);
      Factor=2/pi*z^3/(x^2+z^2)^2;
      Stressfactor=[Stressfactor Factor];
    end
%
else
   Ang1=[];
   % angle between left edge of the distributed load and the points at the extrados%
   for i=1:n+1
      b1 = atan((forcelocation(1,1)-w/2-coordext(i,1))/(Htotal-coordext(i,2)));
      b1degree=angledim(b1,'radians','degrees');
```

```
        Ang1 = [Ang1 b1degree+90];
    end
    Ang2=[];
% angle between right edge of the distributed load and the points at the extrados%
    for i=1:n+1
        b2 = atan((forcelocation(1,1)+w/2-coordext(i,1))/(Htotal-coordext(i,2)));
        b2degree=angledim(b2,'radians','degrees');
        Ang2 = [Ang2 b2degree+90];
    end
   a=find(Ang1 -(disperselangle+90) <= 0 & Ang2 - (90-disperselangle) >= 0);
    %
     index3=[a(1)-1 a a(length(a))+1];
     if  index3(1)==0
         index3(1)=[];
    end
    if  index3(length(index3))>n+1
        index3(length(index3))=[];
    end
    absx=[];
    alfa=[];
    beta=[];
    Stressfactor=[];
    for i=1:length(index3)
        x=abs(coordext(index3(i),1)-forcelocation(1,1));
        al=atan((x-w/2)/(Htotal-coordext(index3(i),2)));
        be=atan((x+w/2)/(Htotal-coordext(index3(i),2)))-al;
        Factor=1/pi*(be+sin(be)*cos(be+2*al));
        Stressfactor=[Stressfactor Factor];
    end
end
% % Force Factors %
    P=zeros(length(Stressfactor),1);
    R=zeros(length(Stressfactor),1);
```

```
    for i=1:length(Stressfactor)-1
        P(i)=(Stressfactor(i)/3+Stressfactor(i+1)/6);
    end
    for i=2:length(Stressfactor)
        R(i)=(Stressfactor(i)/3+Stressfactor(i-1)/6);
    end
    F=P+R;
Forcefactor=[coordext(index3,:) (F./sum(F))];
```

APPENDIX B: GEOMETRIC PROPERTIES AND PREDICTED LIMIT LOADS FOR FICTITOUS ARCH BRIDGES

In order to validate the offered program, the program is tested using several fictitious arch geometries. The following table presents these geometric properties along with the predicted limit loads that are approximated from Barlea and Stratmashie Bridges.

Table B.1. Results of the proposed method on fictitious arches

FICTITIOUS BRIDGE GEOMETRIES				BARLEA APPROXIMATION	STRATMASHIE APPROXIMATION	AVERAGE	Calculated
L (m)	f/L	r^2/fL	H/L	Predicted Collapse Load (kN/m) width	Predicted Collapse Load (kN/m) width	Predicted Collapse Load (kN/m) width	Collapse Load (kN/m) width
12	0.18333	0.01364	0.02917	528.21	275.85	402.03	406.00
13.6	0.22059	0.01036	0.03309	476.03	248.59	362.31	404.07
14.6	0.20548	0.00965	0.03082	456.82	238.56	347.69	354.22
10.6	0.19811	0.01460	0.04245	558.19	291.50	424.85	475.33
8.5	0.38824	0.00570	0.05294	108.72	56.78	82.75	119.00
8	0.37500	0.00667	0.05000	121.58	63.49	92.54	83.58
6	0.33333	0.01333	0.04167	201.45	105.20	153.32	185.31
5.76	0.34722	0.01389	0.04340	206.28	107.72	157.00	169.39
5.9	0.30508	0.01507	0.04237	232.68	121.51	177.10	172.49
9.7	0.18557	0.01035	0.03093	229.04	119.61	174.33	194.12
8.9	0.22472	0.01138	0.03371	254.96	133.15	194.06	148.19
9.4	0.35106	0.01161	0.03191	342.15	178.68	260.42	268.71

FICTITIOUS BRIDGE GEOMETRIES				BARLEA APPROXIMATION	STRATMASHIE APPROXIMATION	AVERAGE	Calculated
L (m)	f/L	r^2/fL	H/L	Predicted Collapse Load (kN/m) width	Predicted Collapse Load (kN/m) width	Predicted Collapse Load (kN/m) width	Collapse Load (kN/m) width
6.6	0.35606	0.01306	0.04924	254.55	132.93	193.74	183.40
6.9	0.34058	0.00987	0.04710	167.13	87.28	127.20	141.02
10.24	0.22949	0.00842	0.03174	197.26	103.02	150.14	154.11
11.3	0.22124	0.00717	0.03097	177.10	92.49	134.79	127.17
11.7	0.24359	0.01080	0.03846	424.05	221.45	322.75	355.14
12.3	0.23171	0.01205	0.04472	581.58	303.72	442.65	487.31
12.76	0.22335	0.01057	0.03918	468.55	244.69	356.62	382.72
13.3	0.23684	0.01008	0.04135	489.18	255.46	372.32	373.51
13.1	0.24046	0.00733	0.04198	281.85	147.19	214.52	224.35
13.7	0.22993	0.00834	0.04015	367.65	192.00	279.82	269.33
14.66	0.21487	0.00915	0.02729	409.43	213.81	311.62	324.43
14.9	0.24832	0.00940	0.03020	486.84	254.24	370.54	369.09
14.5	0.25517	0.00740	0.03103	316.07	165.06	240.57	275.30

FICTITIOUS BRIDGE GEOMETRIES				BARLEA APPROXIMATION	STRATMASHIE APPROXIMATION	AVERAGE	Calculated
L (m)	f/L	r^2/fL	H/L	Predicted Collapse Load (kN/m) width	Predicted Collapse Load (kN/m) width	Predicted Collapse Load (kN/m) width	Collapse Load (kN/m) width
10.66	0.34709	0.01071	0.04221	419.62	219.14	319.38	373.20
12.1	0.30579	0.00944	0.03719	389.86	203.60	296.73	301.49
11.1	0.33333	0.00877	0.04054	313.40	163.67	238.53	207.15
9.36	0.28846	0.01425	0.04808	517.16	270.07	393.62	390.39
7.12	0.37921	0.01300	0.05618	314.46	164.22	239.34	254.00
6.28	0.31847	0.00717	0.04777	80.15	41.86	61.01	65.81
6.88	0.29070	0.01163	0.04360	199.46	104.16	151.81	148.88
7.56	0.27910	0.01269	0.03968	261.79	136.71	199.25	211.22
8.12	0.25985	0.01182	0.04680	274.85	143.53	209.19	183.83
9.34	0.22591	0.01028	0.04069	253.40	132.33	192.87	188.84
10.9	0.26514	0.00794	0.03486	220.82	115.32	168.07	186.08
11.74	0.26831	0.00973	0.04003	378.72	197.78	288.25	306.99
7.4	0.40541	0.01622	0.04054	443.94	231.84	337.89	401.34

REFERENCES

1. Heyman, J., 1995, *The Stone Skeleton*, Cambridge University Press, Cambridge, UK.

2. http://en.wikipedia.org, 2006.

3. Heyman, J., 1982, *The Masonry Arch*, Cambridge University Press, Cambridge, UK.

4. Karaesmen, E., *Lecture Notes: Introduction to Architectural Engineering for CE 480*, Middle East Technical University, Ankara, 110 Pages, 2005.

5. Sevgili, G., B. Küçükdogan and E. Karaesmen,, "Old Masonry in Seismic Zones", *Earthquake Engineering: Essentials and Applications Seminar Series*, Earthquake Engineering Research Center Middle East Technical University, July 18-20 2005, http://eerc.ce.metu.edu.tr/seminer/Karaesmen/ Karaesmen.pdf

6. Bonde,S., R. Mark and E. C. Robison, "Walls and Other Vertical Elements" in MARK, R. (ed.). 1993. *Architectural Technology up to the Scientific Revolution: the Art and Sructure of Large-Scale Buildings*, the MIT Press, London England.

7. Roberts, A. W., "Masonry Arches", *Handbook of Building Construction Data for Architects, Designing and Constructing Engineers and Contractors, Vol1*, McGraw-Hill Book Company Inc.,1920, New York.

8. Yavuz, A. T., 1982, *Anadolu Selçuklu Mimarisinde Tonoz ve Kemer*, Kelaynak Yayınevi ve Matbaası, Ankara.

9. Gay, C. M. and H. Parker, 1943, *Materials and Methods of Architectural Construction*, 2nd edition, John Wiley & Sons Inc., New York, first published in 1932.

10. Jaggard, W. R., and F. E. Drury, 1951, *Architectural Building Construction A text Book for the Architectural and Building Student Vol3*, 2nd edition, Cambridge University Press, first edited in 1923.

11. MC. Kay, W. B., 1963, *Building Construction Vol1* , revised by MC. Kay J. K., 4th edition, Green and Co. Ltd., LONDON, Printed and Photo-Litho by Lowe and Brydone, (Printers) Ltd., London.

12. Ahunbay, Z., Y. Kahya, F. Çili, A. Ersen and A. Güleç, 2000, "Conservation of Uzunkemer aqueduct in Istanbul, Turkey", *Proceedings of Archi2000*, http://www.unesco.org/archi2000/pdf/ahunbay.pdf

13. http://www.past-inc.org/historic-bridges, 2006.

14. Croci, G., 1998, *The Conservation and Structural Restoration of the Architectural Heritage*, Computational Mechanics Publications, Southampton, UK.

15. Lourenço, P. B., *Computational Strategies for Masonry Structures*, Ph.D. Dissertation, Delft University of Technology, Delft, The Netherlands, 1996.

16. Swift, E. H., 1951, *Roman Sources of Christian Art*, Columbia University Press, New York.

17. Mainstone, R., 1975, *Developments in Structural Form*, The MIT Press, Cambridge, Massachusetts.

18. Strong, E., 1970, *Art in Ancient Rome Volume 1*, Greenwood Reprinting, USA.

19. www.citrag.it, 2006.

20. Barker, R. M. and J. A. Puckett, 1997, *Design of Highway Bridges: Based on AASHTO LRFD Bridge Design Specification*, A Wiley-Interscience Publication, John Wiley & Sons, Inc., New York, NY.

21. Brown, D. J., 1993, *Bridges, Macmillan* Publishing Company, New York.

22. http://www.comune.fabricadiroma.vt.it/Cultura.htm, 2005.

23. Ramage, R., H. and A. Ramage, 1991, *Roman art: Romulus to Constantine*, Abrams Inc. Publishers, New York.

24. Mock, E. B., 1949, *The Architecture of Bridges*, The Museum of Modern Art, New York.

25. Jenkins, D. A., 1999, "Arch Structures: Spanning Past, Present and Future", *Proceedings of the Concrete Institute of Australia Conference, Sydney*, http://www.interactiveds.com.au /Conc99-ArchStructures.pdf

26. www.tourismturkey.org, 2006.

27. Çulpan, C., 1975, *Türk Taş Köprüleri Ortaçağdan Osmanlı Devri Sonuna Kadar*, Türk Tarih Kurumu Basımevi, Ankara.

28. Çeçen, K., "Sinan'ın Yaptığı Köprüler", in Bayram, S. (ed.), 1988, *Mimarbaşı Koca Sinan'ın Yaşadığı Çağ ve Eserleri*, Dizergonca Matbaası, İstanbul.

29. Çeçen, K., "Sinan'ın Yaptığı Su Tesisleri", in Bayram, S. (ed.), 1988, *Mimarbaşı Koca Sinan'ın Yaşadığı Çağ ve Eserleri*, Dizergonca Matbaası, İstanbul.

30. Bozkurt, O., 1952, *Koca Sinan'ın Köprüleri XVI. Asır Osmanlı Medeniyeti İçinde Sinan, Köprülerin Mimarı Bakımdan Tetkiki, Siluet ve Abide Kıymetleri*, Pulhan Matbaası, Istanbul.

31. www.turkishculture.org, 2006.

32. Clemente, P., A. Occhiuzzi and A. Raithel, "Limit Behaviour of Stone Arch Bridges", *Journal of Structural Engineering*, Volume 121, Issue 7, pp. 1045-1050, 1995.

33. Huerta, S., "Mechanics of Masonry Vaults: The Equilibrium Approach", *Proceedings of Historical Constructions 2001, 3rd International Seminar*, pp. 47-69.

34. Block, P., *Equilibrium Systems – Studies in Masonry Structures*, M.S. Thesis, Massachusetts Institute of Technology, 2005.

35. Cavicci, A. and L. Gambarotta, "Collapse Analysis of Masonry Arch Bridges Taking Account Arch-Fill Interaction", *Engineering Structures*, Vol. 27, No. 4, pp. 605-615, 2005.

36. Department of Transport: Departmental Advice Note BA16/97, "The Assessment of the Highway Bridges and Structures", Volume 3, Section 4, Part 4, London, 2001.

37. Hughes, T. G. and M. J. Blackler, "A Review of the UK Masonry Arch Assessment Methods", *Proceedings of the Institution of Civil Engineers: Structures and Buildings*, Vol. 122, No. 3, pp. 305-315, 1997.

38. Towler, K. D. S., "Applications of Non-linear Finite Element Codes to Masonry Arches", *Proceedings of the 2nd International Conference on Civil and Structural Engineering Computing*, pp. 218-229, 1985.

39. Crisfield, M. A., "Finite Element and Mechanism Methods for the Analysis of Masonry and Brickwork Arches". *Transport and Road Research Laboratory*, Report 19, London, 1986.

40. Loo, Y. and Y. Yang, "Cracking and Failure Analysis of Masonry Arch Bridges", *Journal of Structural Engineer*, Volume 117, No. 6, pp. 1641-1659, 1991.

41. Ng, K. H., C. A. Fairfield and A. Sibbald, “Finite-Element Analysis of Masonry Arch Bridges”, *Proceedings of the Institution of Civil Engineers – Structures and Buildings*, Volume 134, No. 2, pp. 119-127, 1999.

42. Choo, B. S., M. G. Coutie and N. G. Gong, “Finite Element Analysis of Masonry Arch Bridges Using Tapered Elements”, *Proceedings of the Institution of Civil Engineers*, Part 2, No. 91, pp. 755-770, 1991.

43. NG, K. H. and C. A. Fairfield, "Modifying the Mechanism Method of Masonry Arch Bridge Analysis"*, Construction and Building Materials*, Volume. 18, No. 2, pp. 91-97, 2004.

44. Brencich, A. and C. Colla, “The influence of construction technology on the mechanics of masonry railway bridges”, *Proceedings of Railway Engineering 2002 - V International Conference and Exhibition*, Londra, pp. 44-67, 2002.

45. RING, CLADU, University of Sheffield, UK. http://www.shef.ac.uk/ring, 2005.

46. Lucko, G., *Means and Methods Analysis of a Cast-In-Place Balanced Cantilever Segmental Bridge: The Wilson Creek Bridge Case Study*, M.S. Thesis, Virginia Polytechnic Institute and State University, 1999.

47. Schueller, W., 1996, *The Design of Building Structures*, Prentice Hall Inc., New Jersey.

48. Tunç, G., 1978, *Taş Köprülerimiz*, Karayolları Genel Müdürlüğü Matbaası, Ankara.

49. Smith, R. C., 1967, *Principles and Practices of Heavy Construction*, Prentice- Hall Inc., London, England.

50. Saadet, K., *Development of Arch Form: Exploring the Behaviour of Masonry Arches and Arch Bridges by Finite Element Analysis*. M.S. thesis, Middle East Technical University, Turkey, 2000.

51. Lourenço, P. B., “Computations on Historic Masonry Structures”, *Progress in Structural Engineering and Materials*, Volume 4, Issue 3, pp. 301-319, 2002.

52. Harwey, W. J., “Application of the Mechanism Analysis to Masonry Arches”, *The Structural Engineers*, Vol.66, No.5, pp. 77-84, 1988.

53. Lourenço, P. B., “Experimental and Numerical Issues in the Modeling of the Mechanical Behavior of Masonry”, *Structural Analysis of Historical Constructions*, pp. 57-91, 1998.

54. Brencich, A. and U. De Francesco, “Simplified Approaches to the Assessment of Railway Bridges”, *Proceedings of Railway Engineering 2002 - V International Conference and Exhibition*, Londra, pp.23-43, 2002.

55. Lourenço, P. B., “Computations on Historic Masonry Structures”, *Progress in Structural Engineering*, Volume. 4, Issue. 3, pp. 301-319, 2002.

56. Thomas E. B., ”Analysis of Masonry Arches and Vaults”, *Progress in Structural Engineering*, Volume. 3, Issue. 3, pp. 246-256, 2001.

57. Ahmed, H. M. and M. Gilbert, “The Computational Efficiency of two Rigid Block Analysis Formulations for Application to Masonry Structures”, *Proceedings of the 9th International Conference on Civil and Structural Engineering Computing*, pp. 46-66, Egmond-aan-Zee, Holland, 2003.

58. Boothby, T. E., D. E. Domalik and V. A. Dalal, “Service Load Response of Masonry Arch Bridges”, *Journal of Structural Engineering*, Volume. 124, No. 1, pp. 17-23, 1998.

59. Fanning, P. and T. Boothby, "Assessment Methods for Masonry Arch Bridges", *Proceeding of the 9th International Conference on Structural Faults and Repair*, edited by Forde, pp.66-78, London, 2001.

60. PAGE J., “Load Test to Collapse on Two Arch Bridges at Stratmashie and Barlea”, *Transport Research Laboratory, TRL Research Report 201*, Crowthorne, 1989.

61. Ford, T. E., C. E. Augarde and S. S. Tuxford, “Modeling Masonry Arch Bridges Using Commercial Finite Element Software”, *9th International Conference on Civil and Structural Enginnering Computing*, pp. 88-100, Egmond aan Zee, The Netherlands, 2003.

62. Melbourne, C. and P. J. Walker, “Load Tests to Collapse of Model Brickwork Masonry Arches”, Proceedings of the 8th International Brick and Block Masonry Conference, London, Volume.2, pp. 991-1002, 1988.

63. Gilbert, M. and C. Melbourne, “Rigid-Block Analysis of Masonry Structures”, *The Structural Engineer*, Volume. 72, No. 21, pp. 356-361, 1994.

64. Craig, R. F., 1997, *Soil Mechanics*, Spon Press, London.